Master Thesis in Geosciences

Equatorial Guinea and northern Gabon margins: regional tectonic evolution based on integrated analysis of seismic reflection and potential field data and modeling

by

Ehimen Ebhohimen Williams

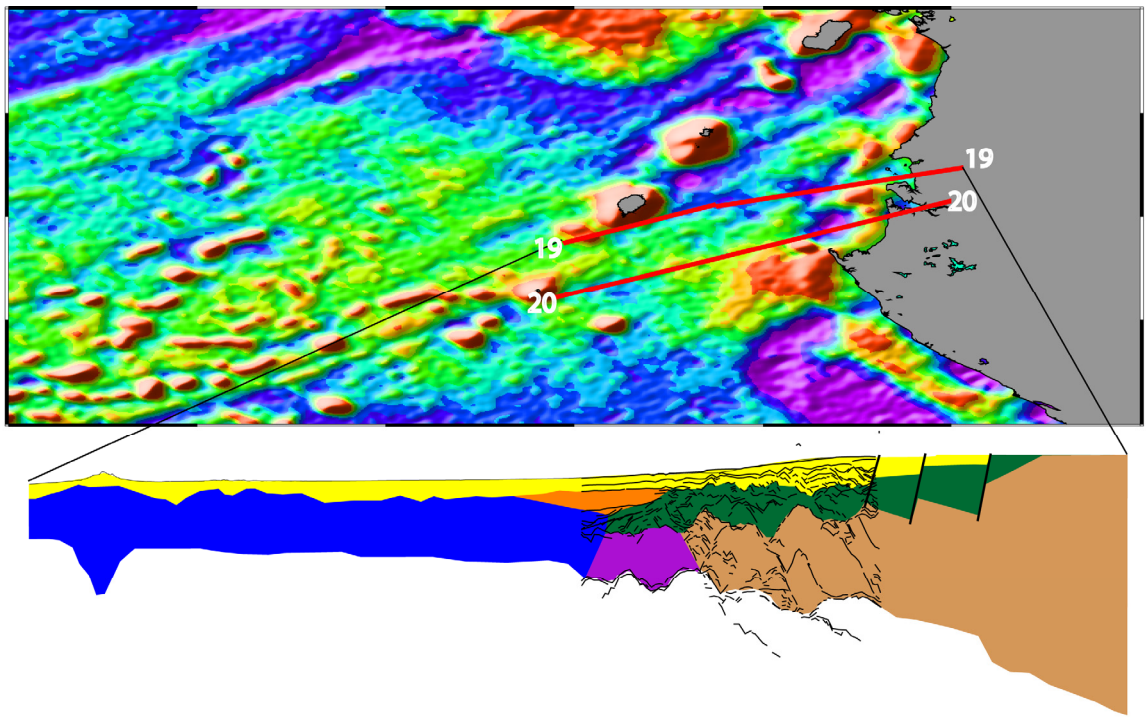

UNIVERSITY OF OSLO

FACULTY OF MATHEMATICS AND NATURAL SCIENCES

Equatorial Guinea and northern Gabon margins: regional tectonic evolution based on integrated seismic reflection and potential field data and modeling

by

Ehimen Ebhohimen Williams

Master Thesis in Geosciences

Discipline: Petroleum Geology and Geophysics

Department of Geosciences

Faculty of Mathematics and Natural Sciences

UNIVERSITY OF OSLO

[June 2008]

Contents

Preface

This master thesis finalizes the two-years master program in Petroleum Geology and Geophysics undertaken at the Department of Geosciences, University of Oslo. The results here-in were derived from an integrated analysis of seismic reflection and potential field data and modeling on the Equatorial Guinea and northern Gabon margins, and supervised by Prof. Jan Inge Faleide and Assoc. Prof. Filippos Tsikalas.

Acknowledgements

First of all, i will like to thank my God and creator for His love and consistency in my life. I will also like to appreciate Dr. Charles O. Ebhohimen and his family for giving me the opportunity to attain this academic status. Many thanks also go to all my siblings and especially to Daniel E. Ebhohimen and Augusta Willem.

My profound gratitude goes to Prof. Jan Inge Faleide and Assoc. Prof. Filippos Tsikalas for their patience, stimulating discussion and critical review of the manuscript. I also owe many thanks to Ph.D. student Olav A. Blaich for his dynamic persuation, constructive criticism, tremendous and technical support to the realisation of this work.

I will also like to commend and thank my dear Julia Mabrey for her kind heart, prayers, patience and understanding during the course of this thesis. Lastly, my appreciation and gratitude goes to Florin Burca (my Romanian friend), Enric Leon and to all my classmates.

University of Oslo, June 2008

Ehimen Ebhohimen Williams

Chapter 1

Introduction

The quest to unravel and better constrain the crustal architecture and related geological processes of South Atlantic margins underscores the importance of this study. This is true considering the huge economic prospect derivable from this region, especially in the petroliferous conjugate margins of West Africa and Brazil (Figure 1.1) (Cameron et al., 1999).

The opening of the South Atlantic Ocean is attributed to the Mesozoic breakup of Gondwana super-continent (Figure 1.1). The breakup led to the splitting of Proterozoic cratonic blocks (e.g. Sao Francisco and Congo cratons) amalgamated during the Late Precambrian when the Brazilian and Pan African orogenies took place in the west and east parts of the cratonic nucleus, respectively (Alkmin, 2004).

The evolution of varied basinal architectures within the South Atlantic conjugate margins took place in response to complex extensional and magmatic regimes initiated during the breakup process. There is a strong rheological control on the overlying Mesozoic-Cenozoic sedimentary basins along the conjugate margins, induced by the underlying different basement terranes which influence the structural evolution of the syn–rift sections (Rosendahl et al., 2005)

There have been ambiguities regarding the exact position of the continent-ocean boundary during plate motion reconstructions and early stages of seafloor spreading in the South Atlantic margins. Firstly, the presence of a magnetic quiet zone from early Aptian to Campanian times is inferred as a major obstacle limiting research into anomalies arising from seafloor spreading at neighboring continental margins (Chang et al., 1992). Secondly, the presence of halokinetic structures (e.g. salt diapirs) along the South Atlantic margins blurs the efficient imaging and effective analysis of the syn-rift features (Katz et al., 2000).

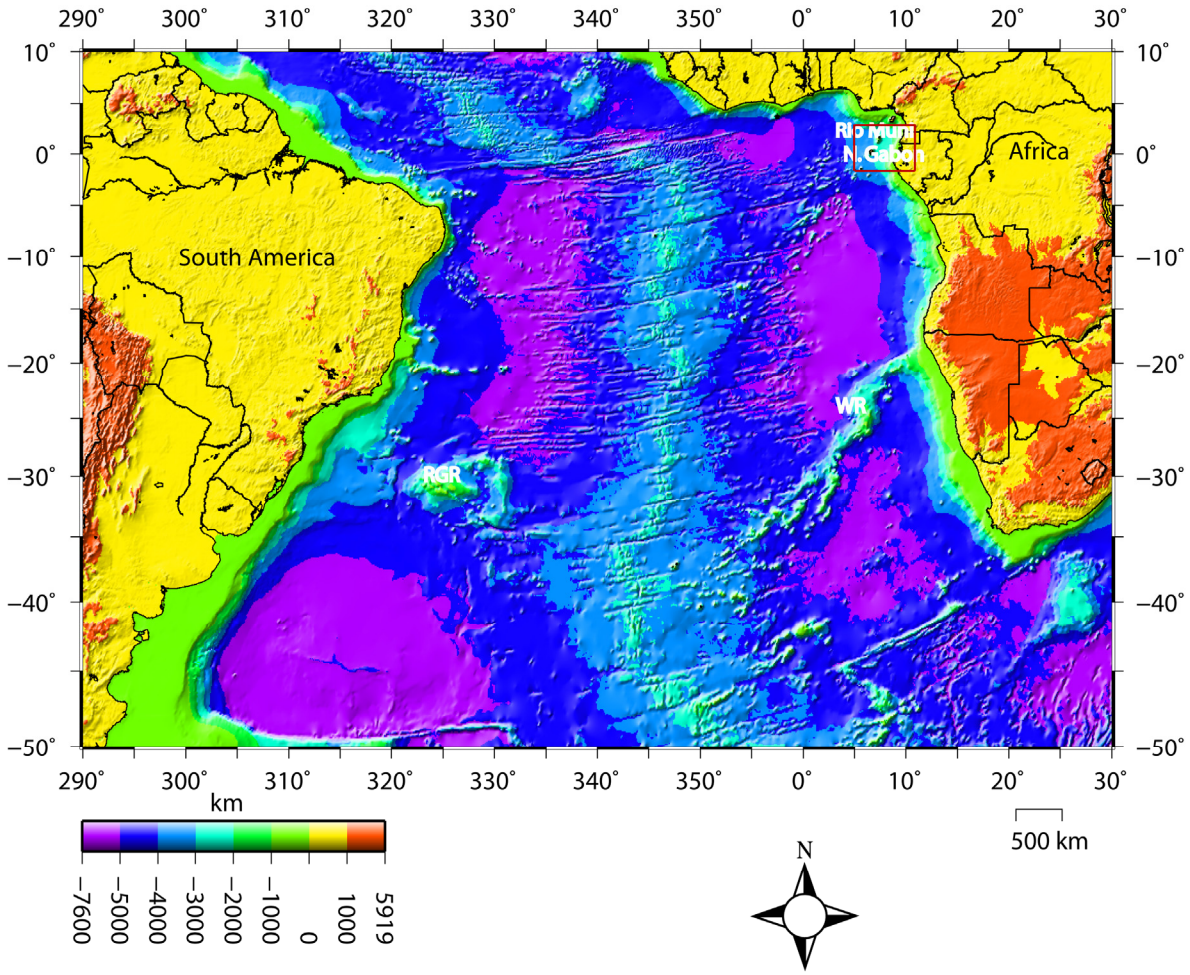

***Figure 1.1**: 1x1 minute elevation grid (GEBCO, General Bathymetric Chart of the Oceans; Jakobsson et al., 2000). Rectangular box outlines the study area. RGR (Rio Grande Rise), WR (Walvis Ridge).*

The bathymetric features in the South Atlantic are fairly symmetric with the central axis being the mid-ocean ridge. This ridge is confined by several structures on both sides of the abyssal plain, the most prominent being the Rio Grande Rise on the South American side and the Walvis Ridge on the African side (Fig. 1.1).

The study area lies between longitude 5ºE–11ºE and latitude 3ºN–3ºS. It stretches from Rio Muni in the NE to central Gabon in the SW (Fig. 1.1). The evolution of these margins is ascribed to the extensional and rifting processes characterizing the South Atlantic development. Fortunately, integration of seismic and potential field data and modeling has advanced our knowledge of the deep crustal structures and fulfills the aims and objectives of this thesis which are to: (1) refine the plate tectonic, rift and shear setting; (2) study and model the crustal structure and refine the

continent-ocean boundary and transition; (3) determine and refine the timing of tectonic events, and the wavelength, amplitude and timing of vertical movements; (4) refine the margin segmentation due to a number of transfer faults systems; (5) within a framework of simplified plate reconstructions, discuss the architecture and development of the conjugate Equatorial Guinea-Gabon and Brazilian margins.

Chapter 2

Geological background

2.1. South Atlantic

The South Atlantic evolved through series of lithospheric stretching and rifting processes which characterized the Mesozoic breakup of the Palaeozoic Gondwana super-continent (e.g. Rabinowitz and LaBrecque, 1979; Mohriak, 2004). The influences of pre-existing (mostly Precambrian) structures have played a major defining role in establishing the line of continental breakup. Therefore, the line of continental separation and the position of the principal failed rifts as presented in Fig. 2.1 were controlled by both the position of boundaries between different ages of basement and the structural grain of the basement (Macdonald et al., 2003).

Moulin et al. (2005) segmented the South Atlantic Ocean between Africa and South America into four parts (Fig. 2.2): (1) the Equatorial segment, located at about 10º N of the Equatorial fracture zones system (Saint-Paul, Vema and Romanche FZ); (2) the central segment between the Romanche FZ and the Walvis-Rio Grande ridges (the segment containing the study area); (3) the southern segment, between the Walvis-Rio Grande ridges and the Falkland-Agulhas FZ and (4) the Falkland segment, south of the Falkland-Agulhas FZ. The initial proposed plate reconstructions for the South Atlantic were characterized by misfits. This was largely due to the failure in acknowledging intraplate deformations. For example in Fig. 2.2, it is impossible to fit the southern segment (between Walvis and Falklands) together with the Equatorial and central segment in the African plate (e.g. Burke and Dewey, 1974; Pindell and Dewey, 1982; Fairhead, 1988; Guiraud and Maurin, 1992), in the South American plate (Curie, 1984) or in both plates (Unternehr et al., 1988; Nürnberg and Müller, 1991; Moulin, 2003).

Distinct structural and depositional evolution characterized these segments. For example, the central segment is known to be dominated by the presence of an Aptian salt cover which is

conspicuously absent south of the Walvis-Rio Grande ridges. On the other hand, seaward dipping reflector sequences (SDRs) are well documented in the southern segment. In addition, dating the early stages of seafloor spreading posed greater challenges and difficulties, ascribed to the absence of well identified magnetic anomalies in the central segments (e.g. Moulin et al., 2005), whereas, in the southern segment M-sequence magnetic anomalies have been recorded (M0-M11, Rabinowitz and LaBrecque, 1979).

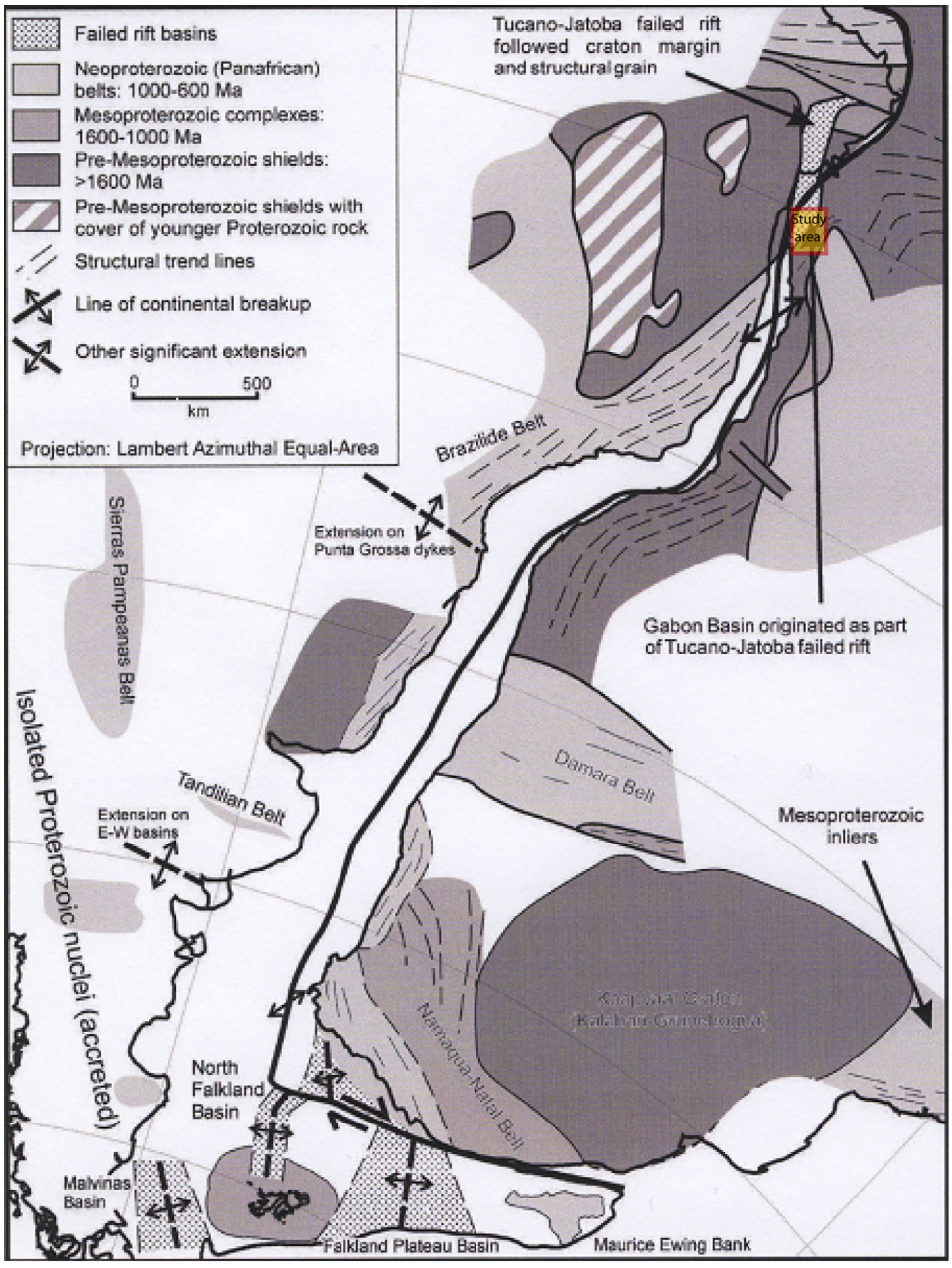

Fig. 2.1 *Structural reconstruction at 135 Ma, immediately prior to South Atlantic opening, illustrating that the line of continental separation and the position of the principal failed rifts in the region were controlled by both*

the positions of boundaries between different ages of basement and the structural grain of the basement (modified from Macdonald et al., 2003). Study area outline in red rectangular box.

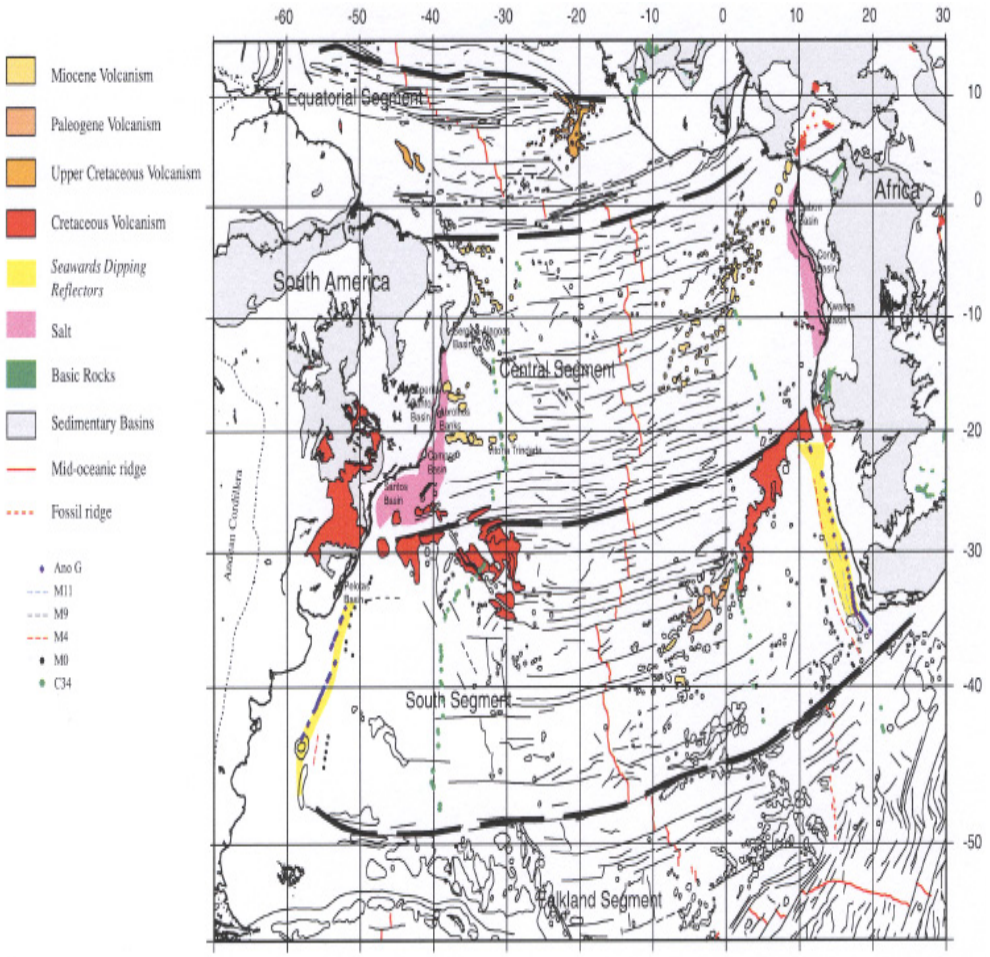

Fig. 2.2: *Regional structural map of the South Atlantic Ocean. Boundaries between the four segments are in broken lines (from Moulin et al., 2005).*

Furthermore, the South Atlantic Ocean is projected to began opening ~130 Ma (Early Cretaceous) in response to extensional regimes which favor the clockwise rotation of the South American plate relative to the fixed African plate (e.g. Rabinowitz and LaBrecque, 1979; Unternehr et al., 1988). The continental rifting sequence between South American and African plates started in the south during the Late Jurassic and propagated to the north during the Early Cretaceous where it finally terminated in the equatorial rift zone during Late Cretaceous times (Fig. 2.3) (e.g. Rabinowitz and LaBrecque, 1979; Ojeda, 1982; Emery and Uchupi, 1984; Scotese et al., 1988; Fairhead, 1988; Popoff, 1988)

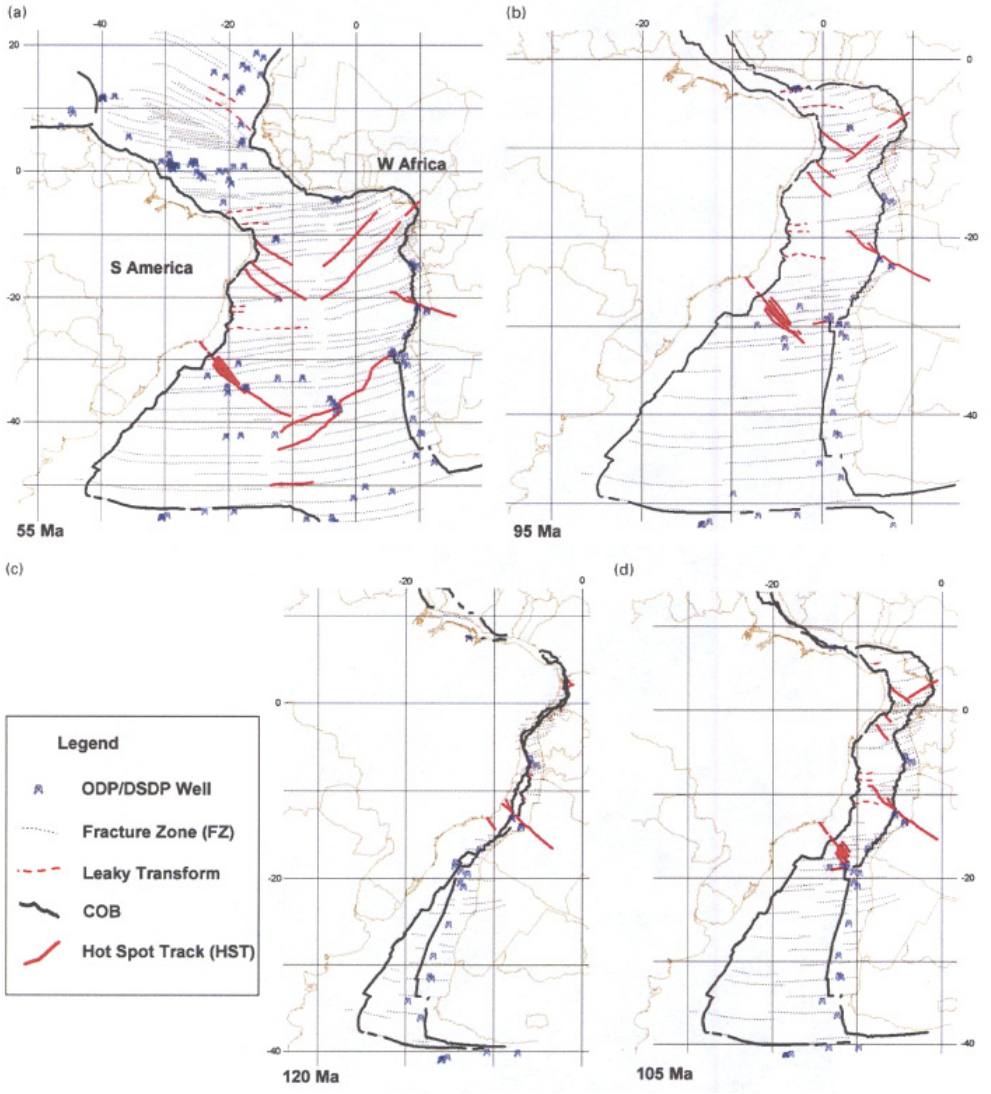

Fig. 2.3: Plate tectonic reconstructions of the South Atlantic (Dickson et al., 2003)

2.1.1 Plate tectonic evolution

The plate tectonic evolution of the South Atlantic can be simplified into three phases: (1) pre-breakup (2) syn-breakup (3) post-breakup.

Pre-breakup (pre-rift) phase

This phase ranged in age from Late Permian to Late Triassic (~255 Ma), when most of Gondwana was enveloped by low-relief basins and swells that preceded the end of the Carboniferous-Permian glaciations, and a change to more arid continental environment in the Triassic. However, this phase was dominated by compressional tectonics which culminated in the formation of part of the Gondwana foreland (e.g. Macdonald et al., 2003).

Breakup (syn-rift) phase

This phase extended from Late Triassic to Early Cretaceous times. Rifting and crustal reorganization were very prominent during this period till the eventual opening of the South Atlantic in the Mesozoic (130 Ma). There have been different geological processes that preceded breakup during Late Triassic to Early Jurassic times (~210-180 Ma). These include: strike-slip faulting, oblique extension and block rotation over the vast south and west part of the Kaapvall Craton (Fig. 2.1) (e.g. Macdonald et al., 2003). Furthermore, the impact of the Karoo plume south of the Kaapvall Craton and the Paraná-Etendeka region is of major importance to the widespread rifting (Macdonald et al., 2003). Oblique extension began in the South Atlantic and led to the NE rotation of the Brazilian microplate, and strike-slip movements along Pernambuco Shear Zone in the northern area of the South Atlantic. This concurrently gave rise to the emergence of transtensional depocentres in Sergipe-Alagoas and Gabon basins, with maximum rift subsidence occurring in the Recôncavo Basin (Milani and Davison, 1988). The linkage between the central and South Atlantic by the latest Aptian was a result of the impact of the Santa Helena Plume which led to the rifting of the Brazilian Equatorial basins and the Benue Trough during late Aptian (Bengtson and Koutsoukos, 1992).

Post-breakup (post-rift) phase

This period is further subdivided into Early post-rift phase (Albian-Cenomanian, mid-Cretaceous) and Later post-rift phase (Cenomanian-Maastrichtian, Late Cretaceous) (Macdonald et al., 2003). The Early post-rift phase is characterized by a change from oblique to margin-normal extension. The rift axis of Recôncavo-Tucano-Jatoba was abandoned and there was continued extension in Sergipe-Alagoas and Gabon basins. Another structural change that occurred during this phase was the cessation of the NE Brazilian microplate rotation, which remained attached to South America. There was also marine linkage of the

Central and South Atlantic, and marine incursion from both north and south. Oceanic basins at this time were in thermal sag phase and transgressed (Macdonald et al., 2003). In the Later post-rift phase, however, the Atlantic was fully open, in a drift stage and its margins were submerged (Fig. 2.3).

2.2 North Gabon-Equatorial Guinea margin

The North Gabon and Equatorial Guinea margin belongs to the West African Atlantic passive margin that developed during the Mesozoic breakup of Africa and South America. This margin is characterized by North Gabon and Rio Muni basins respectively. These basins progressively developed in response to the overall northward opening of the South Atlantic during the latest Jurassic to mid Cretaceous times (e.g. Turner, 1999).

The Gabon sector is made up of three basins: the North Gabon Basin, the South Gabon Basin, and the Interior Basin. The North Gabon Basin is the area of interest for this study and is bounded by Equatorial Guinea in the north and to the south by South Gabon Basin. This basin is described to initially have belonged to the rift system which developed further during the drift period (e.g. Reyre, 1984a). Furthermore, Reyre (1984a) indicated that the North Gabon Basin contains sediments with distinct geological evolution when compared to adjacent basins (e.g. South Gabon Basin).

The Rio Muni (Equatorial Guinea) margin underwent breakup during Late Aptian (ca. 117 Ma; Bradley and Fernandez, 1992). Prior to this time, it was part of the Sergipe-Alagoas basin paired conjugate rift system in NE Brazil. The margin architecture is characterized by stepped normal-faulted segments situated within continental transcurrent fault zones and extending westward into oceanic transform structures (Turner, 1999).

2.2.1 Structural framework

The Congo Craton being very prominent in the study area was once connected to the Sao Francisco Craton in east Brazil. The Congo Craton is considered to be an amalgamation of

Archean geotectonic units that is believed to have been reworked during the Transamazonian cycles (Early Proterozoic) (e.g. Ledru et al., 1989; Bertrand and de Sá, 1990; Teixeira and Figueiredo, 1991). Furthermore, the Proterozoic mobile belts are made up of subservient geotectonic units that accreted to the African plate during the collision of Transamazonian and Pan-African/Braziliano phases (e.g. Torquato and Cordani, 1981; Ledru et al., 1989; Porada, 1989; Bertrand and de Sá, 1990; D' Agrella-Filho et al., 1990; Teixeira and Figueiredo, 1991; de Brito and Cordani, 1991; de Matos, 1992; Chang et al., 1992). The origin of the Pan-African belt has been ascribed to rifting (ca 1.2 Ga) and successive closure and obduction (ca 0.6 Ga) of 2 Ga old high-grade gneisses associated with a younger phase of granitic magmatism, imparting a NE-SW oriented structural fabric in Cameroon and northeastern Brazil (e.g. Torquato and Cordani, 1981; Cahen et al., 1984; Porada, 1989; Ekwueme et al., 1991). Until the eventual breakup of Gondwana in the Mesozoic, there was no substantial record of Paleozoic tectonism for this region. However, Garcia (1991) reported the occurrence of Jurassic continental sediments deposited in the Afro-Brazilian depression, an intracratonic sag basin that propagates over the Gabon and Douala Basins before rifting.

The study margin is characterized by rift structures and subbasins which are separated by ~50-150 km northeast oriented fracture zones and corresponding transfer zones. The nearshore and onshore areas are covered by deep seated lineaments which continue offshore and correlate with the oceanic fracture zones. These lineaments have been referred to as: N'Komi lineament, Breme lineament, Kango lineament (e.g. Davison, 1999), while the fault zones are referred to as: Cape San Juan Fault Zone, Campo Fault Zone (e.g. Turner, 1995). The segmentation of the rift zones in the study area spans in age from Barremian to Aptian, and is younger when compared to the Neocomian phase of rifting for the adjacent South Gabon Basin (e.g. Reyre, 1984a; Teisserenc and Villemin, 1990). This younging in age from south to north has been speculated to be a result of northward rift propagation or ambiguities in sampling or drilling the syn-rift sediments of the North Gabon Basin that has been deeply buried by deltaic sediments from the Ogooue River (e.g. Meyers et al., 1996). Prominent bathymetric features which characterize this margin include: major oceanic fracture zones, transfer fault terrains, elevated islands and seamounts, volcanic chain lines and hotspots (Fig. 2.4). The onshore and offshore geology of the study areas is largely correlative but minor differences exist in their stratigraphic history.

The Gabon Basin lies on a suture zone that is bounded by the ancient Congo and Sao Paulo cratons. This suture is projected along the southwest side of the Congo craton as the Mayumbe Range fold zone, dated 1300-1100 Ma (e.g. Bessoles, 1977; Fig. 2.5). An upper Precambrian basin (Nyanga syncline) which has undergone slight deformation during the Panafrican tectonic event (~650 Ma) occupied the area. The presence of this suture zone which defines a probable weakness may have favored the rift evolution which subsequently developed into the South Atlantic Ocean.

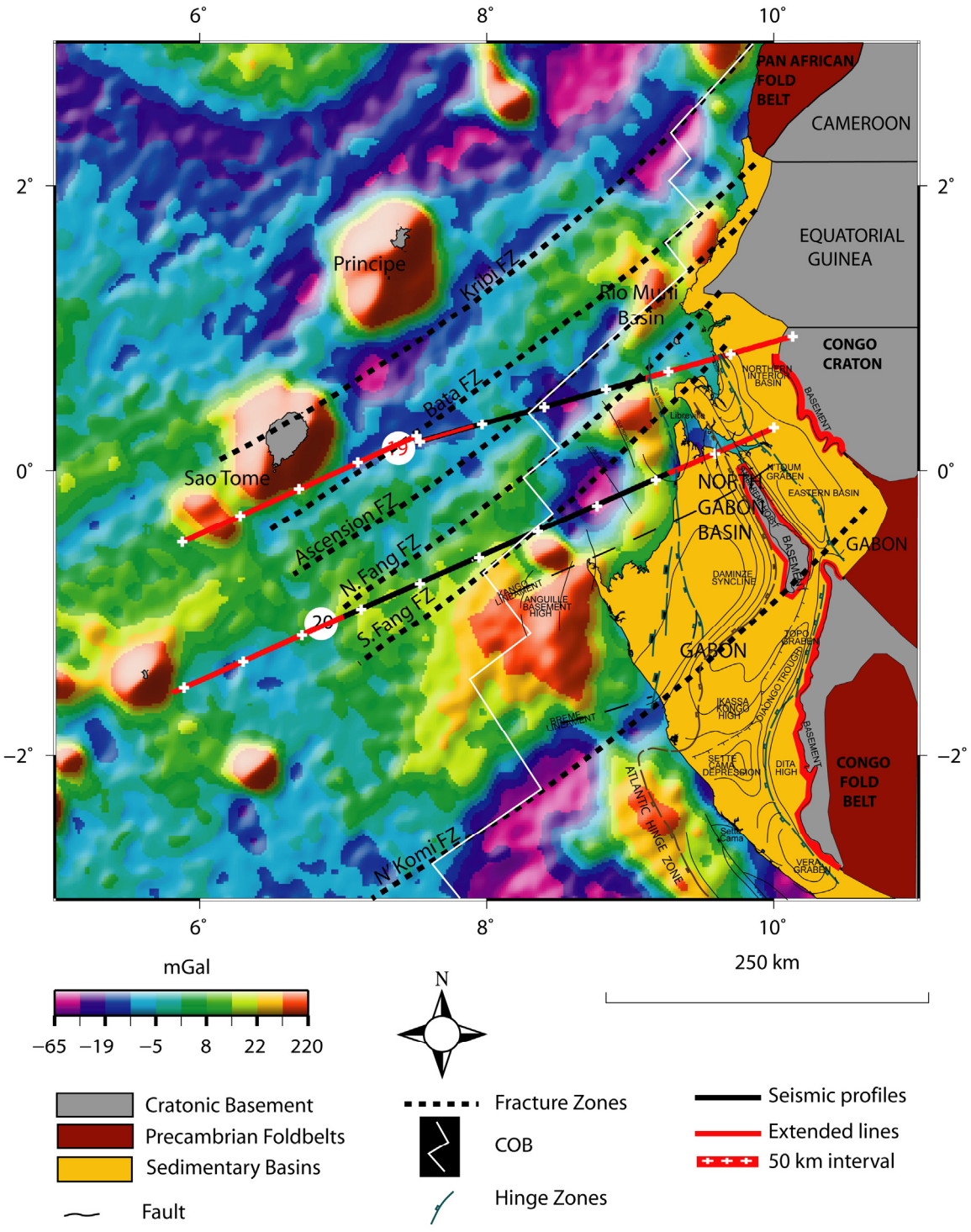

***Fig. 2.4**: Structural map of the study area imposed on 1x1 minute gridded satellite-radar-altimeter free-air gravity anomaly field (Sandwell and Smith, 1997; version 10.1). Geological structures modified after Davison, (1999), Meyers et al.(1996) and Dailly, (2000).*

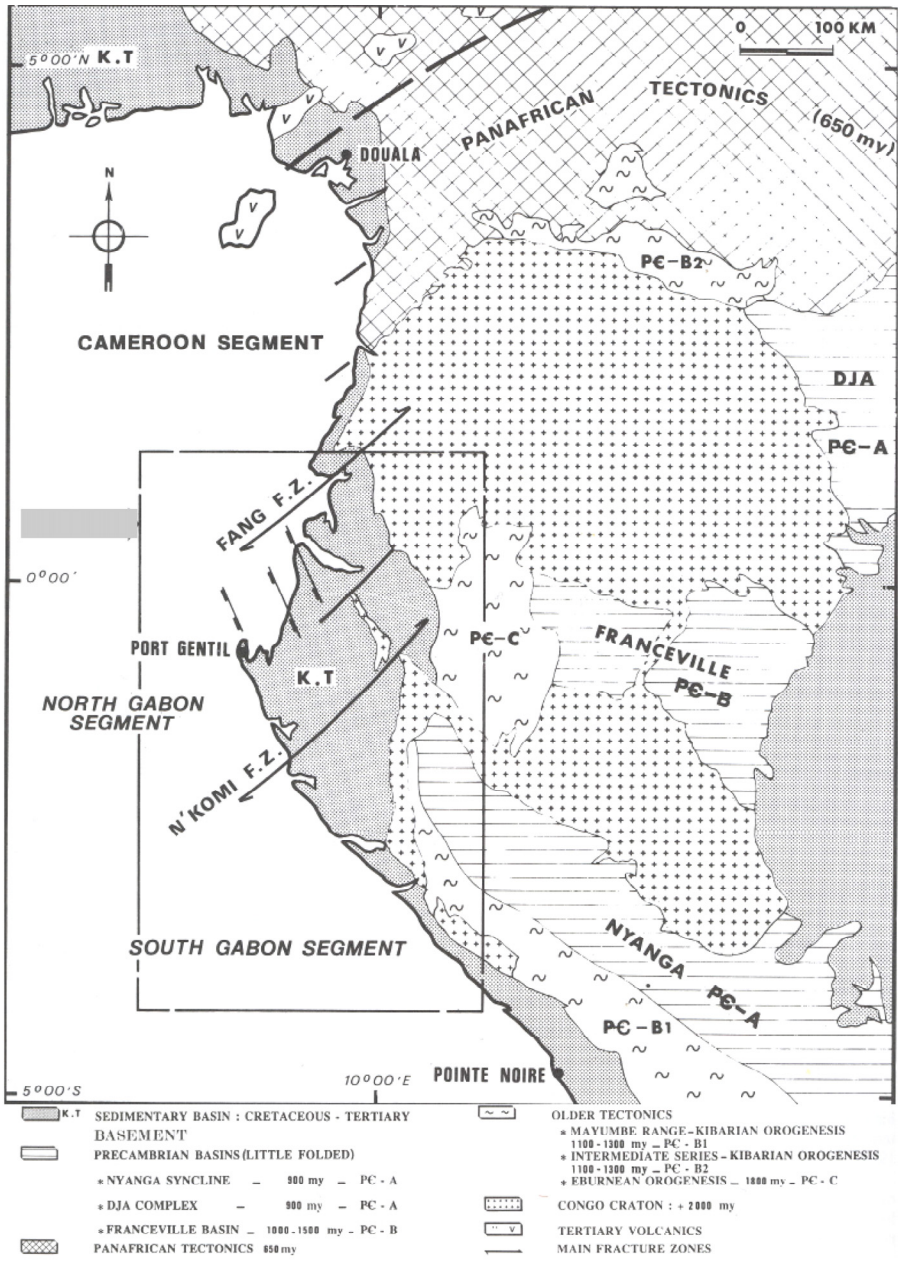

Fig. 2.5: *Schematic geological features of Gabon basin (Teisserenc and Villemin, 1990).*

The North Gabon Basin is separated from the adjacent South Gabon Basin by the N'Komi fracture zone, a wrench fault system trending N60 ^{o}E (Teisserenc and Villemin, 1990). Furthermore, the rift period in the North Gabon Basin is younger than in the South Gabon Basin, as evidenced by the draping of fault blocks in the north which is mid-Aptian in age, as opposed to late Barremian in the south (Teisserenc and Villemin, 1990). In the offshore areas northwest of the N'Komi fault zone, a thick depocenter of Upper Cretaceous to Tertiary sediments on salt resulted in a complex development of diapiric structures. However, a third

basin situated northeast of the North Gabon Basin is the Interior Basin, which formed during the early Neocomian to Albian rifting but did not develop after that time.

The Rio Muni Basin is isolated from the North Gabon Basin to the south, the Douala Basin of Cameroon to the north, and bounded by prominent fault zones (e.g. Campo and Cape San Juan) (Turner, 1995). These fault zones are made up of the continental extensions of deep-seated oceanic fracture zones which compartmentalize the Atlantic margin basin system along its length (Turner, 1995). The geometry of the basin is confined by two conspicuous transcurrent fault zones ~100 km apart that meet the coast at approximately 30º (Turner, 1999). The Bata Fracture Zone separates Rio Muni from Douala Basin in Cameroon to the north, while to the south the North and South Fang fracture zones border the Rio Muni margin from North Gabon (Fig. 2.4). However, the Rio Muni margin is postulated to be directly intersected by the Ascension Fracture Zone, a 200 km long transform faulted boundary which has been described as one of the major oceanic fracture zones and the site of whole lithosphere failure (Burke, 1969; Rosendahl and Groschel-Becker, 1999).

2.2.2 Geological evolution and stratigraphy

The geological evolution of these basins has been a source of debate. Several authors have argued that the mechanism leading to the formation of these basins is related to that responsible for the east Brazilian margin. The studies of Ussami et al. (1986) and de Matos (1992), proposed a simple-shear mode for the early rifting history of these basins. They connected R-T-J (Reconcavo, Tucano and Jatoba) with NG-D-SA (Northern Gabon, Douala; and Sergipe Alagoas) rift branches along low-angle detachments within the lower crust. Ussami et al. (1986) argued that there is no shallowing of the mantle below the Tucano Graben which is within the R-T-J rift branch. They linked the formation of Tucano and Jatoba grabens to NG-D-SA rift branch and argued that their formation were related to extension along an east-dipping detachment fault. Milani and Davison (1988) in their study disagreed with the concept of Ussami et al. (1986). They argued that there is shallowing of the mantle below the Tucano and Jatoba basins and therefore preferred a separate rift system. However, Castro (1987) in his study suggested a paired simple-shear mechanism for these rift branches. He based his argument on the location of the rift basin being over east-dipping detachments that flatten into the lower crust and then step down to Moho. Davison (1988) further argued

that such crustal connection involving these basins as proposed by other authors is very unlikely because their opening direction lies at high-angle to each other and separated by a wide area of non-rifted continental crust (i.e. East Brazilian microplate).

Stratigraphically the development of North Gabon and Equatorial Guinea margin is best described in a simplified order of pre-rift, syn-rift, Early drift and Late drift (i.e. both Early and Late drift sequences form the post-rift sequence).

Pre-rift sequence

The pre-rift sequences are best exposed along the east flank of the Interior Basin in North Gabon. They are made up of continental, fluviatile, and lacustrine deposits. This sequence extends through Upper Carboniferous, Permian, and Triassic-Jurassic times. The upper Carboniferous (e.g. Nkhom Formation) consists of glacial deposits: tillites and thinly laminated black shales. Permian (e.g. Agoula Formation) constituents are made up of continental sediments such as: conglomerate, bituminous black shale, phosphatic deposits, lacustrine dolomite, anhydrite and anhydritic limestone, culminating in shale and sandstone. Lastly, Triassic-Jurassic (e.g. Mvone Formation) constituents are mostly fluviatile sediments such as: sandstone and red to violet shale in the upper part (Teisserenc and Villemin, 1990).

Syn-rift sequence

The syn-rift sequences of these basins (i.e. North Gabon and Rio Muni) span from late Barremian-middle Aptian times. According to Teisserenc and Villemin (1990), the N'Toum Formation is the oldest and was deposited in a lacustrine environment as fan-delta turbidites, made up of coarse- to medium-grained sandstone with rock fragments which are poorly sorted and cemented by micaceous shale. Succeeding the N'Toum is the Lower Aptian Coniquet Formation, made up of well differentiated clastics; fine- to medium-grained sandstone, commonly feldspathic, micaceous, and shaly, and in most places cemented by carbonates or silica. Coarse- to very coarse-grained, poorly sorted sandstones are found locally near the edge of the basin. Occurrence of silty shale and organic laminated shale abound locally in the southern part of the basin. Their depositional environments are representative of continental to

lacustrine which vary from fluvial through littoral sediments, delta front, and fan delta to basinal turbidites.

In addition, Teisserenc and Villemin (1990) argued that there is a transitional phase (Aptian-Albian) in these basins that are characterized by reactivation of syn-rift fault zones and a change towards marine conditions. In the North Gabon Basin, this phase is represented by the Como Formation and it is characterized by mixtures of coarse to very coarse-grained sandstone, fine to medium-grained sandstone, siltstone, and laminated, organic rich, carbonaceous, and pyrite bearing shale. The Como Formation correlates with the Gamba Formation of the South Gabon Basin. In the Rio Muni Basin, this phase consists of a two part coarsening-upward succession that is made up of two sub-sequences: the saliferous sequence and the turbidite sequence (Turner, 1995).

Early drift sequence

This sequence of Albian-Cenomanian age consists of successions of allochthonous shelf carbonates that have been emplaced in a deep, basinal setting by post-depositional, gravity driven nappes (Turner, 1995). Lithologically, the early drift sequence is characterized by repetitive cycles of oolitic limestones and calcarenite arranged in a shallowing-upward sequence, which record the earliest marine flooding of the basin (e.g. Turner, 1995).

Late drift sequence

This sequence is characterized by post-Cenomanian stratigraphy which comprises a shoreward tapering prism of clastics containing open-marine foraminifera and dinoflagellate fauna. The sequence lies above the drift unconformity, a sharply erosive unconformity that truncates the faulted and folded early drift sequence with marked angularity. The drift unconformity is interpreted as recording major uplift in response to the thermal re-equilibration of the crust and mantle at the close of continental rifting and extension. The drift unconformity signals the onset of oceanic crust production and earliest Atlantic opening in this part of the West African margin basin system (e.g. Turner, 1995).

This phase characterized by the opening of the ocean basin during the Upper Aptian-Turonian-Holocene led to the accumulation of progradational marine sediments. Widespread distribution of facies which ranges from continental through carbonate platform and/or siliciclastic platform to basinal environment has been recorded during this phase. The main progradational trend for sediment in this phase is westward, and the depocenter is situated in Port Gentil area with a total thickness of about 3-4 km (Teisserenc and Villemin, 1990).

Salt tectonics characterized the development of the post-rift sedimentary sequence. Possibly, the deposition of salt occurred in the proto-South Atlantic basin during Aptian to Albian times. The undisturbed salt layer onshore and beneath the shelf is 1 km thick (e.g. Brink, 1974; Lehner and de Ruiter, 1977; de Ruiter, 1979; Reyre, 1984a; Teisserenc and Villemin, 1989), however, west of the shelf break, its thickness is doubtful. Salt mobilization has been attributed to sediment loading in Late Cretaceous, leading to the formation of salt anticlines, piercement diapirs and turtle backs (e.g. Leyden et al., 1972; Brink, 1974; Reyre, 1984a; Teisserenc and Villemin, 1989). The presence of salt sink-holes is abundant in areas where the top of the salt dome is just beneath the shelf and onshore basins are susceptible to dissolution from surface waters (e.g. Brink, 1974; Teisserenc and Villemin, 1989). Reactivated faults consequent upon the Late Cretaceous tectonism (Santonian to Coniacian) cut across the Aptian salt horizon in the North Gabon Basin (e.g. Teisserenc and Villemin, 1989).

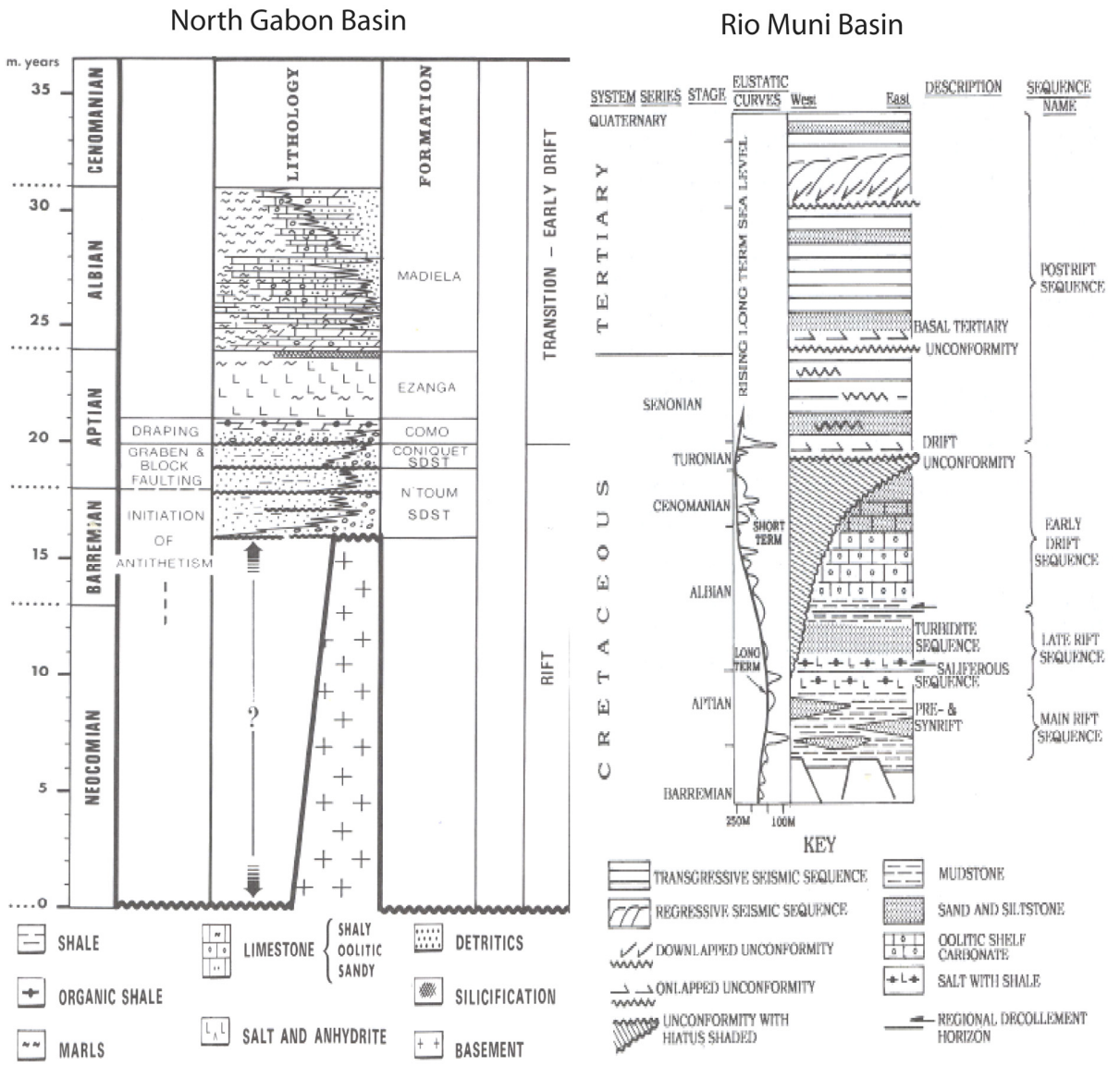

Fig. 2.6: *Stratigraphic column showing rift formations in the North Gabon and Rio Muni basins (Teisserenc and Villemin, 1990; Turner, 1995).*

Chapter 3

Data

The data used for this study were mainly geophysical and geological resources which included: published multi-channel seismic (MCS) reflection profiles (Fig. 3.1), academic ship-tracks (Fig. 3.2) which were employed in extracting magnetic, gravity and bathymetric data derived from LDEO (Lamont-Doherty Earth Obeservatory, Columbia University, USA), 1x1 minute gridded satellite-radar-altimeter free-air gravity anomalies (Sandwell and Smith, 1997; version 10.1); 2x2 minute global free-air gravity data from ERS-1 and GEOSAT satellite altimetry (KMS; Andersen and Knudsen, 1998); 1x1' minute elevation grid (GEBCO, General Bathymetric Chart of the Oceans; Jakobsson, M., 2000); and additional magnetic data from EOS (Earth Observing System, NASA, USA). Other input sources are: line drawings from published seismic profiles; Bouguer-corrected gravity anomalies extracted from gridded data; 5x5 minute grid of the total sediment thickness of the World's Oceans and Marginal Seas (NOAA; National Oceanic and Atmospheric Administration, USA); and along track and grid single-channel seismic reflection profiles.

3.1 Margin setting

The margin setting identifying the locations of the published profiles, the coastline and onshore relief, academic ship-tracks of the study area and potential field grids are displayed in the basemaps created with GMT software package (Generic Mapping Tools; Wessel and Smith, 1998) at a Mercator projection. GMT is an academic, interactive software package used in the editing, reduction, management, and visualization of geophysical data. GMT was also used to extract bathymetric, gravity and magnetic data along academic ship-tracks.

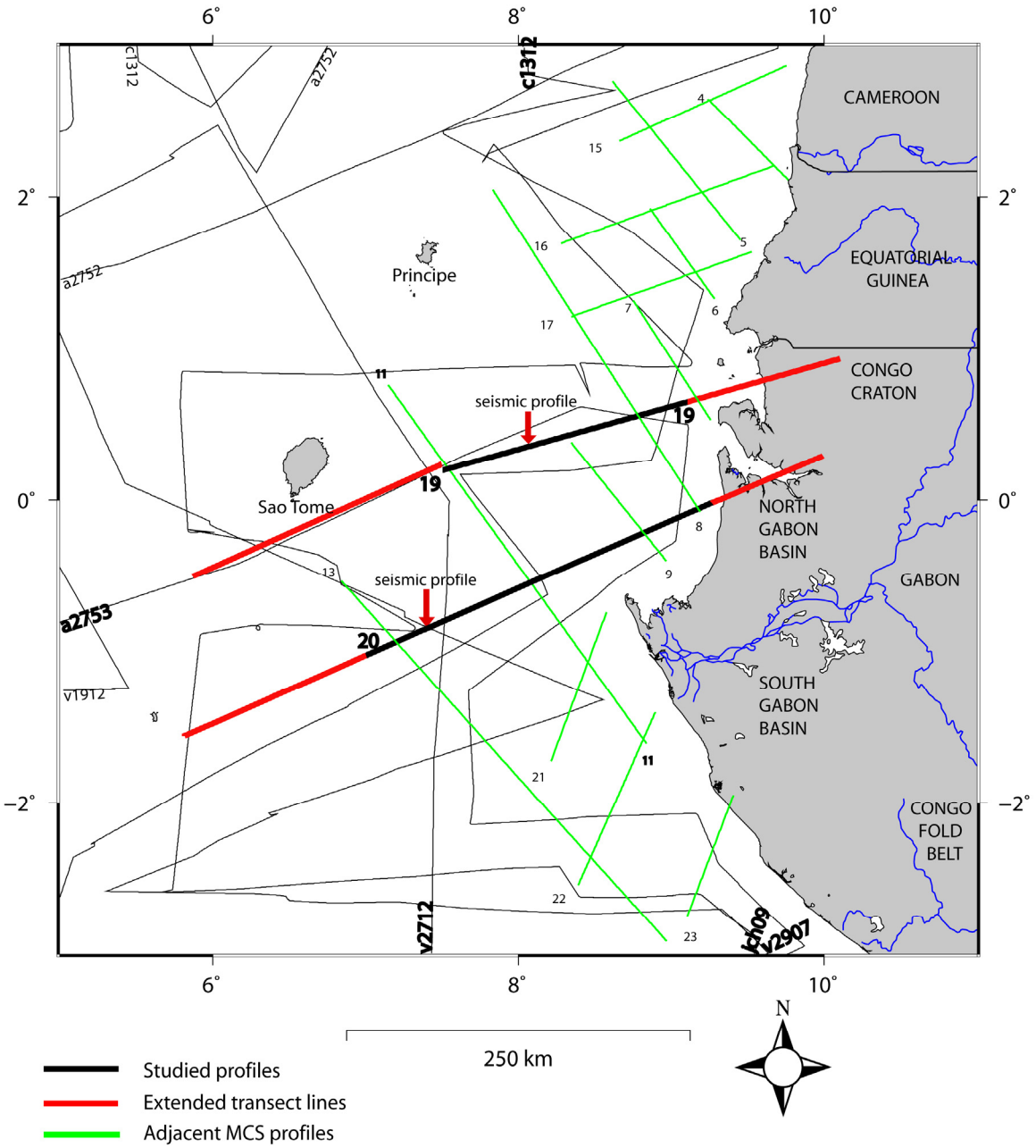

Fig. 3.1: *Location of published seismic reflection profiles along the Gabon margin (after Rosendahl and Groschel-Becker, 2000), constructed crustal transects (bold), extended lines, and selected academic (LDEO) ship-tracks.*

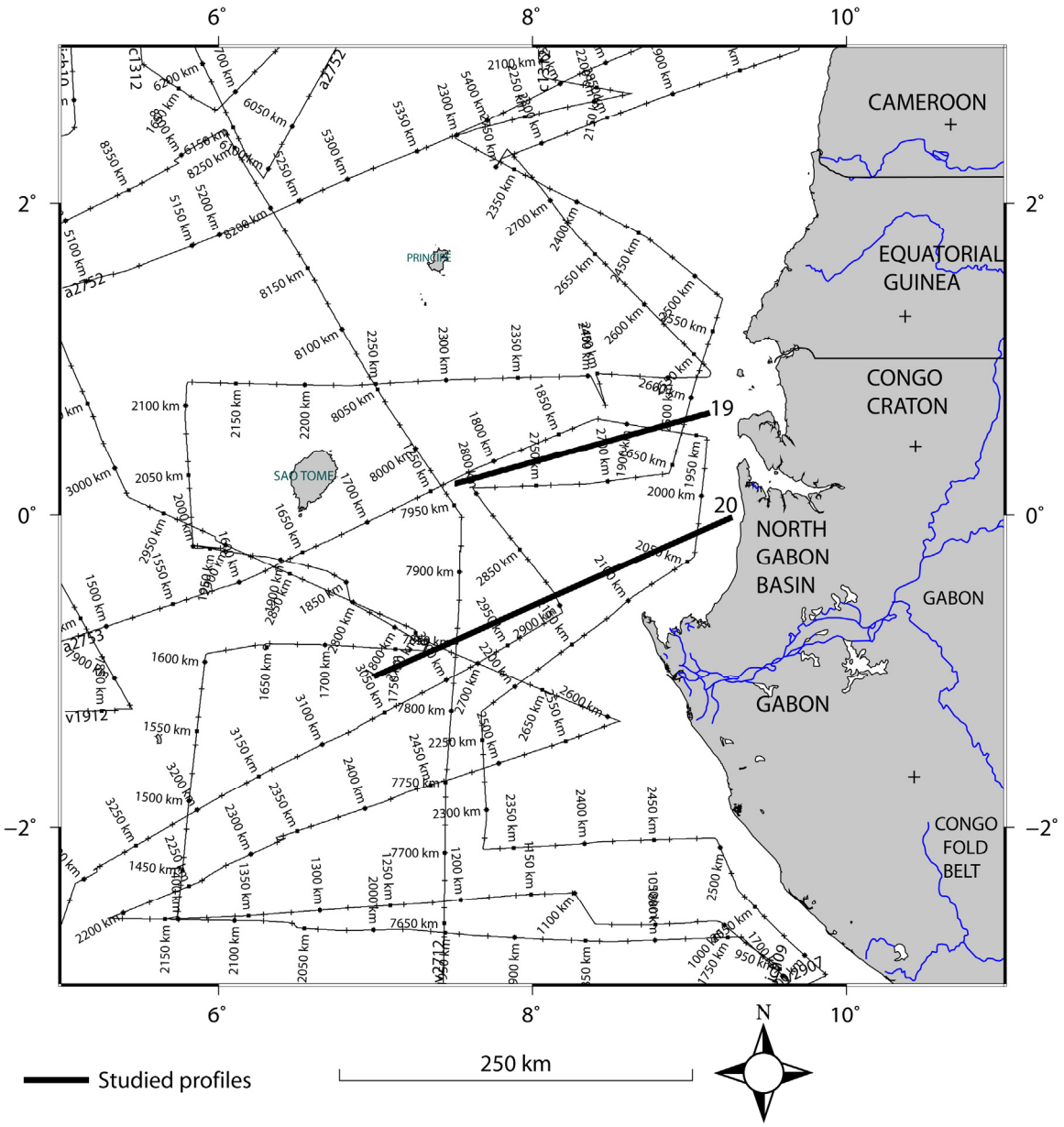

***Fig. 3.2**: Location of seismic reflection profiles and LDEO academic ship-tracks of the study area*

In this thesis, two published seismic profiles in two way travel time (twt) were taken from Rosendahl et al. (2005). The locations of the published profiles and other adjacent profiles on the West African margin have been indicated (Fig. 3.1).

The effectiveness of potential field data complementing seismic interpretation in this study can not be overemphasized. It has proven to be a powerful tool for: deep crustal and regional constraints of the margins, simulating the structural and morphological trend of the crust, and depicting the Moho relief. The result from applying this kind of integrated approach to basin

modeling is very realistic. It provides good constraints for better resolving and refining studies related to the COB/COT (continent-ocean boundary/transition) and defining basinal architecture, which is imperative especially in exploring and evaluating frontier areas in ultra-deep waters.

Potential field data can be acquired along ship tracks situated parallel to transect lines and from gridded data. Obviously, data acquired along ship tracks are more detailed and representative of the subsurface morphology. This is primarily due to proximity as compared to gridded data which utilizes all available regional data inherent with varied averaging and filtering techniques, and in addition is taken from satellites. The implication in using gridded data is in the quality of its resolution which might obscure tiny details. An example of this difference is shown in the along track and grid diagrams in chapter 4. However, in this study, along grid method was chosen to extract bathymetric and potential field data, primarily because it is more representative with the extended lines, while along academic ship-track (monitored by LDEO) 'a2753 and c1312'for both Transects 19 and 20 do not cover the entire extended profiles (Fig. 3.1).

3.1.1 Bathymetry

The Bathymetry/elevation basemap for the study area (Fig. 3.3) was derived from ship-borne tracks and gridded data covering the modeled profiles. However, for this study, the bathymetric input was extracted from the 1x1 minute GEBCO elevation grid. The importance of this data is in defining the morphological features inherent within the study area, the width of the continental shelf and as input to generate the Bouguer-corrected gravity anomaly map. Structural trends such as oceanic fracture zones and shear related structures are not conspicuous from this bathymetric basemap as they probably could have been blurred by sediments. However, morphological features were observed along the northwestern areas of this study, e.g. local elevations in the ultra deep-water provinces. The presence of these elevated bodies have been interpreted to be oceanic basement highs (seamounts) and corroborated by other geophysical basemaps in this study. The continental platform and width in accordance with the oblique nature of this margin is shallower and narrower along Equatorial Guinea but becomes progressively wider along the Gabon sector. The location of the proposed COB (continent-ocean boundary) of Meyers et al. (1996) is closest to the

continental margins of Equatorial Guinea (Rio Muni basin) and progressively farther along the Gabon margin.

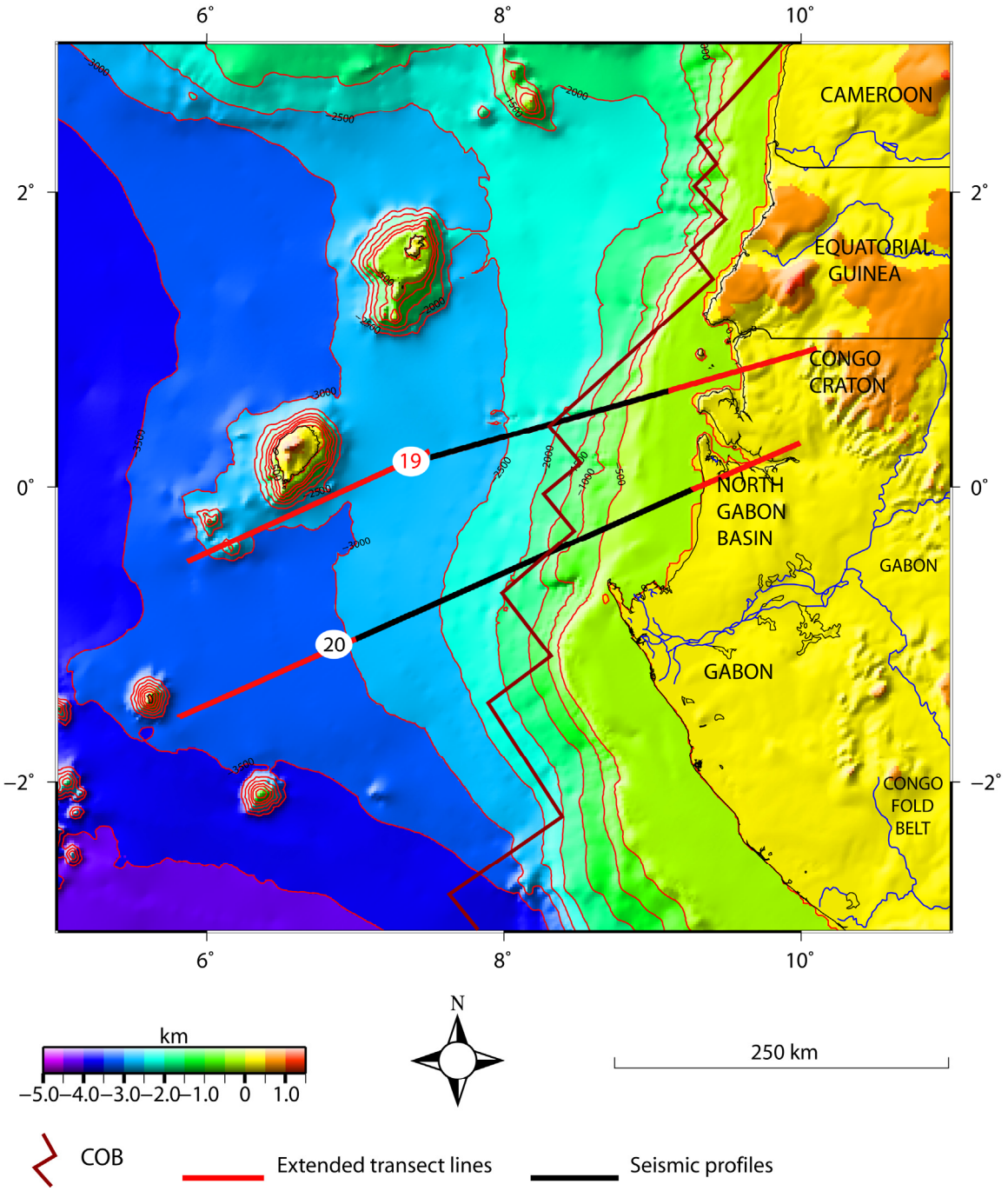

Fig. 3.3: *1x1 elevation grid (GEBCO, General Bathymetric Chart of the Oceans; Jakobsson et al., 2000) of the study area. COB interpreted by Meyers et al. (1996).*

3.1.2 Gravity

Gravity anomaly reflects lateral changes in surface and subsurface bodies and structures as a function of density. Where the numeric value of gravity anomaly is high, it indicates presence of denser bodies or structures and where there is a low, it indicates the presence of less dense bodies or structures. This scenario is best described in a faulted terrain where the horst exhibits excessive lateral mass which translates into high densities as compared to the graben filled with sediments having less mass and therefore lower densities.

The gravity data for the study area were extracted from ship-borne tracks and gridded profiles. The 2x2 minute gridded free-air gravity, based on satellite-radar-altimeter (KMS-grid, Andersen and Knudsen, 1998; version 10.1) was used to generate the gravity basemap for the study area (Fig. 3.4), to define an initial Moho relief and for gravity modeling. The gridded gravity basemap was further used as input for the Bouguer-corrected gravity anomaly. The gravity map clearly highlights larger masses in areas with corresponding high amplitude, situated along oceanic fracture zones, submarine volcanic highs (e.g. seamounts), which are orientated in a NE – SW direction. The presence of these structures and volcanic ridges, according to Gomes et al. (1997) is probably related to the occurrence of the oceanic fracture zones. In the incipient phases of sea floor spreading and drifting, magmatic leakage(s) from the mantle is highly possible along oceanic fracture zones which could develop into lower crustal bodies or extrude as seamounts. The expression of anomalously high amplitudes observed adjacent to the continental margin of Gabon is probably induced by 3D edge-effect, lithified sedimentary basin or presence of intrusives.

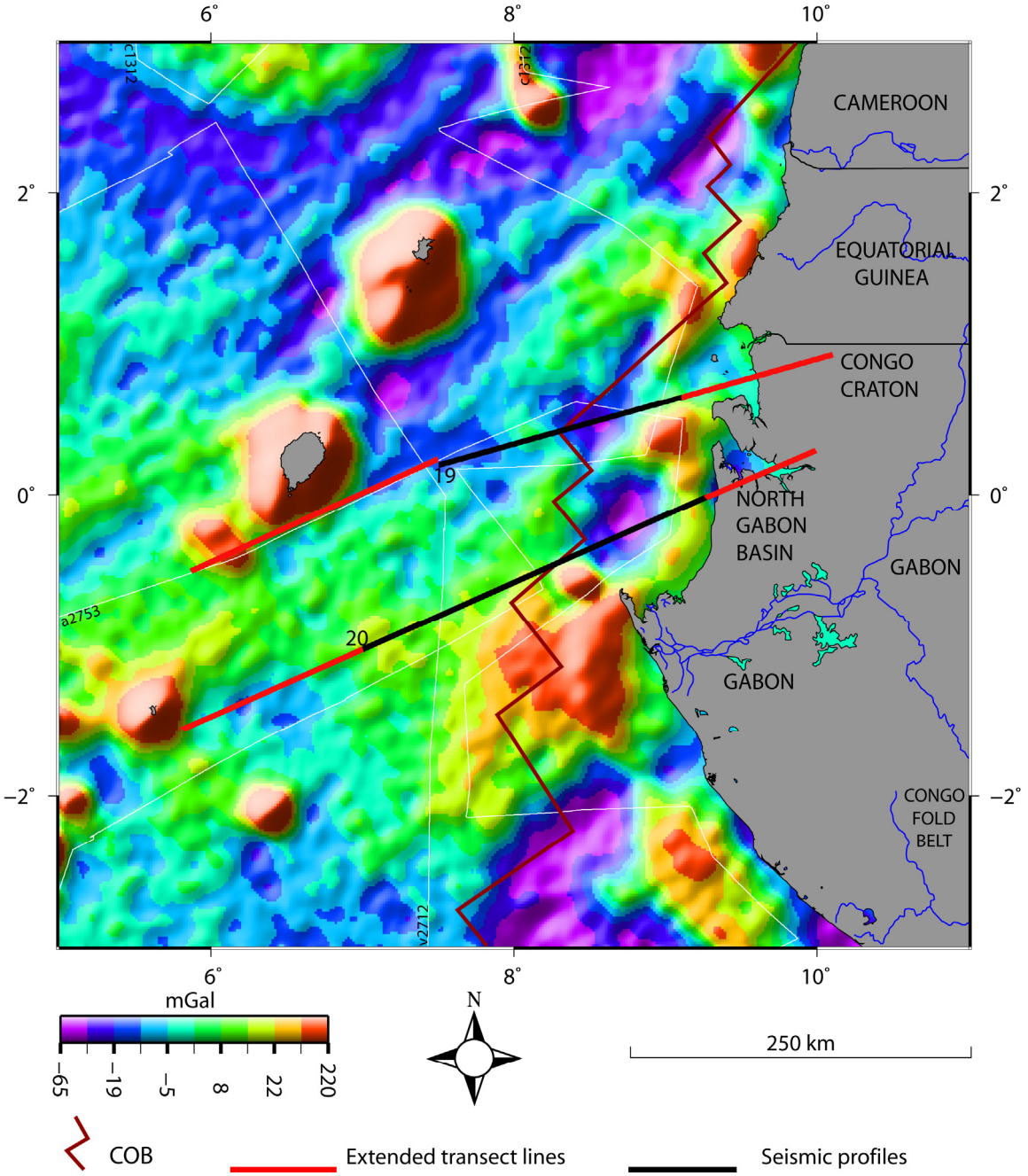

Fig. 3.4: *2x2' minute satellite-radar-altimeter free-air gravity grid (KMS-grid, Andersen and Knudsen, 1998). COB interpreted by Meyers et al. (1996).*

The Bouguer-corrected gravity response was introduced using GMT software. This was necessary in order to arrive at a more realistic trend of the subsurface devoid of the overwhelming influence of variations in gravity anomaly effect of the bathymetric relief,

thereby eliminating the strong lateral density variation between the water-layer and lithological units (e.g. top sediment/basement). Bouguer-corrected data enhances better imaging of the basement and Moho configuration (Fig. 3.5).

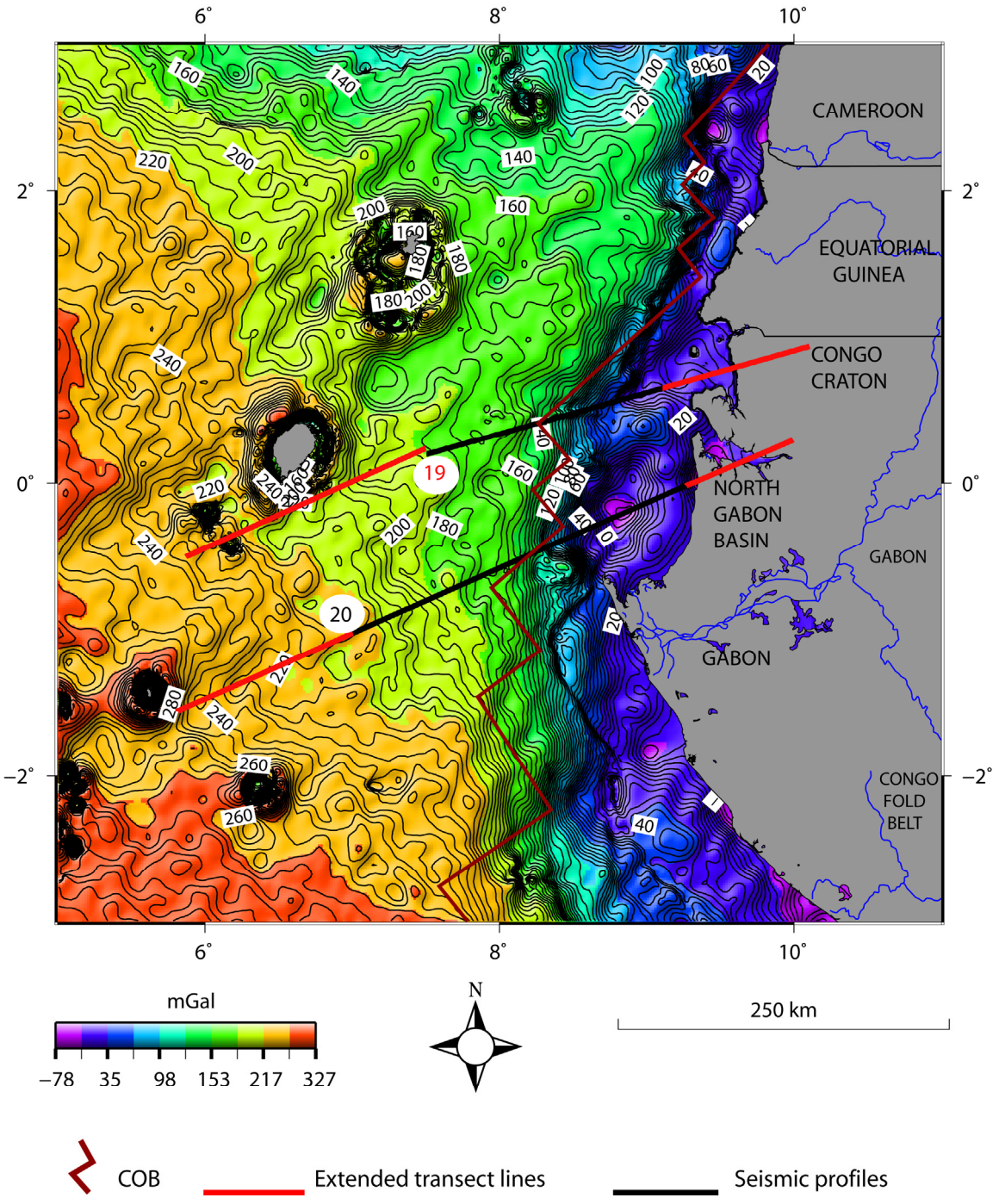

Fig. 3.5: *Bouguer-corrected gravity anomaly grid. COB interpreted by Meyers et al. (1996).*

3.1.3 Magnetic

Magmatic susceptibility is a function of the concentration, orientation, latitude, geometry of the source body and the magnetic properties. Rocks with high content of iron bearing minerals (e.g. magnetite) and beneath the Curie temperature will be more prone to remanent magnetisation irrespective of the source. Alan and Khan (2000) proposed that igneous rocks are prone to higher magnetic susceptibility than other rock types. The usefulness in applying this geophysical parameter in geology can be seen in delineating stratigraphical horizons, characterization of magmatic intrusions, configuring the depth to/and composition of basement and determining boundaries (e.g. COB / COT).

Most magnetic data maps display a chaotic style for magnetic anomaly which makes it rather complex to decipher structural features (Figs. 3.6a and 3.6b). In this study, magnetic data was extracted both from academic ship-tracks (Fig. 3.6a; LDEO) and from grid (i.e. EOS; Fig. 3.6b). As earlier stated, data from LDEO is much more representative as a function of proximity than grid obtained data (EOS). However, the anomalous features are more or less similar (cf. Figs. 3.6a and 3.6b). Where the magnetic trend shows high values/numbers and narrow/short amplitude will conform to proximal basement areas and intrusives, but where the trend is reversed and records low magnetic values/numbers and broader/longer amplitudes will correspond to sedimentary terrains.

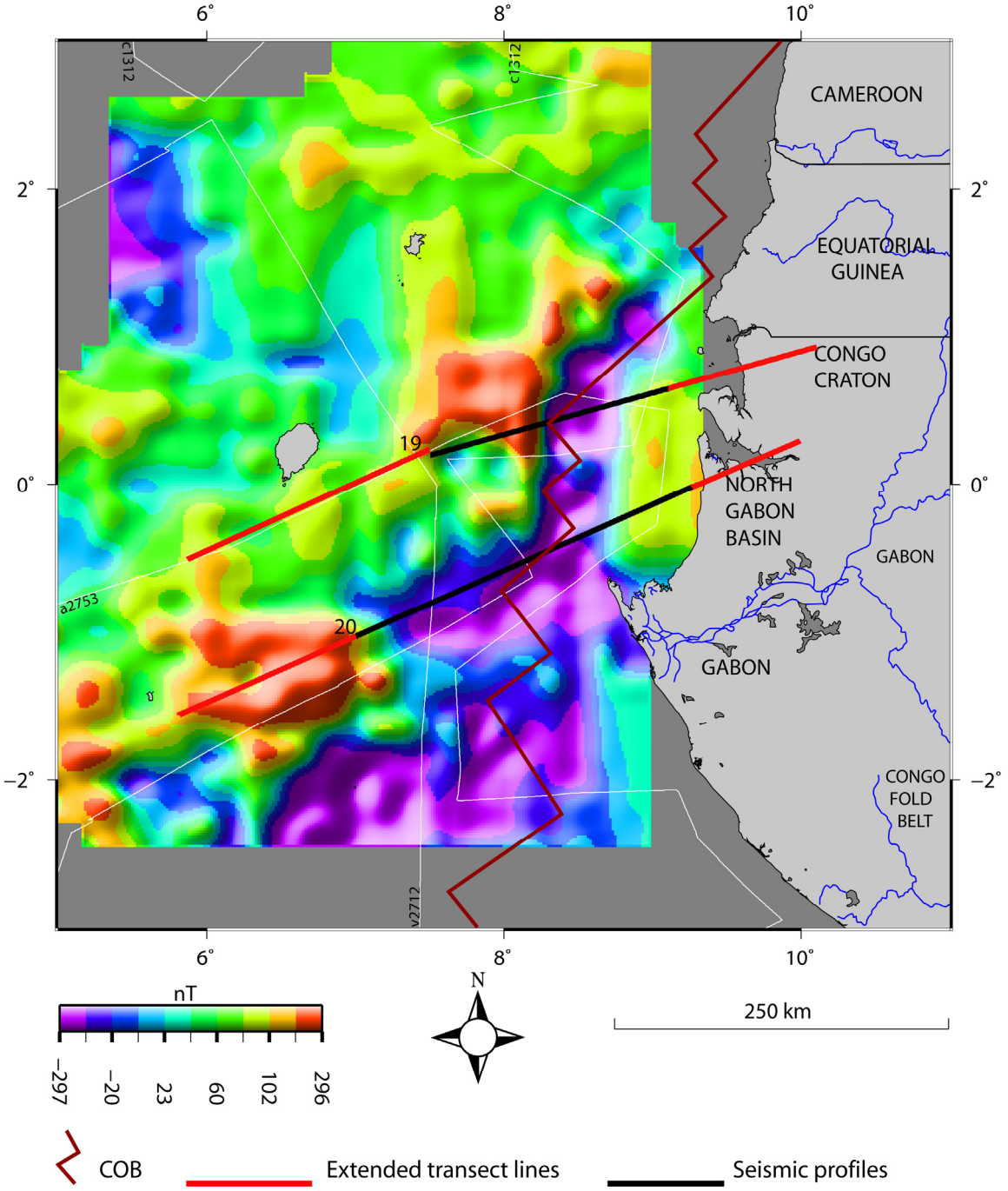

Fig. 3.6a: *Magnetic anomaly map of the study area extracted from LDEO (Lamont-Doherty Earth Observatory, Columbia Univ. USA) ship-tracks. COB interpreted by Meyers et al. (1996).*

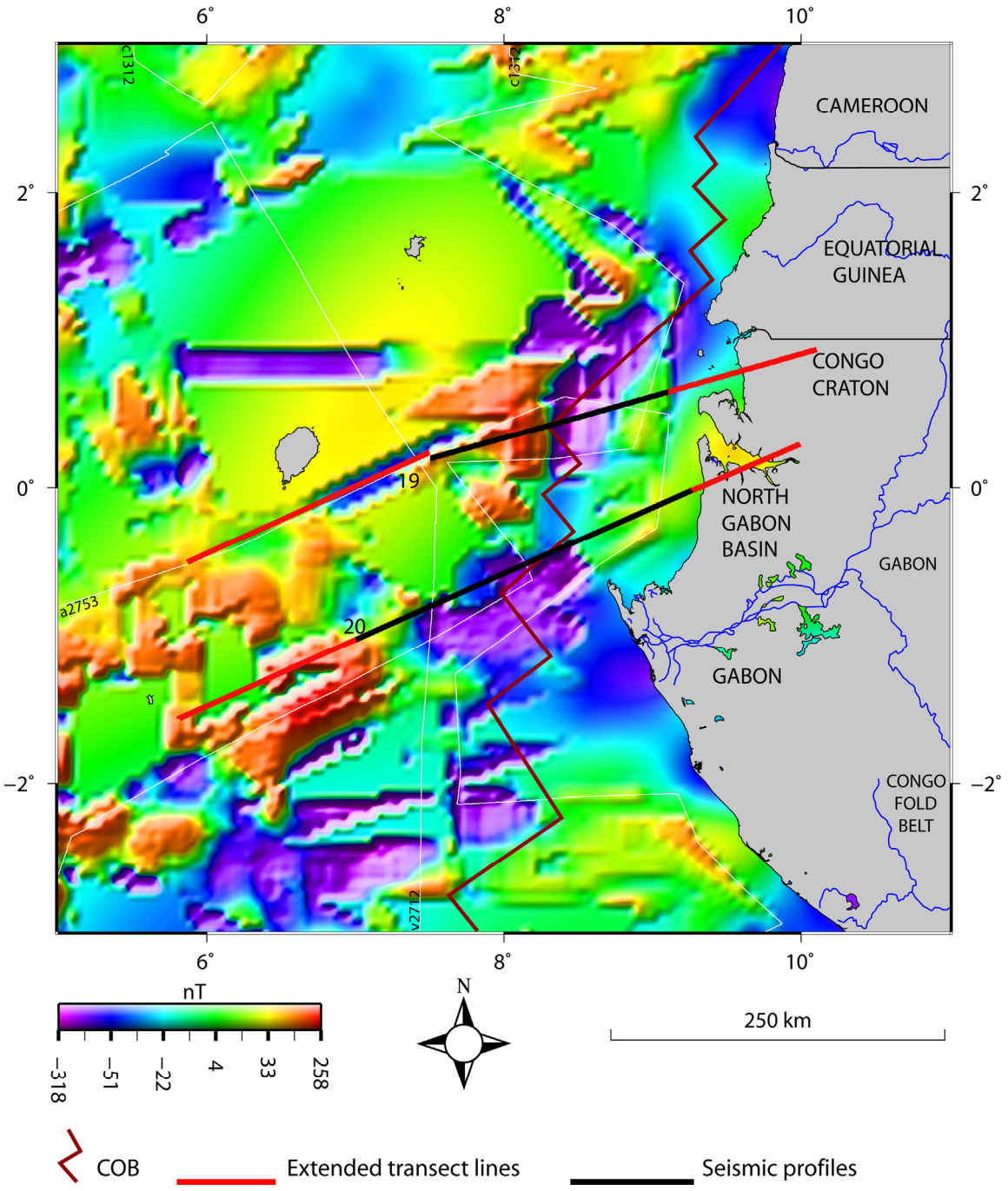

***Fig. 3.6b**: Magnetic anomaly map of the study area, extracted from EOS (Earth Observing System, NASA, USA) grids. COB interpreted by Meyers et al. (1996).*

3.1.4 Sediment thickness

The sediment thickness map (Fig. 3.7) for the study area was derived from 5x5 grid of total sediment thickness of the World's Oceans and Marginal Seas (NOAA, National Oceanic and Atmospheric Administration, USA). The sediment thickness data represents offshore isopachs for the interval between the sea bottom and the acoustic basement. These data reveal that higher sediment packages are prominent adjacent to the continental margin and lower packages within the vicinity of the oceanic crust. This distribution of sedimentary packages is in conformity with the morphology of the continental and oceanic setting. This means that sedimentary units are favorably accommodated within continental margins as compared to oceanic basement.

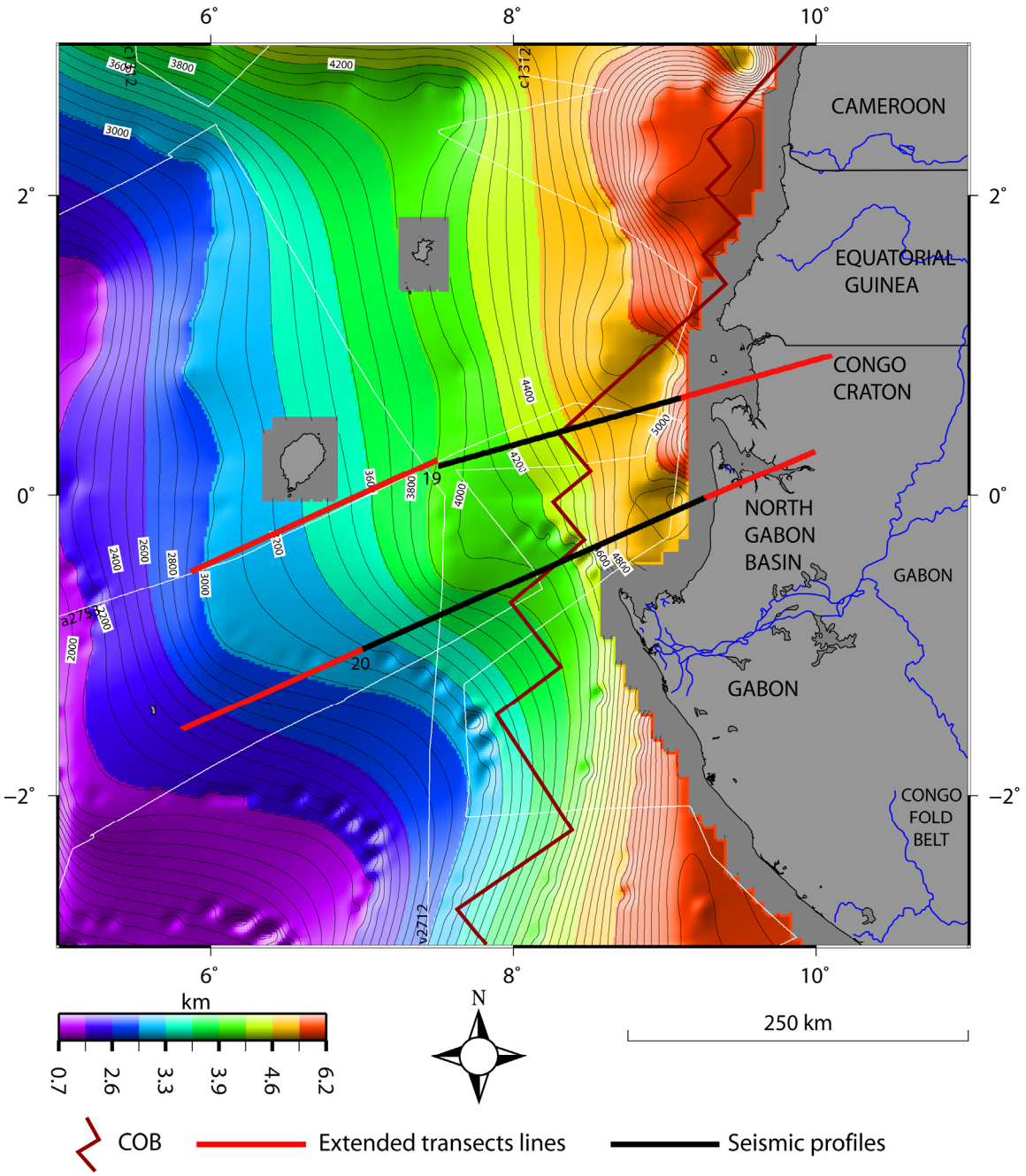

Fig. 3.7: *Sediment thickness map extracted from 5x5 minute grid of total sediment thickness of the World's Oceans and Marginal Seas (NOAA, National Oceanic and Atmospheric Administration, USA). COB interpreted by Meyers et al. (1996).*

3.2 Seismic reflection profiles

The studied seismic lines were extracted from previous studies done within the study area and interpreted by Rosendahl et al. (2005). They were extended into the onshore areas to the east and far into the oceanic crust to the west of the section (Fig. 3.1). These extensions were necessary in order to better constrain the crustal architecture through the aforementioned geophysical parameters (e.g. gravity and magnetic). The study profiles are shown in table 3.1 while the location of the published lines is shown in Fig. 3.1. Digitization of the studied seismic lines was achieved with the aid of the 'in-house' software application named SECTION (Planke, 1993). The digitized profile was subsequently introduced during gravity modeling to tie the observed crustal configuration.

Published seismic profile	Reference
Seismic line 19	Rosendahl et al. (2005)
Seismic line 20	Rosendahl et al. (2005)

Table 3.1 *Published seismic reflection lines for the study area.*

The two seismic profiles used in this study were part of the deep-imaging multichannel seismic (DIMCS) data set from the Proto Rifts and ocean Basin Evolution (PROBE) study (Rosendahl et al., 1991). The data were acquired using a semi-tuned, Arrich air gun source array arranged in a chevron configuration. The data consisted of thirty-six (36) elements operated at 2,000 psi, with a total nominal volume of 7,500 to 7,800 cu. in. The active cable length was 6,000 m, divided into 240 channels, and had a lead-in length of 600-1000 m. Shot spacing was 50 m, producing nominal 60-fold coverage. Sample rate was 4 ms and recording time 20 seconds. The acquisition method allowed for deep crustal reflection imaging and some velocity control. The data are processed by Seismograph Services Limited (SSL), and were demultiplexed, resampled to 8 ms and 16 s record lengths, corrected for spherical divergence, trace equalized over 7-15 s, dip moveout (DMO) corrected from normal moveout (NMO) velocity spectra every 10 km and predictively deconvolved. The data was further subjected to semblance velocity analyses, NMO corrected, muted by NMO stretch, CMP stacked, trace normalized for far offset, post-stack deconvolved, trace mixed and band pass filtered. Meyers et al. (1996) stated that the stacking velocity were within effective moveout to the top of acoustic basement and occasionally to reflection Moho in areas underlain by thin

crustal sections (basement thickness less than 3 s twt) and that it shows clearly interpretable Moho reflections (e.g. Figs. 3.8 and 3.9). Seismic profiles 19 and 20 extend ~142 km and 283 km respectively. They were recorded and processed to a time length of 12 s twt.

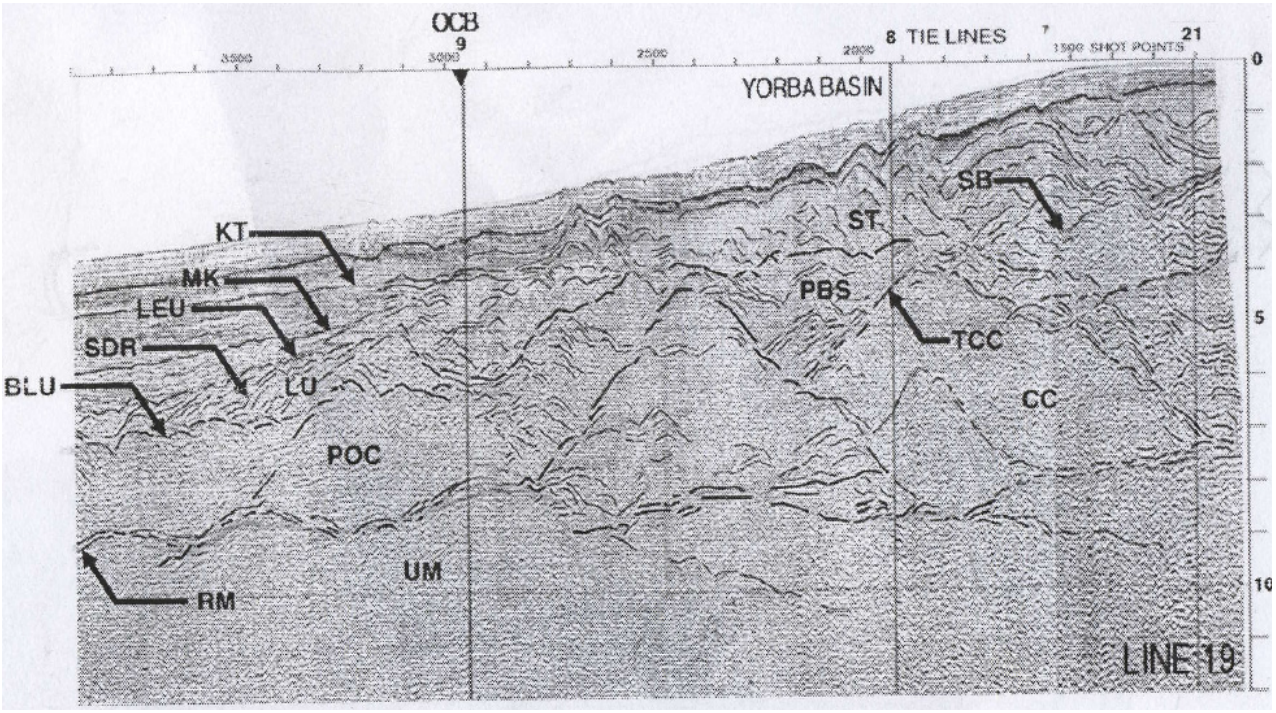

***Fig. 3.8**a: Published seismic reflection line 19 (Rosendahl et al., 2005)*

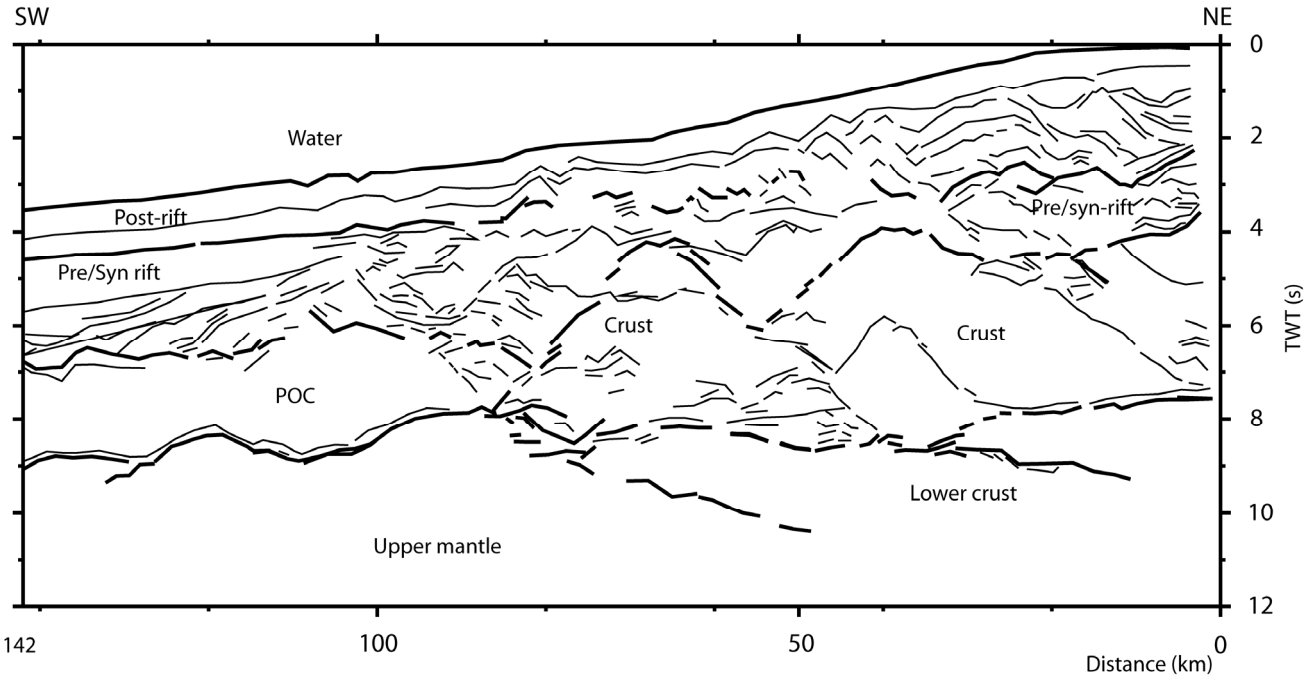

***Fig. 3.8b**: Line-drawing interpretation of seismic line 19 in TWT (after Rosendahl et al., 2005)*

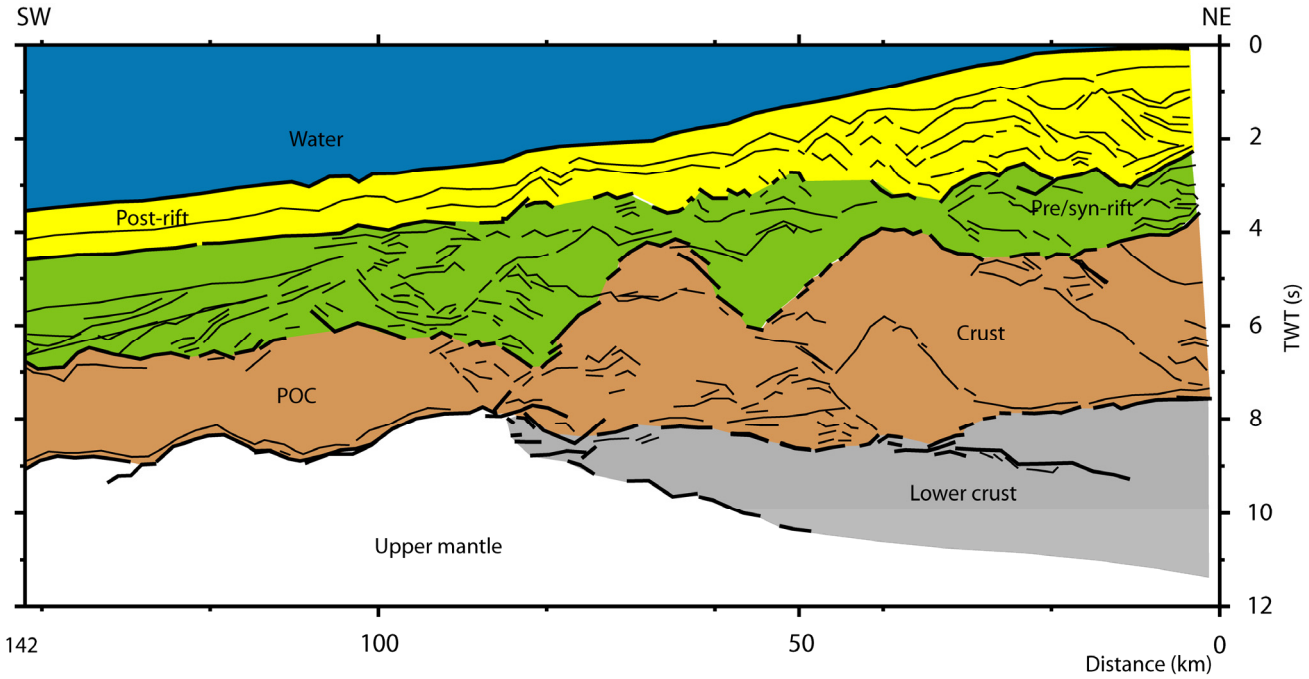

Fig. 3.8c: *Interpreted seismic reflection line 19 in TWT (after Rosendahl et al., 2005).*

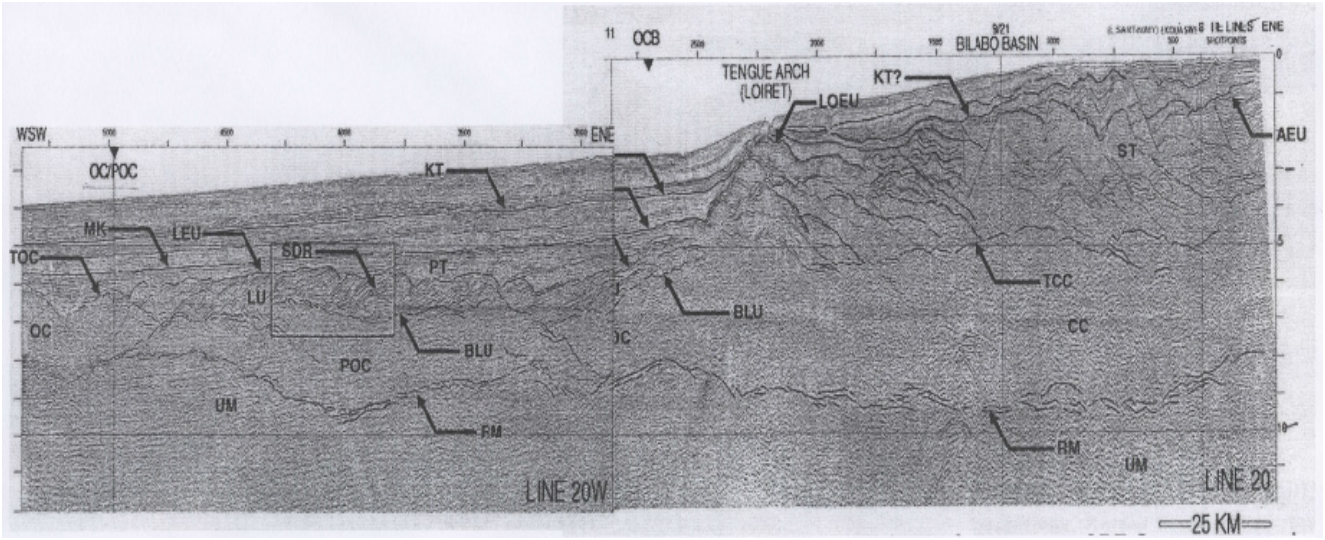

Fig. 3.9a: *Published seismic reflection line 20 (Rosendahl et al., 2005).*

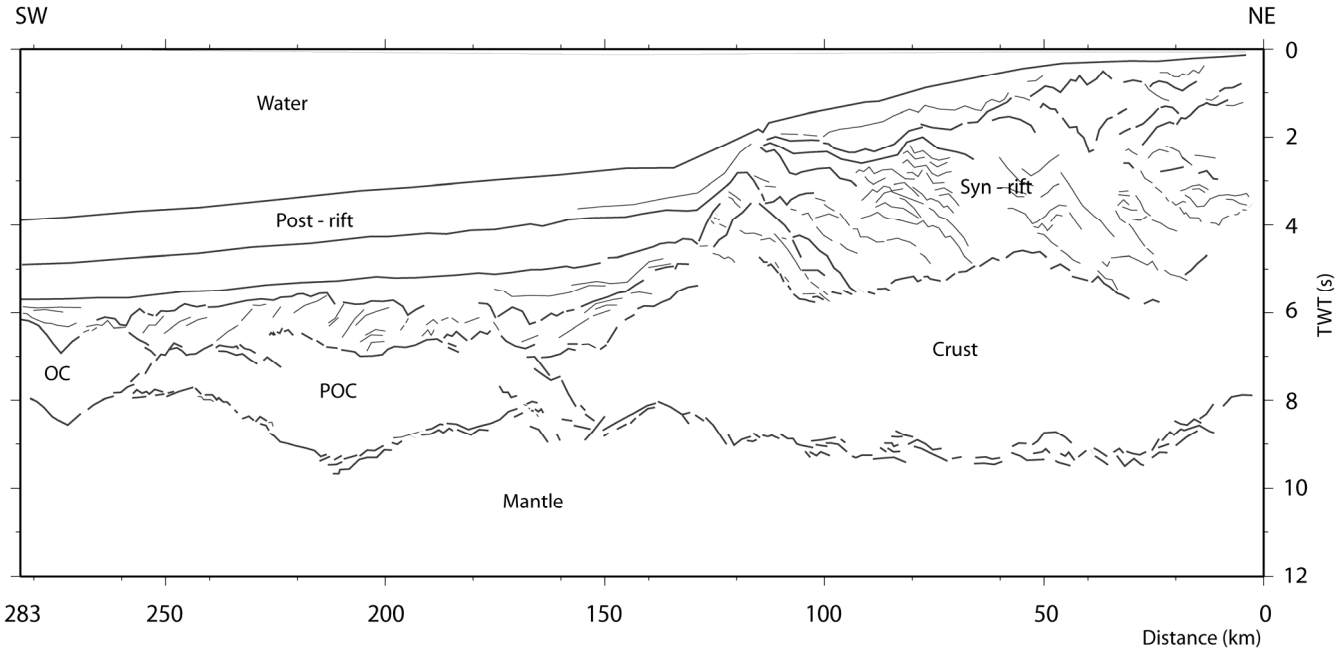

***Fig. 3.9b**: Line-drawing interpretation of seismic line 20 (after Rosendahl et al., 2005).*

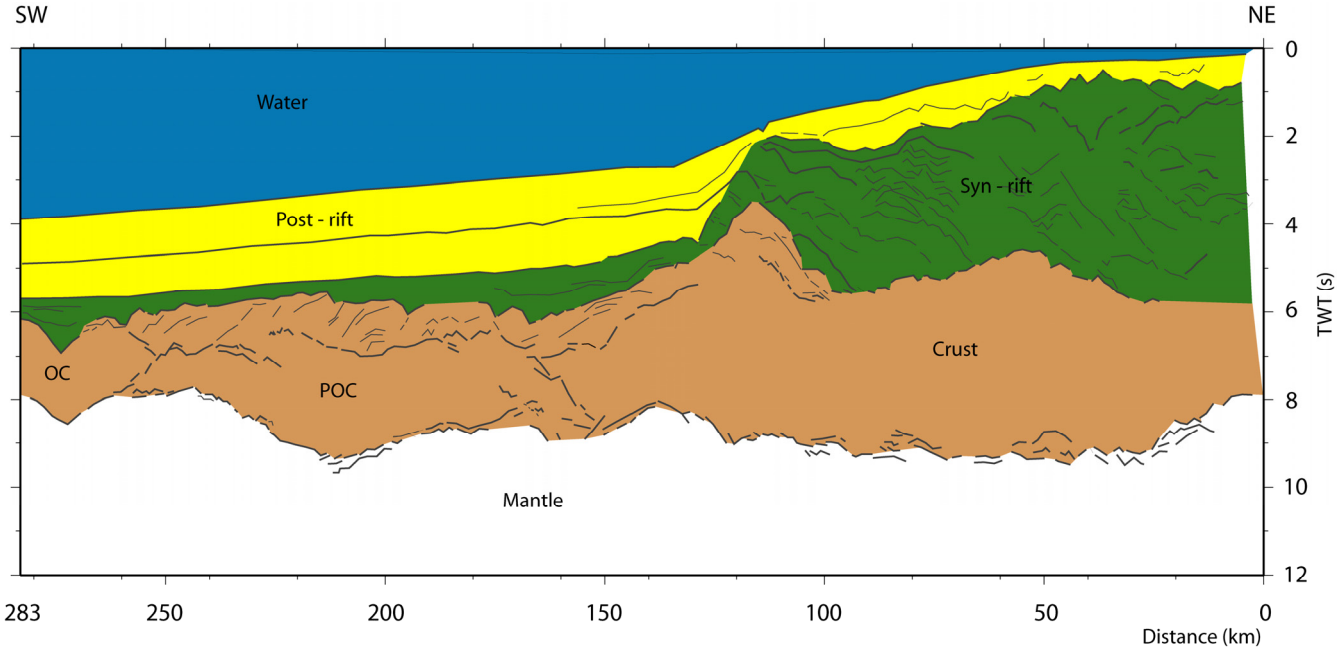

***Fig. 3.9c**: Depth converted interpreted seismic reflection profile 20 (after Rosendahl et al., 2005).*

Chapter 4

Methods and approach

4.1 Interpretation of seismic and depth conversion

As stated in the preceding chapter and displayed in Table 3.1, two interpreted published seismic lines were used for this study. Except for the line drawings, modifications and refinement were effected on the published profiles of Rosendahl et al. (2005) by using alternative published line drawings of the same lines by Rosendahl and Groschel-Becker (2000) (this will be discussed in chapter 6), in order to constrain the gravity modeling.

4.1.1 General stratigraphic attributes

Nøttvedt et al. (1995) characterized seismic stratigraphic interpretations into three distinct sedimentary sequences: pre-rift, syn-rift, and post-rift. The pre-rift sedimentary package is characterized by uniform thickness inferring that deposition occurred in a broad and slowly subsiding basin devoid of major fault regime at the onset of flexural subsidence. The underlying effect of mantle upwelling and the associated high heat flow could induce the formation of domal bodies thereby obstructing basinal subsidence. The syn-rift packages have a disorganized trend and are mostly deposited as a consequence of extensional regimes (i.e. stretching) and fault-block rotation. Generally, the mechanism for subsidence is in response to lithospheric stretching, thinning, mantle upwelling, thermal contraction and relaxation of the heated crust and its attendant effect is greatest at the initial stage of cooling due to the exponential nature of thermal decay. The obvious effect of these processes will be extensive erosion on the shoulders of the fault-blocks. Fault-block rotation and local footwall uplift causes the syn-rift geometry to be wedge-shaped. Syn-rift sequences exhibiting less developed wedge-shape characteristics can be inferred to have undergone relatively low rate of tilting. The post-rift units are characterized by thick deposits in the center of the basin slowly thinning towards the flanks. Post-rift sediments could also display wedge-shape

geometry especially in basins that have been starved of sediments. These two scenarios posed by syn- and post-rift sequences are indeed challenging. However, divergence of the syn-rift strata with respect to the active footwall is fundamental in differentiating and defining syn-rift sediments from post-rift sediments. On the contrary, post-rift units build up and onlap against the footwall after cessation of fault-movements.

4.1.2 Seismic interpretation

The seismic lines showed the different reflections down to 12 s twt. The syn-rift and post-rift sediments were imaged, while the top of the basement (i.e. the upper continental crust) and also the oceanic crust were identified. Dipping reflector sequences that thicken down-dip, just below the Aptian salt, have been interpreted to be syn-rift basins, with a time depth of ~4-6 s twt. The Libreville units and erosional unconformity sequences were also expressed on both seismic lines. The post-rift and passive margin sequences overlie the syn-rift sequences. They are homogeneous, extending from the continental shelf to the oceanic basins (Fig. 3.8a and 3.9a).

Generally, the offshore sectors of the West African margin are subdivided into three crustal types separated by two boundaries. Oceanic crust is separated from proto-oceanic crust by the oceanic crust/proto-oceanic crust boundary; proto-oceanic crust is separated from continental crust by the ocean-continent boundary. Meyers et al. (1996) characterized three main crustal types to be recurrent in the West African PROBE study multichannel seismic profiles: (1) rifted continental crust (RCC), (2) oceanic crust (OC) and (3) proto-oceanic crust (POC), which is described as transitional form of crust found between RCC and OC.

Rifted continental crust

RCC (rifted continental crust) characterized by: (1) a discontinuous reflection geometry and high relief at the top of acoustic basement; (2) a band of discontinuous reflection pattern described as a weakly defined reflection Moho; (3) 2-7 s twt seismic thicknesses from the top of acoustic basement to reflection Moho; and (4) exhibiting less intense long wavelength

magnetic anomalies (< 100 nT). The RCC is occasionally overlain by syn-rift sediments and structured Aptian salt.

Oceanic crust

Oceanic crust is also characterized by: (1) a pronounced top of acoustic basement with more subdued relief between fracture zones; (2) conspicuous high amplitude reflection Moho (2 cycles in the 10-12 Hz range); (3) 1.5-2 s twt seismic thickness from the top of acoustic basement to reflection Moho; (4) basement which contains few internal reflections; and (5) subdued, long wavelength magnetic anomalies (> 20 km wide peaks and troughs, and < 200 nT amplitude).

The most notable seismic characteristics of African oceanic crust are its uniform thickness between fracture zones and lack of seismic structure between top of the oceanic crust and reflection Moho (e.g. Rosendahl et al., 1992a). The total range in African oceanic crust thickness is ~1.3-2.0 s twt, or ~4.2-6.5 km. Rarely does the thickness between fracture zones vary by more than 10 percent. There are subtle differences in the acoustic character of oceanic crust but they are neither definitive nor systematic. For the most part, African oceanic crust is seismically unlayered and structureless away from fracture zones (e.g. Rosendahl et al., 1992a).

Proto-oceanic crust

Proto-oceanic crust (POC) is interpreted to occur along fracture zones between rifted continental crust (RCC) and typical oceanic crust (OC) (e.g. Meyers et al, 1996). It is usually overlain by seaward-dipping reflector sequences (SDRs) and Aptian salt within the study area. Seismically, proto-oceanic crust (POC) expression varies from location to location due to variance in the degree of faulting, volcanism and concentrations of detached blocks of continental crust.

In addition, Meyers et al. (1996) characterized the seismic signature of proto-oceanic crust by: (1) a well defined top of acoustic basement, which occurs at the boundary between flat

sedimentary reflectors and underlying higher velocity dipping reflectors or transparent basement; (2) high seismic relief between high velocity dipping reflectors and seismically transparent basement; (3) a band of high amplitude, discontinuous reflections representing reflection Moho; (4) 2-5 s twt seismic thickness from the top of acoustic basement to reflection Moho; and (6) well-defined magnetic anomaly corresponding to the RCC-POC boundary.

Continental rift basins

The rift basin evolution and compositions of the pre-, syn-, and post–rift have been discussed in chapter two. However, the seismic expressions are obscured by diffraction, side echoes, weaker seismic transmission, and multiple reflections which are due to the presence of salt structures and layers. Complementing this poor seismic imagery is the lack of borehole data below salt in the North Gabon Basin, thus making interpretation speculative (Meyers et al., 1996).

4.1.3 Depth conversion

All seismic reflection profiles used for this study were in two-way travel time, and then depth-converted with the in-house software 'SECTION' (Planke, 1993). This depth conversion was necessary in order to convert the seismic section from time domain into depth domain which is suitable for gravity modeling and further geologic analyses. The depth-conversion was carried out by using velocity functions along individual profiles. The input file for depth-conversion contains the digitized transect and the velocity function parameter file. The operation of this program (i.e. SECTION) requires that the distance along the x-axis be given in kilometers and that velocity functions are added beyond both ends of the profiles in order to prevent edge effects. The program also requires that each velocity layer is continuous through the profile, while each point along the digitized profile is depth-converted using the two closest velocity functions. The velocity-depth functions input used for depth conversion were derived from averaging published values of three layers (i.e. syn-rift, upper continental crust, lower continental crust) of Wannesson et al. (1991) (Fig. 4.1; Table 4.1) which is the most adjacent to the study area; and inversion of the world ocean-floor sediment thickness

map (NGDC, National Geophysical Data Center). Regional considerations were taken into account for the post-rift and upper mantle layers,

In seismic line 19, a total of 16 velocity stations have been constructed along the profile. These were positioned at every 10 km distance along the profile. Six velocity layers were used for the seismic profile 19 and the interval velocities are shown in Table 4.2 for the respective layers. In seismic line 20, a total of 30 velocity stations were constructed along the profile at every 10 km distance. However, five velocity layers were interpreted and used for depth conversion of this profile. The interval velocities are the same as in Table 4.2 with the exception of the lower crust. The corresponding depth-converted sections are presented in Figs 4.2 and 4.3. The position of Moho is well resolved in both sections. However, the average velocity value of 5.60 km/s for the crust, derived from Wannesson et al. (1991), was rather too low when compared to other world-wide values for the continental crust. Therefore, a more realistic value of 6.10 km/s which is within global acceptable range was used.

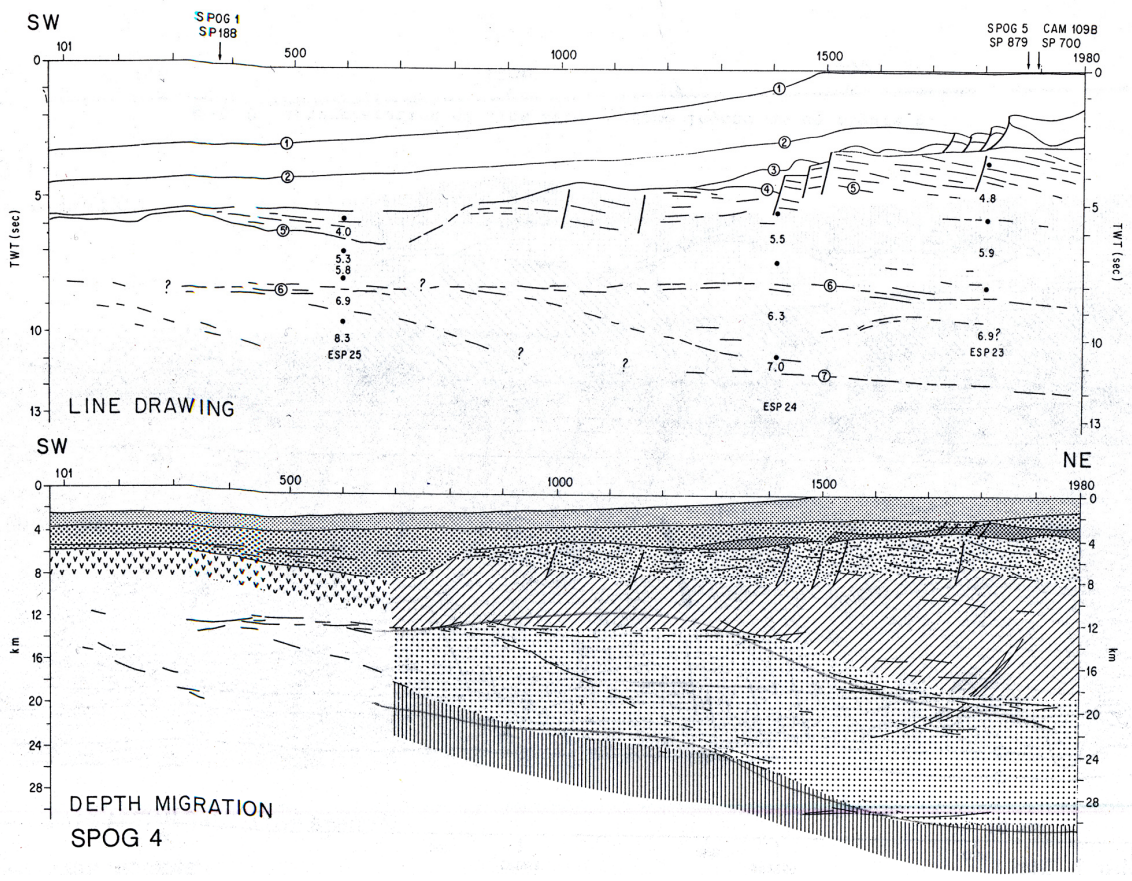

Fig. 4.1: *Line drawing interpretation of Wannesson et al. (1991) for the northern segment of Gabon Margin.*

Layer	Velocity values (km/s)
Syn-rift	4.0, 4.8
Upper continental crust	5.3, 5.5, 5.8, 5.9
Lower continental crust	6.3, 6.9, 6.9, 7.0

Table 4.1: *Velocity functions of Wannesson et al. (1991) for the northern segment of Gabon Margin.*

Layer	**Average interval velocity (km/s)**
Water	1.48
Post-rift	2.50
Syn-rift	4.40
Crust	5.60/6.10
Lower crust	6.70
Mantle	8.10

Table 4.2: *Velocity values representing each seismic layer used in depth conversion.*

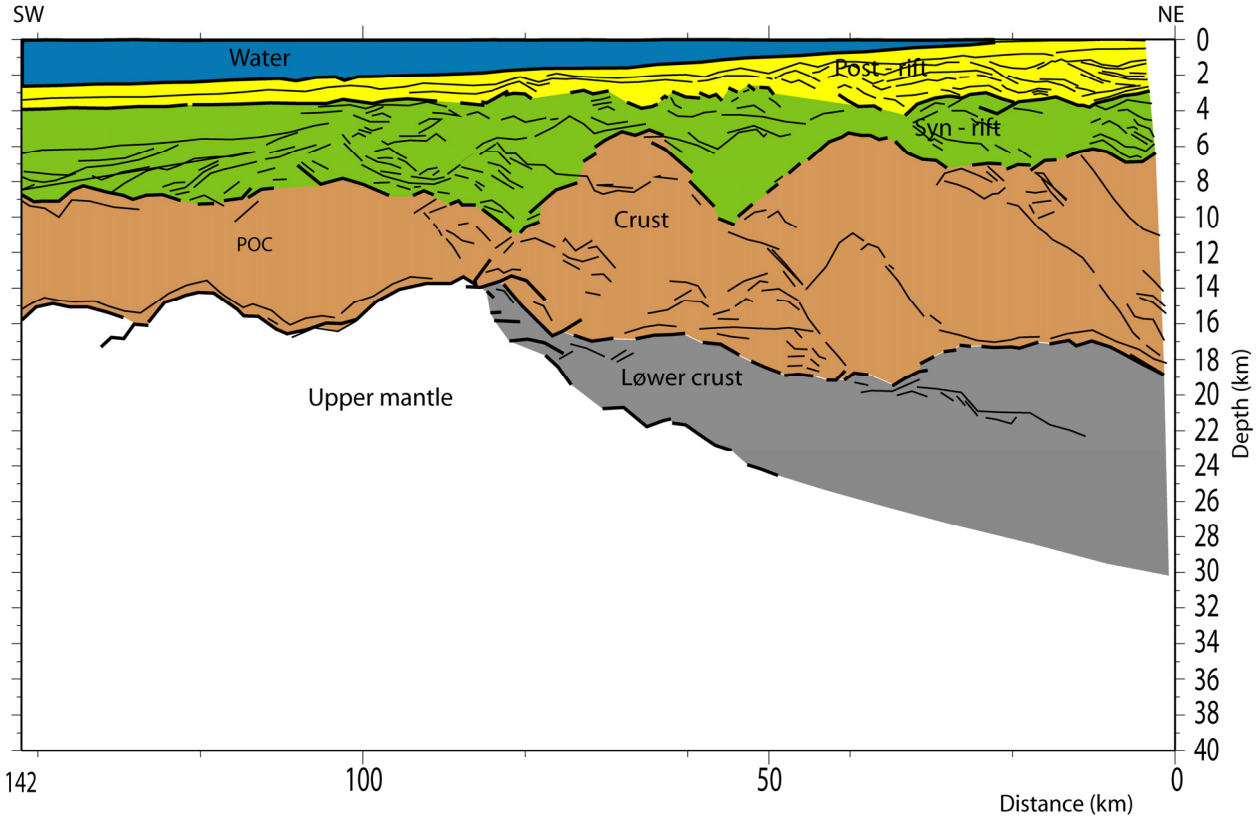

Fig. 4.2: *Depth-converted seismic line 19. Seismic interpretation is based on Rosendahl et al. (2005). POC refers to proto-oceanic crust.*

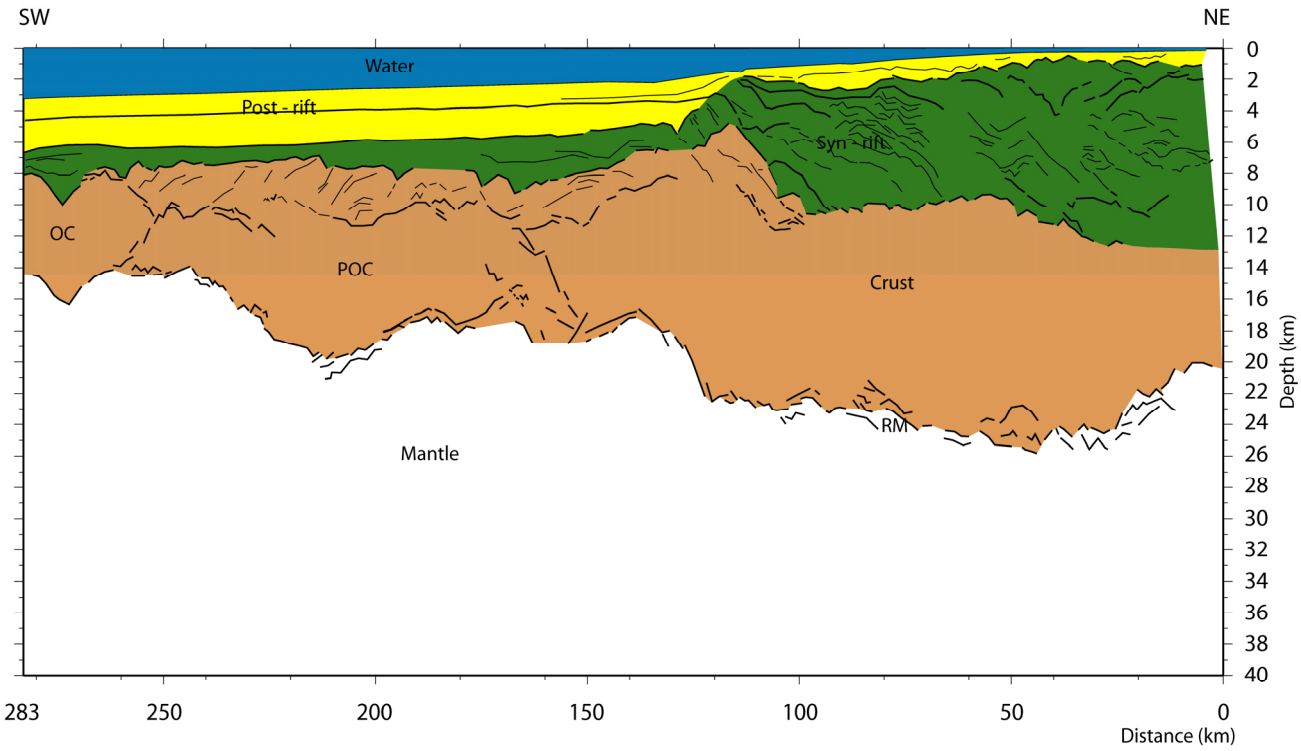

Fig. 4.3: *Depth-converted seismic line 20. Seismic interpretation is based on Rosendahl et al. (2005). OC, POC, and RM refers to oceanic crust, proto-oceanic crust, and reflection Moho respectively.*

4.2 Initial Moho relief estimates

The Mohorovicic discontinuity is described as the boundary separating the crust and the mantle. Seismically, it is that surface at which seismic P-wave velocity abruptly increases from less than 7.6 km/s to at least 8 km/s (Condie, 2005). There is also a conspicuous abrupt discrepancy in density, transiting from the lower crust to the upper mantle. Changes in mineralogy as well as phase changes ascribed to pressure differentials (Condie, 1989) have been adduced to be possible reasons for the seismic velocity and density contrast.

The initial Moho relief is achieved along constructed transects by incorporating two methods: forward isostatic balancing and inverse modeling, with the aid of the in-house software TAMP (Breivik et al., 1990). TAMP executes its operations by defining polygon models of the crust and displaying calculated gravity anomaly results for each model in graphic form. The expressed simplified Earth models produced via TAMP are presented by three polygons: water, crust and mantle. The first polygon expressed the water column with a density of 1.03 g/cm^3 and the bathymetry input was extracted from the gridded data, its importance in

defining the boundary between the water and the crustal polygons; the second polygon expressed the crust and was modeled with different densities in the order of 2.70 g/cm^3, 2.80 g/cm^3, and 2.90 g/cm^3; and finally, a lower polygon which expresses the mantle has a density of 3.20 g/cm^3, and a maximum depth of 50 km was assigned.

Transect name	Total length (km)	Position of anchor point
Transect 19	502	480
Transect 20	511	480

Table 4.3 *Composite transects modeled with TAMP. See Fig. 3.1 for locations.*

4.2.1 Forward isostatic balancing

The idea behind forward isostatic modeling is the assumption of an isostatically balanced Moho based on Airy isostasy along the constructed transects. Airy isostasy compensates the unevenness in crustal geometry and thicknesses in response to loading with a corresponding constant density. In the computation of a balanced Moho, TAMP was introduced to define the geometry of a simplified crustal model and the only variable input was bathymetry, allowing therefore direct correlation of the Moho relief to changes in the bathymetric morphology. Extracted gravity along grid was also put into the TAMP computation and the final result was a simulated crustal model of the **observed** and **calculated** gravity trend along the section (Figs. 4.4 and 4.5). Areas of anomalous discrepancies in the resulted curves along the section will be eventually fine-tuned, based on the seismic profile and local geology during 2D forward crustal-scale gravity modeling. Furthermore, anchor point (i.e. a point where the depth to Moho is suspected) was selected in the oceanic crust domain during the modeling process to better resolve the Moho geometry (Table 4.2). The position of the anchor point has a corresponding water depth value which was added to the acceptable value for the world average thickness of the oceanic-crust (6.5 km).

Transect 19

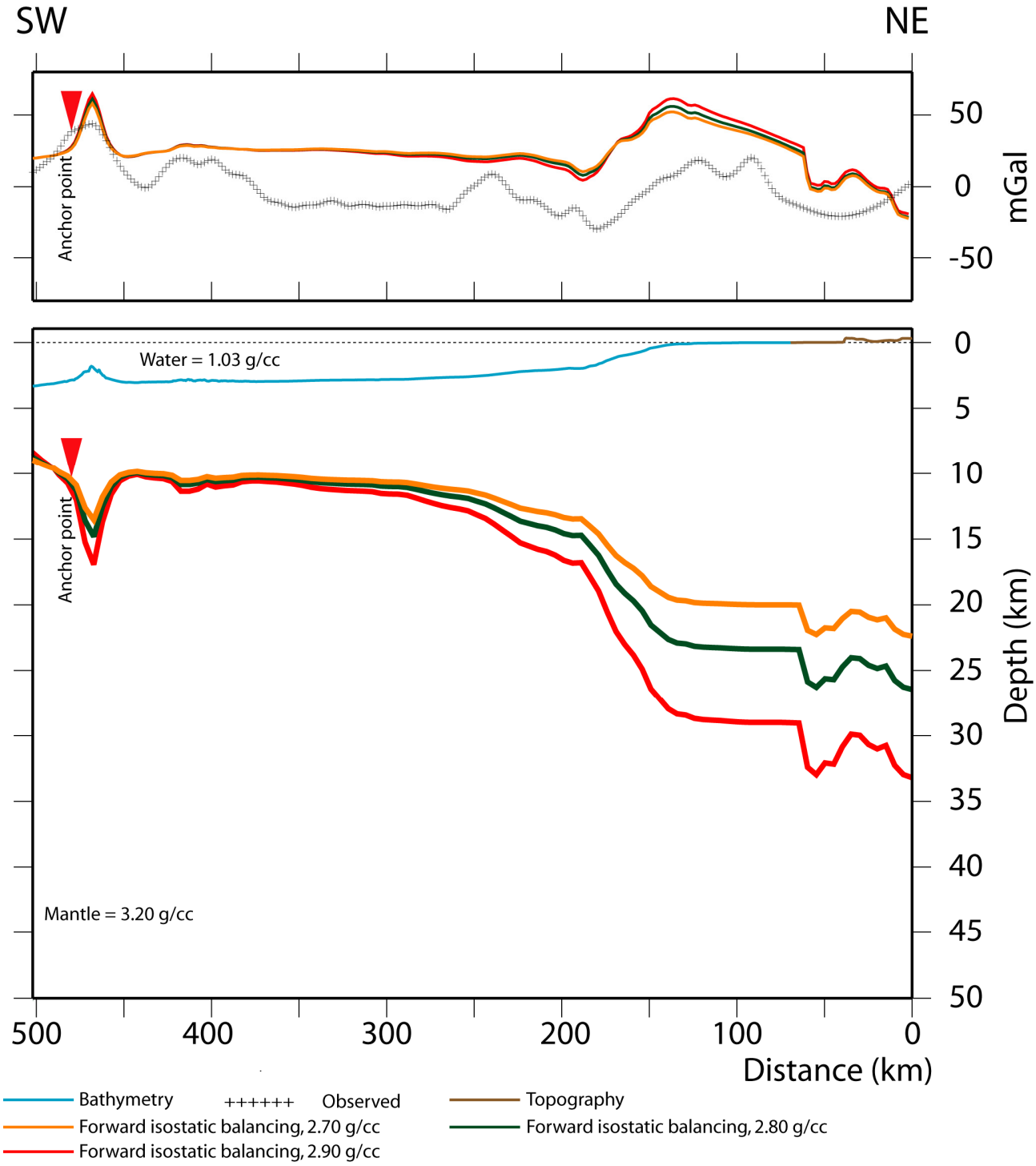

Fig. 4.4: *Moho relief calculated along Transect 19 by forward isostatic balancing. Variations in color indicate different crustal densities.*

Transect 20

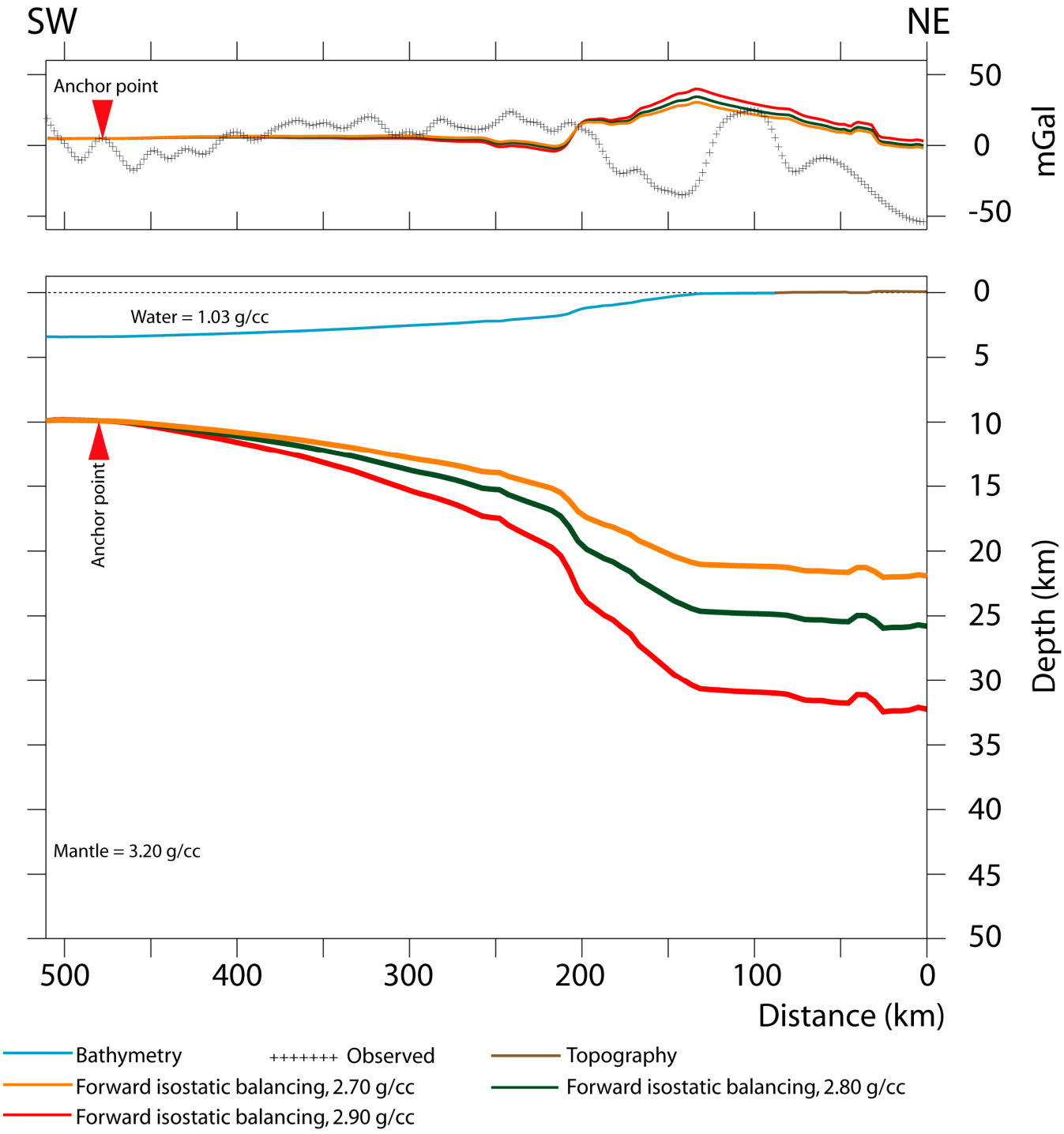

Fig. 4.5: *Moho relief calculated along Transect 20 by forward isostatic balancing. Variations in color indicate different crustal densities.*

4.2.2 Inverse modeling

The use of this technique was initiated by Cordell and Henderson (1968). The idea is based on iteration of computed three-dimensional structural models for gravity anomaly with respect to the Moho geometry. Therefore, the result will be a hypothetically derived Moho relief with the expressions of the **calculated** gravity curve being adjusted to fit the **observed** gravity (Figs. 4.6 and 4.7). TAMP was employed in the modeling process and the input data were the same as for the forward isostatic modeling. However, an initially planar Moho relief was assumed for the program to function and iterative computation of the gravity data was effected until an agreeable correlation between the **observed** and **calculated** curves was achieved.

In addition, the calculated Moho relief based on the two techniques is compared for each profile in Figs. 4.8 and 4.9.

Transect 19

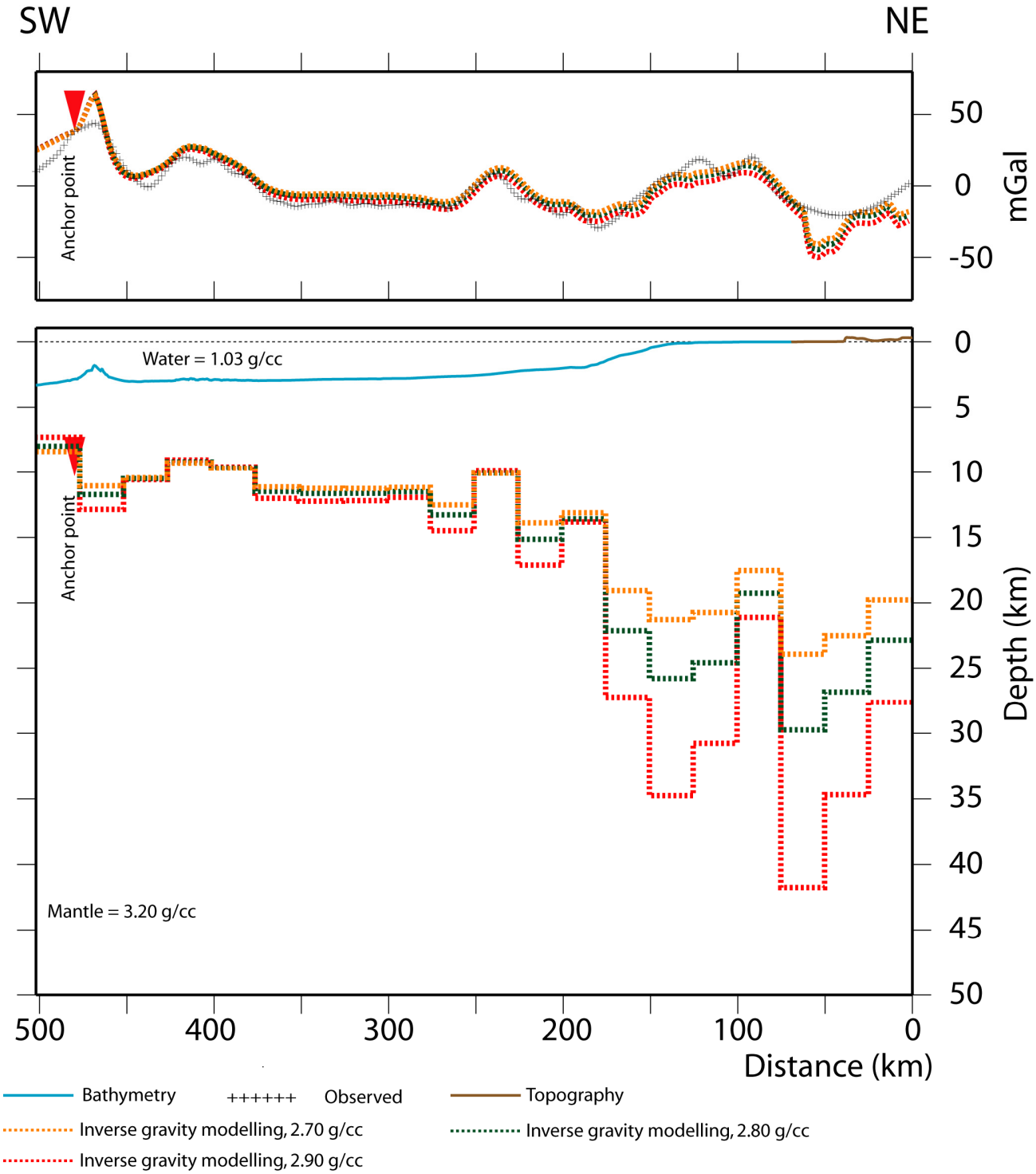

Fig. 4.6: *Moho relief calculated along Transect 19 using inverse modeling.*

Transect 20

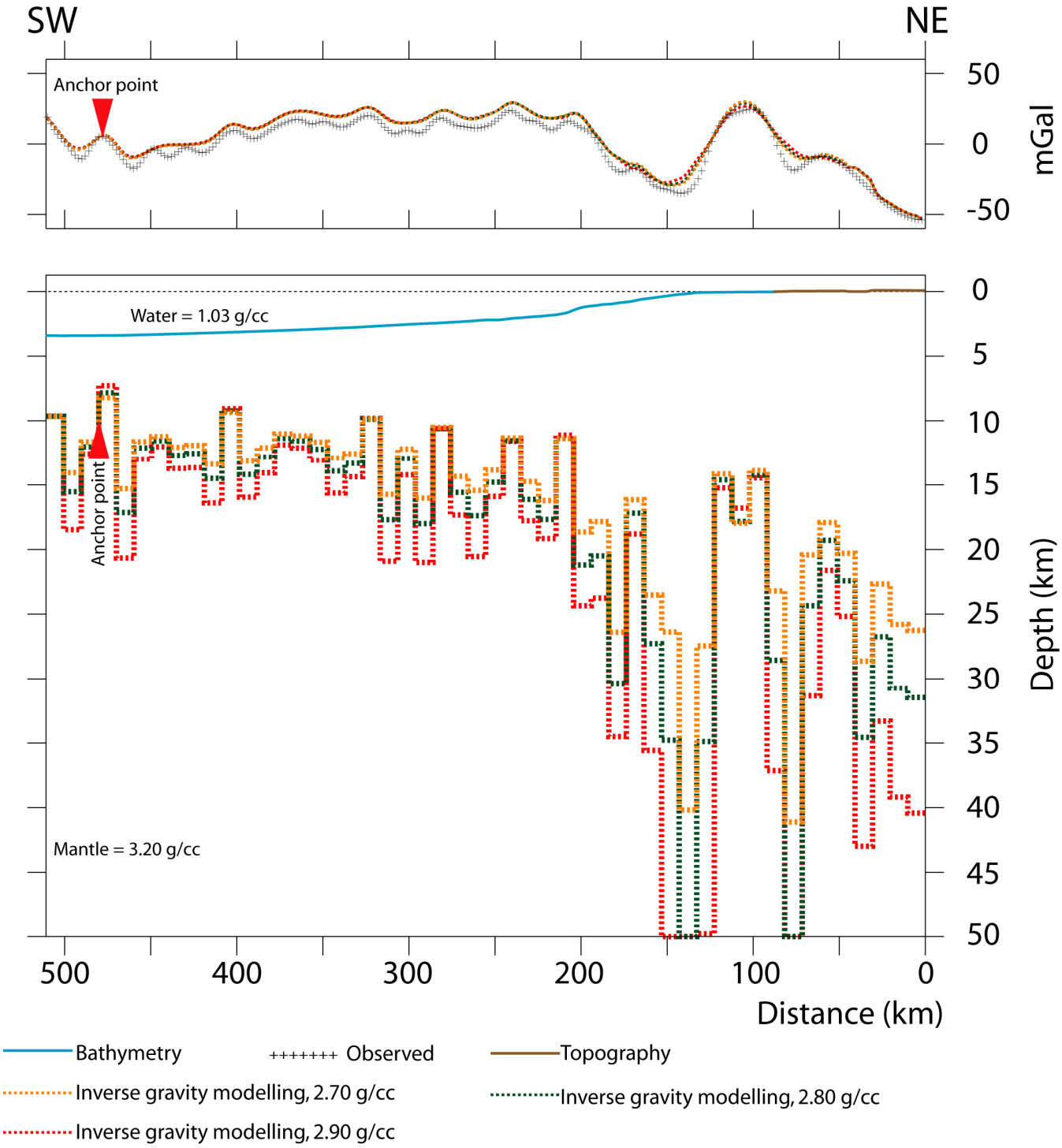

Fig. 4.7: *Moho relief calculated along Transect 20 using inverse modeling.*

Transect 19

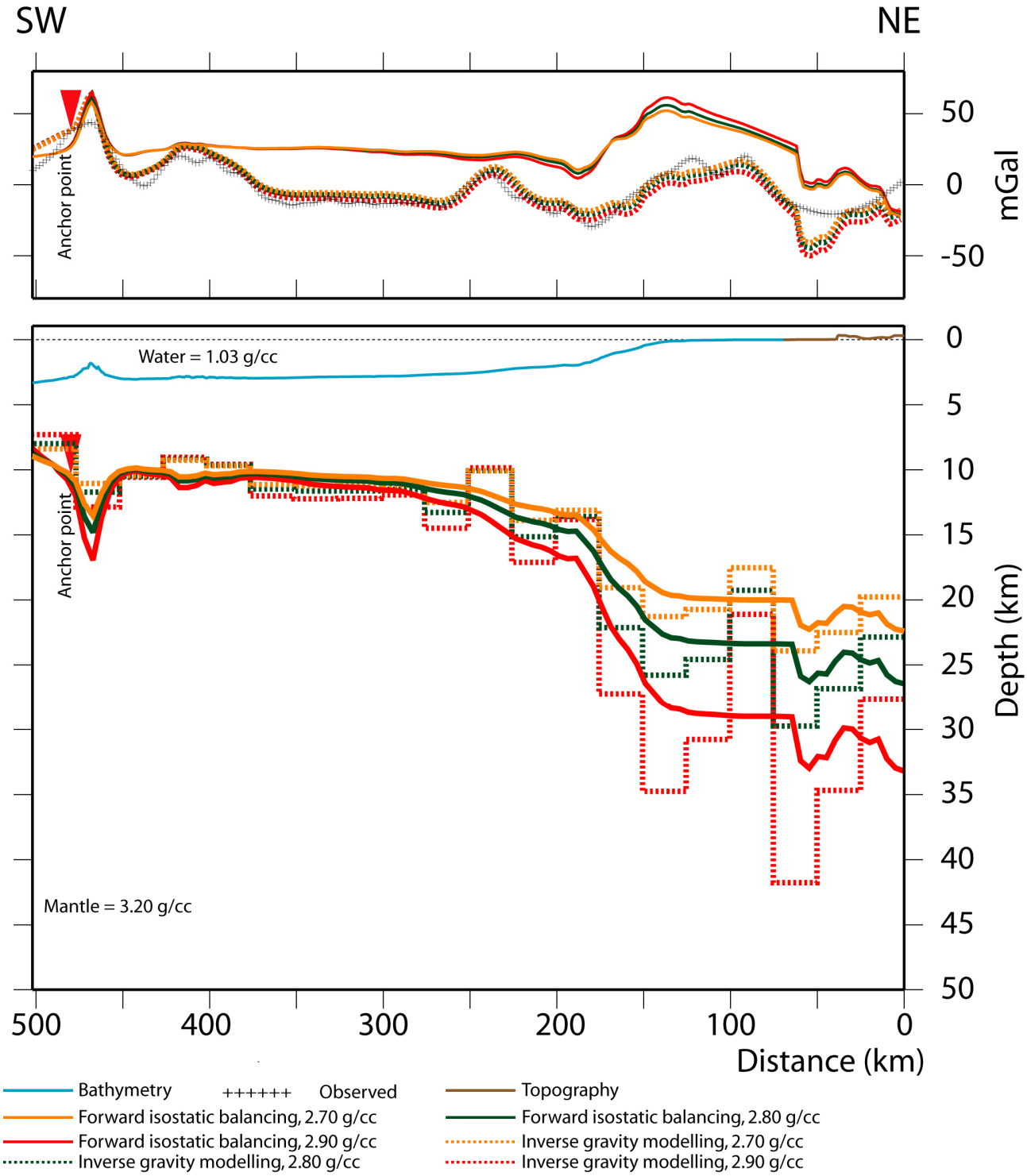

Fig. 4.8: *Moho relief calculated along Transect 19 using isostatic balancing and inverse modeling.*

Transect 20

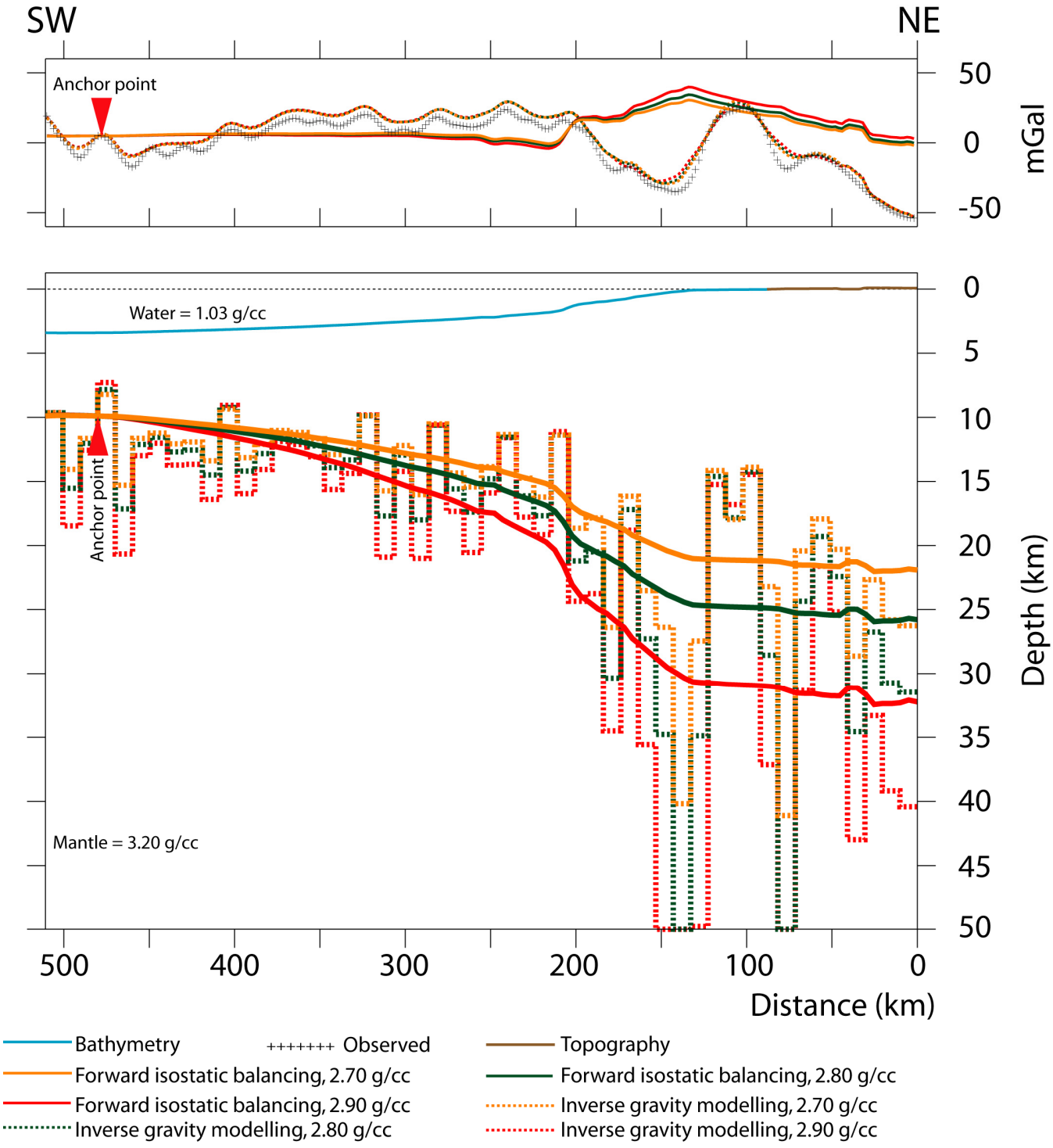

Fig. 4.9: *Moho relief calculated along Transect 20 using isostatic balancing and inverse modeling.*

4.3 Potential field gradient and continent-ocean boundary/transition

The demarcation of the line of initial rifting in passive continental margin settings is highly significant in discussing breakup and drift episodes as it concerns basinal and crustal evolution. To this end, the exact reconstruction of the continent-ocean boundary, which has generated extensive debate even within the study area, is at best complex and challenging, thus giving credence to the different processes and configurations that characterize the development of the margins. To effectively conceptualize the configuration of deep crustal processes, seismic alone, for many obvious reasons, will be inadequate in critically assessing the detail architecture of rift margins (e.g. beneath salt domes, volcanic rocks, and associated problems derived from multiples within a sedimentary column) and in affirming the existence or absence of decollement surfaces (Watts and Stewart, 1998). The use of geophysical technique (i.e. potential field data and modeling) to approach the characterization of the continent-ocean transition/boundary has been successful to a larger degree. The manifestation of gravity and magnetic anomalies has been ascribed to morphological changes in oceanic and continental domains (Talwani and Eldholm, 1973). Notable changes with respect to basement elevations have been observed to occur at the boundary separating oceanic and continental crust, primarily due to the contrast in density between these bodies, evoking a corresponding isostatic response and expressed as a steep gradient on the gravity anomaly curves. The same contrasted magnetic anomalous response will be expressed.

Karner (2000) proposed that the continent-ocean boundary is broadly aligned with a steep Bouguer gravity gradient (negative-positive). Tsikalas et al. (2005) defined the continent-ocean transition as a zone of rapid crustal thinning. This is true in instantaneous extensions with greater degree of strain, as expressed in seismic profiles for this study and corroborated with the result from TAMP (Figs. 4.4-4.9). The configuration of the proposed COB/COT by Meyers et al. (1996) on the study area is some-what segmented or step-like (i.e. uneven) and it has been attributed to the effect of oceanic transform zones and normal faults that characterized the oblique evolution of the margin (e.g. Meyers et al., 1996; Wilson et al., 2003).

In this study, Bouguer-corrected gravity anomaly, gravity data, magnetic data, bathymetric dated and interpreted line drawing seismic profiles were incorporated to obtain an initial approximation of the COB/COT. Bouguer assumes a planar reference surface devoid of topographic gravity anomalies. This is achieved by subtracting all topographic effects from a constant reference level and it only represents the bathymetric gravity anomalies. Thus, topographic areas will record as positive, and a negative correction is needed, while over the sea-surface, the replacement of the water layer with an assumed rock slab of crustal density will increase the values of the residual gravity anomaly. Therefore, a positive-negative landward gradient is expressed.

The observed Bouguer-corrected gravity anomaly contrast in gradient between the oceanic domain and continental domain is best explained by the lateral variation in density between the lithospheric mantle and crystalline crust beneath the continent-ocean transitional zone. The Moho relief within this zone is a causative factor for regional Bouguer-corrected gravity gradient expressed between two main regional gravity domains (e.g. oceanic and continental). Figs. 4.10-4.11 depict this type of contrast in regional Bouguer gravity trend where sudden lateral density variations within the basement reflect relative steepness, thus a probable candidate for COB/COT. However, this proposal will be further constrained with 2D forward crustal-scale gravity modeling.

Transect 19

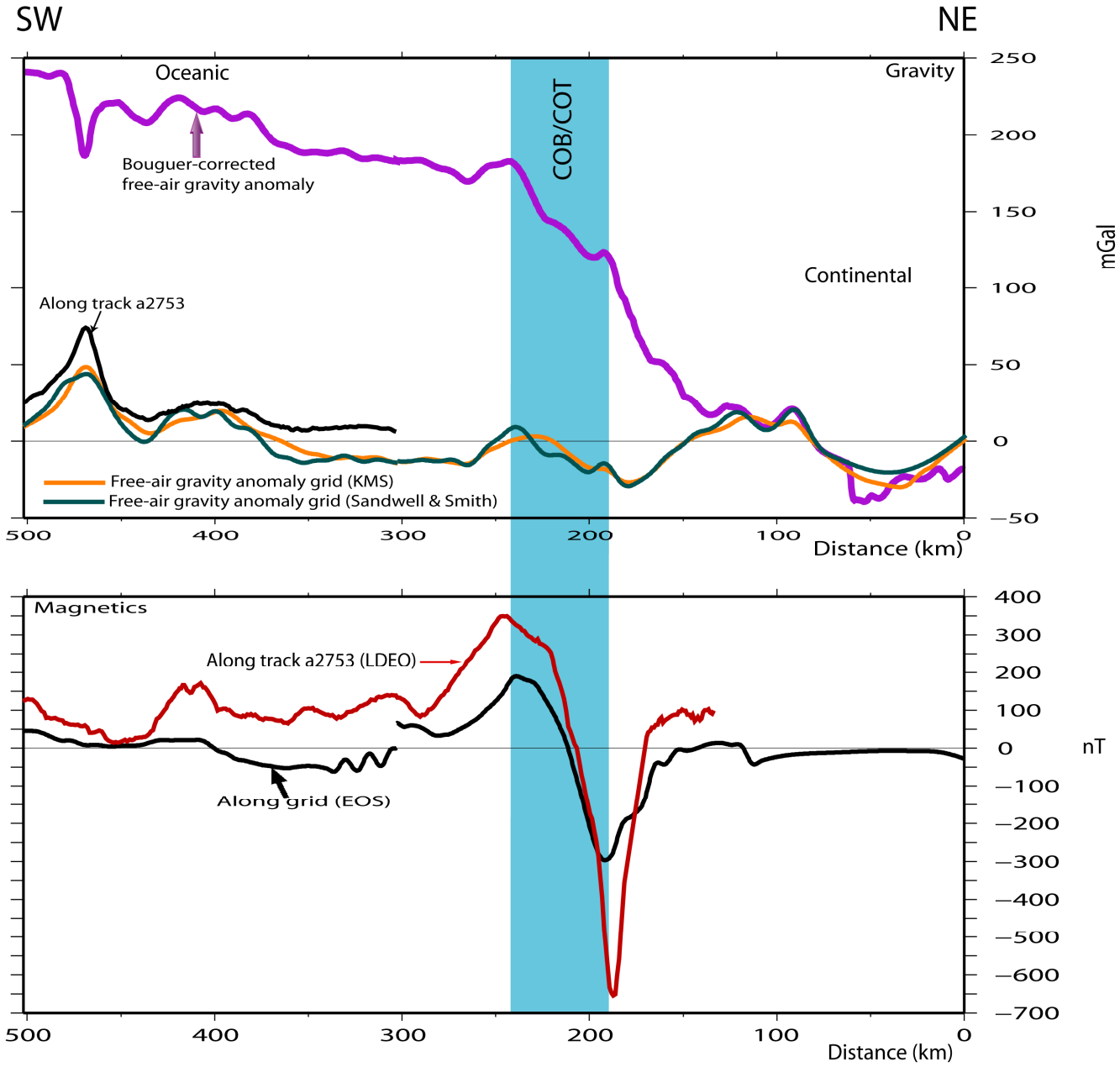

Fig. 4.10: *Bouguer-corrected gravity anomaly, free-air gravity anomaly (Sandwell and Smith, 1997, and KMS99 grids), and magnetic anomaly along track and grid (EOS, and LDEO), along constructed Transect 19. Inferred continent-ocean boundary/transition (COB/COT) indicated.*

Transect 20

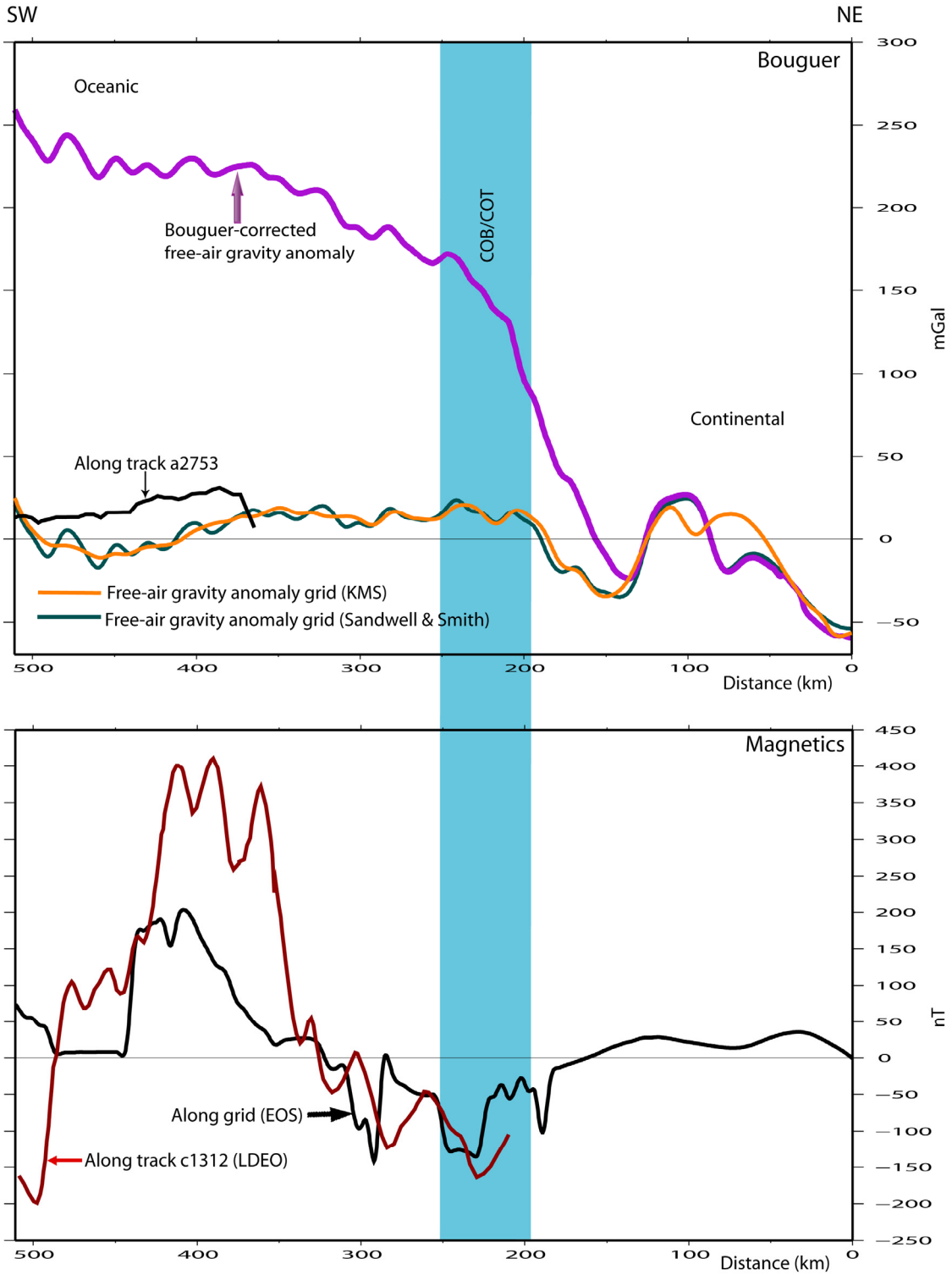

Fig. 4.11: *Bouguer-corrected gravity anomaly, free-air gravity anomaly (Sandwell and Smith, 1997, and KMS99 grids), and magnetic anomaly along track and grid (EOS, and LDEO), along constructed Transect 20. Inferred continent-ocean boundary/transition (COB/COT) indicated.*

Chapter 5

Gravity Modeling

5.1 Modeling parameters

Gravity modeling is a complimentary tool to seismic interpretation, as it offers a robust approach for unraveling the deep crustal architecture which is beyond seismic resolution. In this study, a two-dimensional forward gravity modeling was applied by using GMSYS v.4.7 software (Northwest Geophysical Associates, Inc., www.nga.com). GMSYS is an interactive gravity and magnetic modeling software that enables generation of verifiable geological models by comparing their gravity and/or magnetic responses against the observed measured responses along a reference section. The input data include the depth-converted MCS profiles, the estimated Moho relief constrained from TAMP and grid-extracted gravity anomalies. Consequently, the structural architecture of the margins along the constructed transects were further probed through gravity modeling. The GMSYS modeling approach allows for the creation of polygons with representative density value for each crustal unit along the constructed transects. Anomalous gravity responses due to edge effects arising from polygons that extend beyond the modeling area are avoided by extrapolating the polygon at the start and end of the transects to a distance of 30,000 km on each side.

The format for GMSYS operation involves a reiterative improvement of the model through changes in the geometry and/or the density of the polygons, until the residual gravity response (i.e. the difference between the calculated and the observed values) falls within the generally acceptable margin of error, i.e. below mean residual error of 10 mGal for this regional study. The observed gravity anomaly response along each transect was extracted from the 1x1 free-air gravity anomaly grid (Sandwell and Smith, 1997, v.10.1). In the course of gravity modeling of the constructed transects, notable discrepancies were observed in the gravity field between the calculated and observed gravity responses which were expressed as long-wavelength and short-wavelength variations. The longer wavelength variations can be considered as regional and related to lower crustal features and to the Moho relief, while the short-wavelength variations can be considered as local and attributed to upper crustal features

and essentially to the crystalline basement relief. The robust approach in gravity modeling is flawed by its none uniqueness. This implies that manipulations of the calculated gravity response to fit the observed gravity response are possible in spite of the resulted model being geologically unfeasible. However, the key is to simulate realistic solutions that define a geological model correlated with available and verifiable geologic constraints and ensuring minimal uncertainty.

The seismic lines used for this study were interpreted by Rosendahl et al. (2005) in time domain, and then depth converted (refer to chapter 3 and 4) with the in-house software 'SECTION' (Planke, 1993). The subsequent results were further utilized in TAMP and introduced into GMSYS gravity modeling. However, the regional velocity functions (refer to chapter 4) utilized for this study were taken from Wannesson et al. (1991). These velocity functions were averaged for the different layers starting from the syn-rift layer to the lower crust.

The building of the gravity models for each transect was premised on an initial simplified model constrained by earlier interpreted seismic reflection boundaries and the Moho relief derived from TAMP. The corresponding density values assigned to each unit were inferred from seismic velocity-density conversion tables derived from the empirical Nafe and Drake (1957) relationship (Table 5.1 and Fig. 5.1). Assigned velocity-density relationships on related rifted continental margin studies were also taken into account (e.g. NE Brazilian margin: Blaich et al., 2008; NE Atlantic margins: Tsikalas et al., 2005).

Vel. (km/s)	Den. (g/cm^3)	Vel. (km/s)	Den. (g/cm^3)	Vel. (km/s)	Den. (g/cm^3)	Vel. (km/s)	Den. (g/cm^3)
1.5	1.47	3.2	2.24	4.9	2.55	6.6	2.93
1.6	1.66	3.3	2.26	5.0	2.57	6.7	2.95
1.7	1.73	3.4	2.28	5.1	2.59	6.8	2.98
1.8	1.80	3.5	2.30	5.2	2.61	6.9	3.01
1.9	1.86	3.6	2.32	5.3	2.62	7.0	3.04
2.0	1.92	3.7	2.34	5.4	2.64	7.1	3.07
2.1	1.98	3.8	2.36	5.5	2.66	7.2	3.10
2.2	2.01	3.9	2.38	5.6	2.68	7.3	3.13
2.3	2.03	4.0	2.39	5.7	2.70	7.4	3.16
2.4	2.06	4.1	2.41	5.8	2.72	7.5	3.19
2.5	2.09	4.2	2.43	5.9	2.74	7.6	3.22
2.6	2.11	4.3	2.44	6.0	2.77	7.7	3.25
2.7	2.13	4.4	2.46	6.1	2.80	7.8	3.28
2.8	2.15	4.5	2.48	6.2	2.83	7.9	3.31
2.9	2.18	4.6	2.50	6.3	2.85	8.0	3.34
3.0	2.21	4.7	2.52	6.4	2.87	8.1	3.38
3.1	2.23	4.8	2.53	6.5	2.90	8.2	3.42

Table 5.1: *Mean velocity-density conversion values (from Nafe and Drake, 1957).*

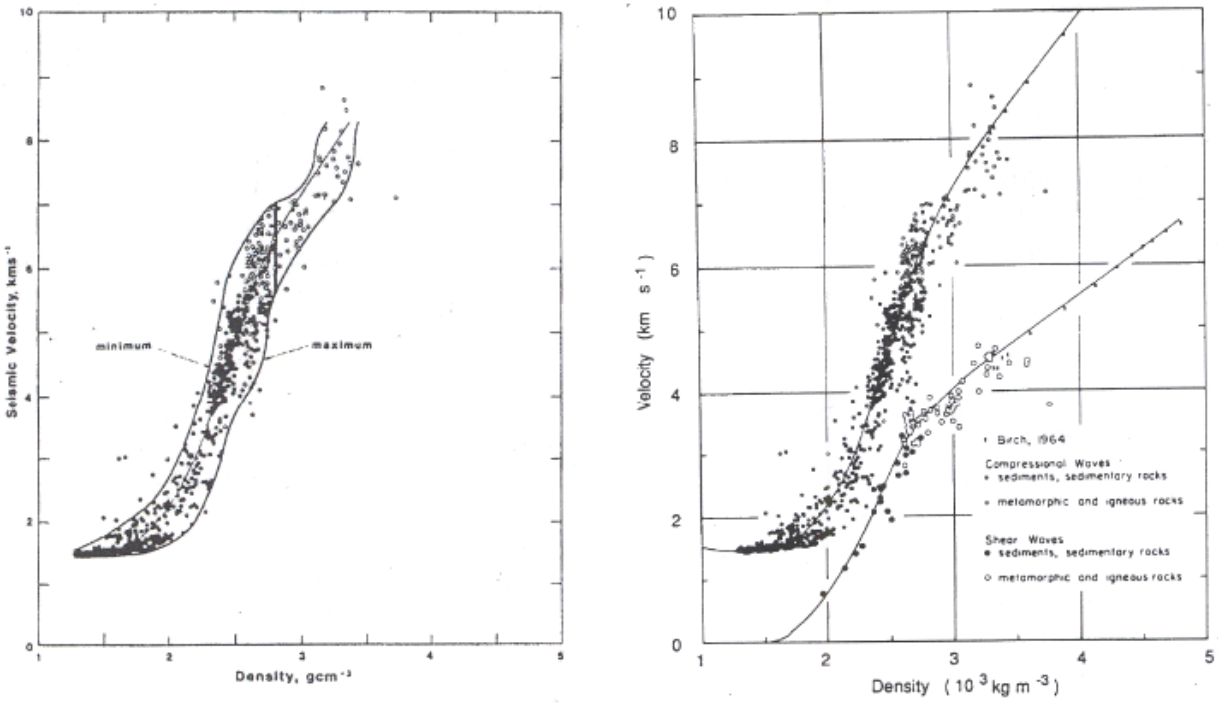

Fig. 5.1: *Mean velocity-density relationship curve (from Nafe and Drake, 1957).*

The initial density values assigned to each block were: water (1.03 g/cm^3); post-rift sediments (2.09 g/cm^3); syn-rift sediments (2.46 g/cm^3); continental crust (2.80 g/cm^3); oceanic crust (2.83-2.85 g/cm^3); upper mantle (3.20 g/cm^3). However, constant densities of 2.80 g/cm^3 and 2.83 g/cm^3 were assigned to the continental and oceanic crusts, respectively, in order to obtain homogeneous crustal densities. Furthermore, the crystalline crust was subdivided into three segments and two boundaries. These are: (1) continental crust, bounded by the continent-ocean boundary; (2) proto-oceanic crust, i.e. intermediate crust between continental and oceanic crust; (3) oceanic crust, bounded by the proto-oceanic crust and the continent-ocean boundary. It has been postulated that the African proto-oceanic crust densities vary considerably, being at least as great as the density of the oceanic crust, and possibly higher (Rosendahl et al., 2005). Similarly, gravity modeling along the West African margin has also shown higher density values for proto-oceanic crust ranging within 2.85-3.11 g/cm^3 (e.g. Weger et al., 2001; Wilson et al., 2003). These high density values have been attributed to the presence of varying amount of serpentinite (Wilson et al., 2003). However, a constant density value of 3.04 g/cm^3 was assigned to the performed gravity modeling in this study for the proto-oceanic crust and was found to be satisfactorily. The position of the continent-ocean boundary (COB) is placed to correspond to that region of maximum negative-positive gradient as expressed in the Bouguer anomaly.

5.2 Modeling results

In this study, two transects (i.e. Transect 19 and Transect 20) were constructed and gravity modeling was applied along the sections. Anchor points have been placed over known positions of oceanic crust. An initial model was constructed (Transect 19A) based on the interpreted depth-converted seismic profile and a corresponding mean residual error of ~41. mGal resulted. The misfits observed in this model were mostly restricted to the continental domain while the best match was observed along the oceanic crust domain. There is a correlative trend in the long-wavelength distribution with the deeper structural relief especially along the oceanic crust. This could be ascribed to the oceanic crust relative uniformity in terms of its gravity response. Where this trend is interrupted, it could be related to high frequency gravity fluctuations induced by oceanic basement relief. On the other hand, within the continental basement the large anomalous expression is most probably related to the short-wavelengths derived from basement relief features. Several modification processes were applied mainly through trial and error and constraints from published geological data, until a reasonable geological gravity model was attained with a correspondingly acceptable mean residual errors of less than 10 mGal. Knowledge gained from Transect 19 was further applied to Transect 20 to obtain a reasonable match and acceptable mean residual error.

The successive final gravity models for both transects evolved from a complex mix consisting of refined seismic data and onshore geologic data of the study area. However, uncertainties still abound on the exact position of the interpreted seismic boundaries, velocities, and the lack of onshore gravity data. Uncertainties also arose in quantifying to what extent the 2D lines used in gravity modeling are influenced by 3D gravity effects. In spite of these setbacks, a reasonable geologic model was achieved with an acceptable mean residual error. Therefore the robustness of gravity modeling as a viable tool for understanding crustal architecture has been justified and interpretational uncertainties inherent in poorly resolved seismic reflection/refraction profiling are better constrained. An additional importance of gravity modeling is in extrapolating geologic information on areas not covered by seismic data. The output of gravity modeling consists of a plot of the 2D crustal-scale forward gravity modeling, ‘calculated’ and ‘observed’ gravity anomaly curves along constructed transects. Progressive improvements in the gravity modeling for both transects are presented (Figs. 5.2-5.5) along with the representative densities for each unit.

5.2.1 Transects 19

The gravity modeling of this transect, as mentioned earlier, has been divided into two progressive steps of improvement. Transect 19A (Fig. 5.2) represents the initial regional gradient based on the interpreted depth-converted seismic profile of Rosendahl et al. (2005). The model portrays a stepwise dipping from the continental domain to the oceanic domain, following the deepening in bathymetry. Seven compartments were modeled and listed as: post-rift; syn-rift; crust; lower crustal body; proto-oceanic crust and oceanic crust. All segments were assigned representative densities on the basis of the velocity used for depth conversion.

The anchored point is positioned far into the oceanic crust and the discrepancies between the calculated and the observed gravity anomalies were very minimal or virtually absent within the oceanic crust domain, except around the oceanic seamount at about 470 km. The existence of this seamount has also been observed on the gravity map (Fig.3.4) and the seamount is probably related to fault leakages along the Cameroonian volcanic line or along flow lines. The important areas of concern in gravity modeling are related to the continental crust and basement relief where the discrepancies/misfits between the calculated and observed gravity responses were quite high, with a mean residual gravity error of ~41 mGal (Fig 5.2).

This considerable misfit in the initial model resulted in questioning the geological geometry and re-evaluating the interpreted published seismic reflection data of Rosendahl et al. (2005) with the same seismic lines interpreted by Rosendahl and Groschel-Becker (2000). The following steps were taken in an effort to minimize the misfit: (1) re-configuring the geometry of the basement relief (i.e. excluding the lower crustal body, LCB); (2) varying the densities within the shallower parts of the basement relief to reflect the influence of intrusives/volcanics on the sedimentary units; (3) inclusion of onshore structural and stratigraphic features; (4) placing the faults related to the shallower parts of the basement relief at their appropriate positions and (5) finally, constraining the onshore areas based on published geological input.

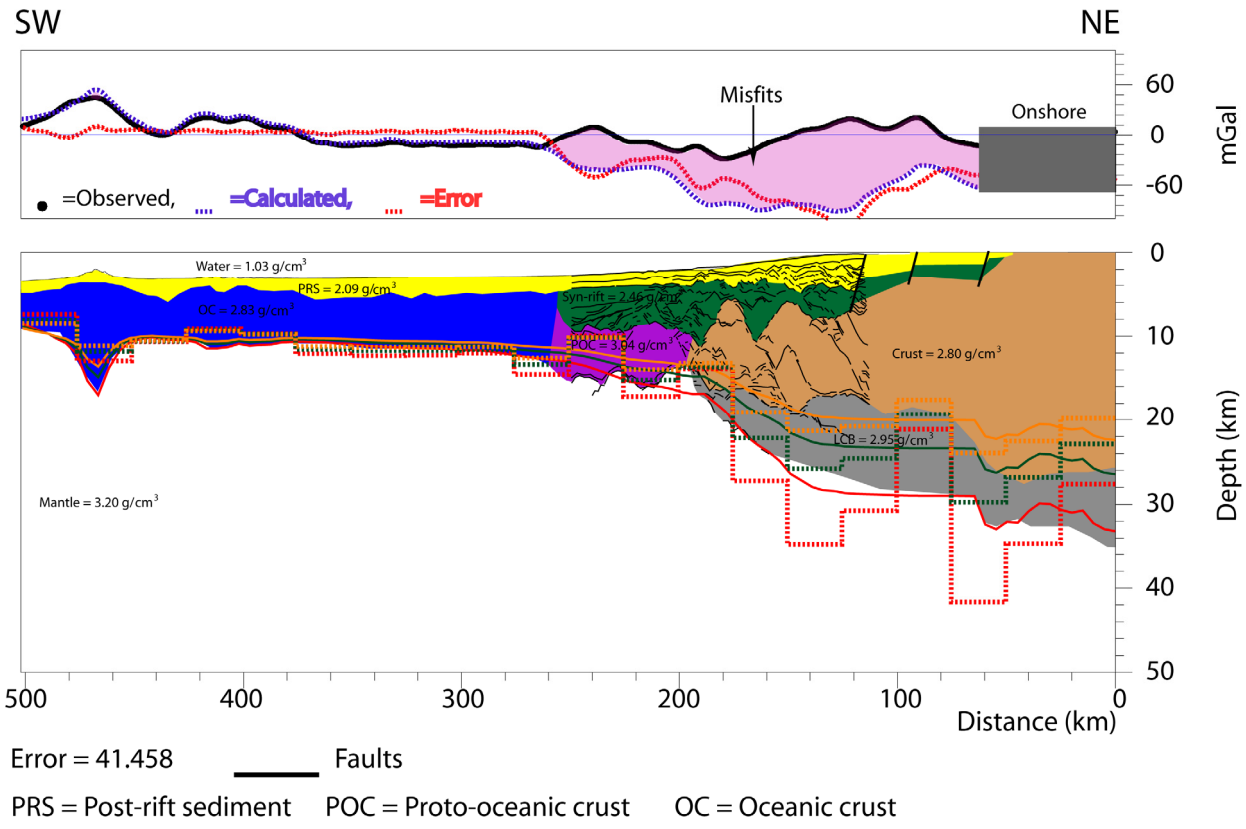

Fig. 5.2: *Initial crustal-scale 2D forward gravity modeling for Transect 19 (A). Transect location in Fig.3.1.*

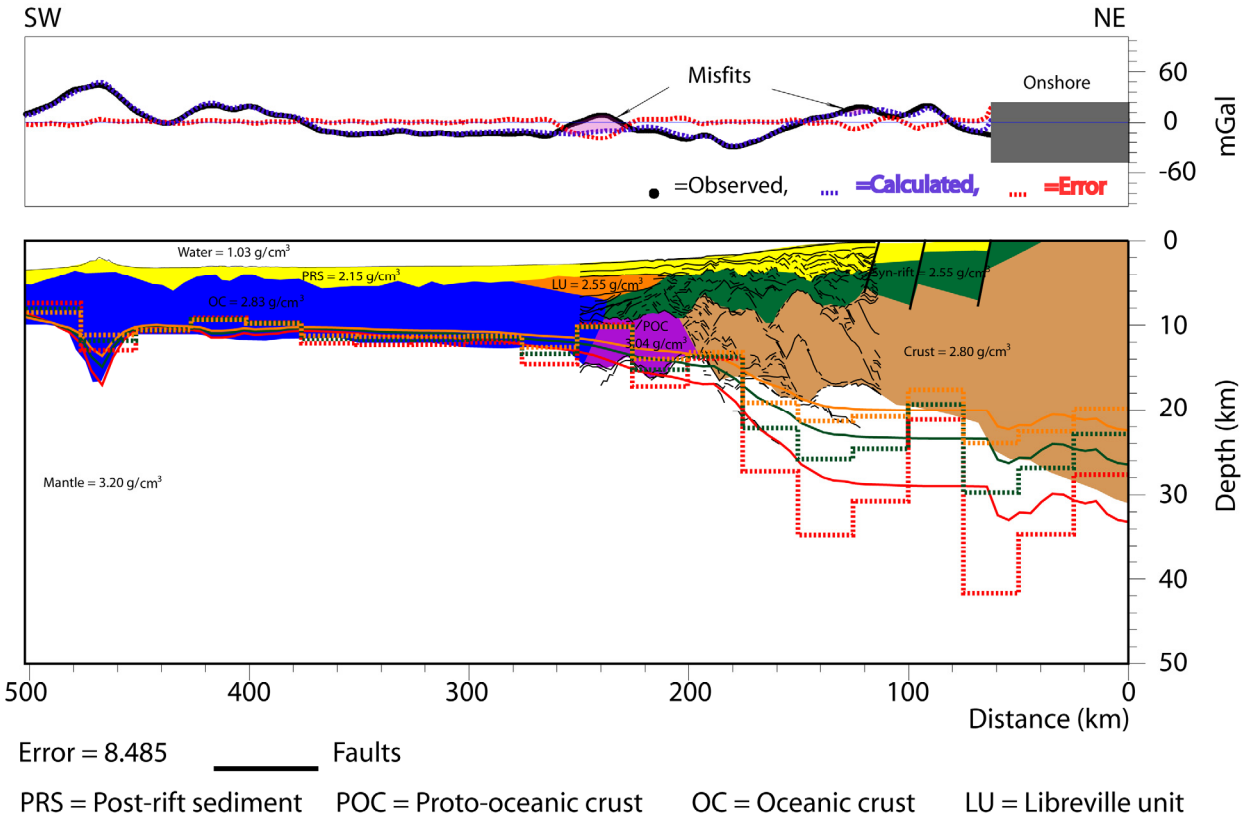

Fig. 5.3: *Final crustal-scale 2D forward gravity modeling for Transect 19. Notice the improvement.*

Incorporating these measures/steps in gravity modeling of Transect 19 ensured that most uncertainties are reduced to a minimum and at the same time evolving a model that is geologically realistic. There is now a better correlation between the calculated and observed gravity anomalies in Fig. 5.3, although few misfits are still evident at distances of 220-250 km (the most prominent one) and ~120 km. The resulting mean residual error of 8 mGal in gravity modeling is within the acceptable margin of error for a regional transect.

5.2.2 Transect 20

The gravity modeling of Transect 20 was constrained in part by the knowledge gained from Transect 19 and two progressive steps were also evolved in the modeling of the transect. The initial Transect 20A (Fig. 5.4) reflects the initial crustal geometry based on the interpreted depth-converted seismic profile and corresponding densities. The result of this modeling solution showed a mean residual error of ~21 mGal and very pronounced misfits between the calculated and observed gravity anomalies. The only exception to this trend is along the oceanic crust domain at ~370 km seaward, where there is a good fit between the observed and calculated gravity responses. There are also obvious discrepancies in the long and short wavelength distribution relating to deeper structural features and shallower basement relief, respectively. The gravity anomaly curves along this transect express a gentle undulating trend landward but increase rapidly seaward. This trend could be an expression of stretching of the crust prior to breakup or presence of pockets of local fault block shoulders seaward.

In resolving the considerable misfits of this initial gravity model, the following steps were taken: (1) referring to the interpreted seismic profiles of Rosendahl et al. (2005) compared with Rosendahl and Groschel-Becker (2000) for Transect 20, e.g. placing the position of the top continental crust (as interpreted by Rosendahl and Groschel-Becker, 2000) higher than the position interpreted by Rosendahl et al. (2005); (2) placing the faults on the structural map at their exact position during the modeling process; (3) the onshore geology, structural architecture, and stratigraphic distribution was also evaluated and incorporated in to the final model; (4) better constrained densities were assigned to the sedimentary units on the basis of burial and thickness, volcanic intrusions, presence of seaward dipping reflectors, and the consideration of Libreville unit to be volcanic as earlier proposed (e.g. Rosendahl et al.,

2005); and (5) insertion of an intra-crustal body with higher density to account for the large discrepancy between the calculated and observed gravity anomaly at ~85-130 km distance.

The need for the insertion of this intra-crustal body is further supported by the inverse modeling gravity response derived with TAMP, at about equivalent distance. The inverse modeling response on this part of the crystalline basement is abruptly elevated in comparison to adjacent trends. Thus, the presence of a massive body within the crust is suspected. The final gravity modeling (Fig. 5.5) is better improved, geologically more realistic and the corresponding residual error is within acceptable mean margin of ~10 mGal.

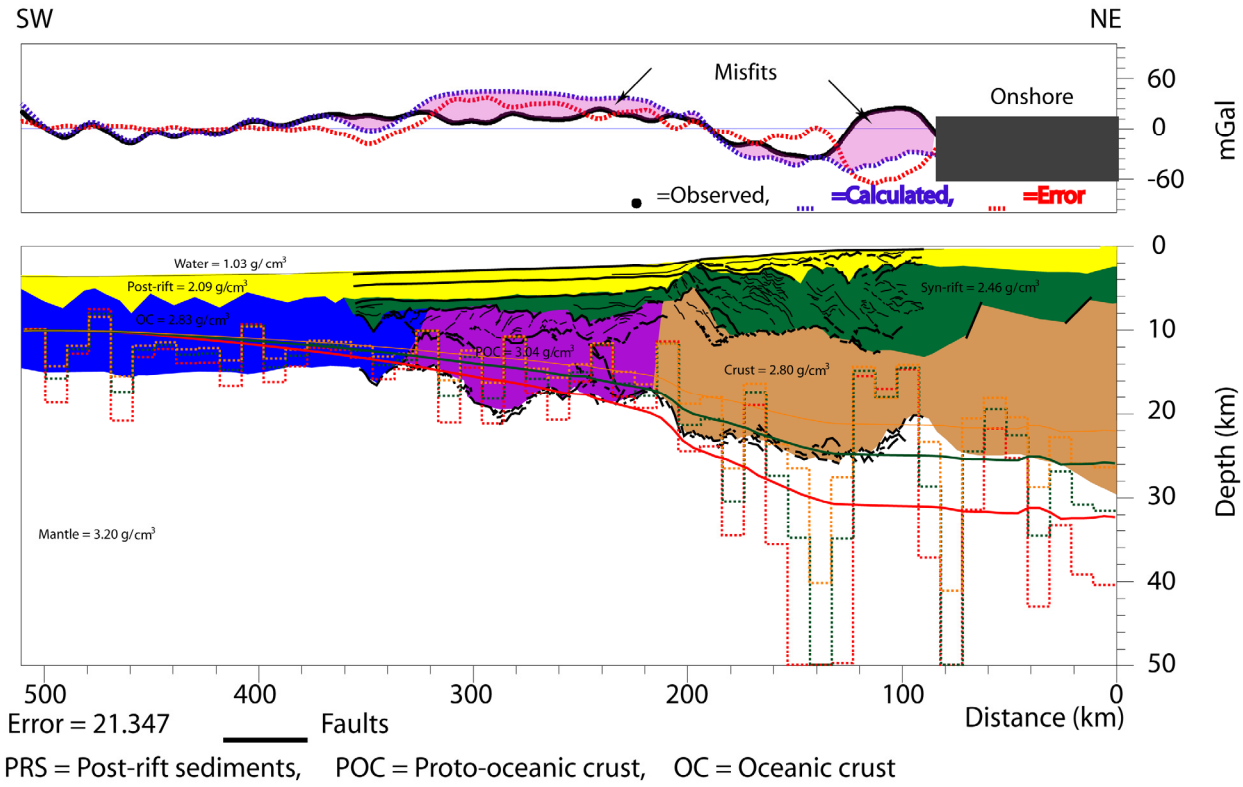

Fig. 5.4: *Initial crustal-scale 2D forward gravity modeling for Transect 20 (A). Transect location in Fig.3.1.*

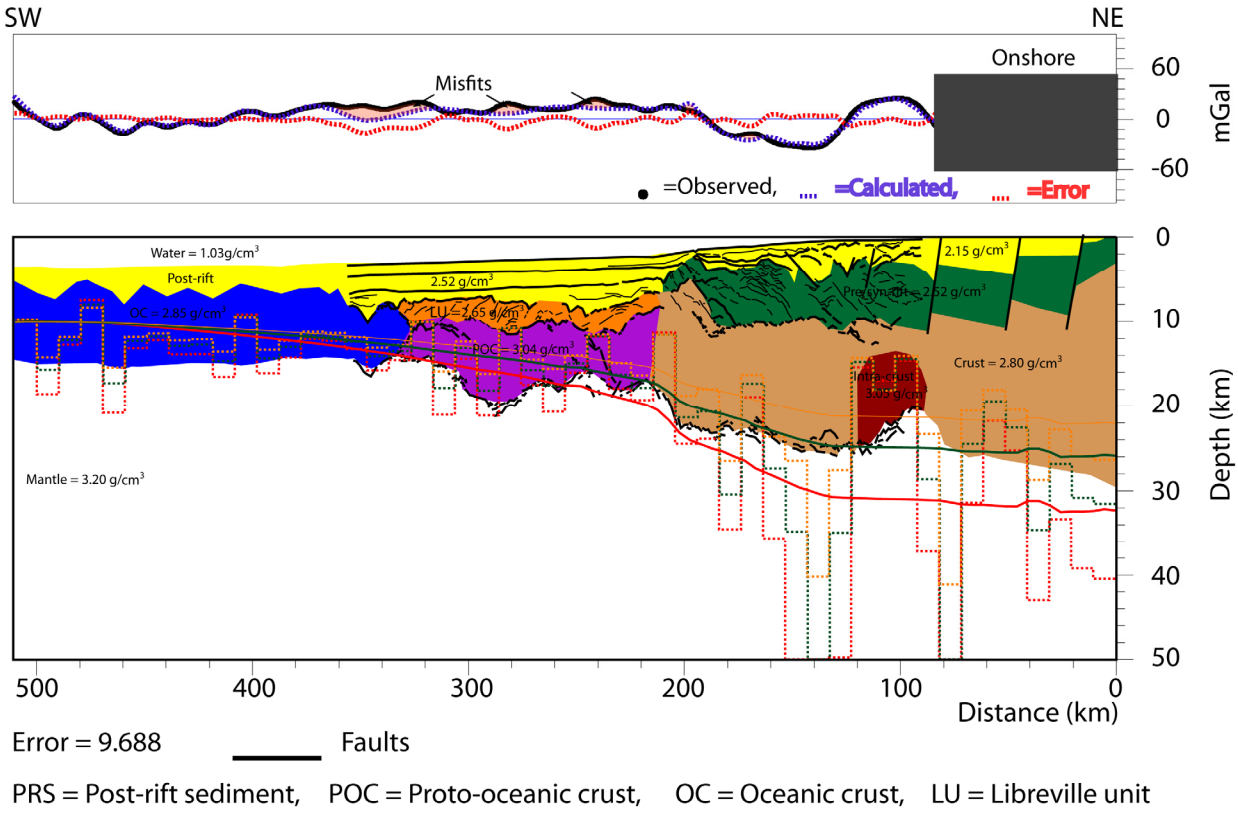

Fig. 5.5: *Final crustal-scale 2D forward gravity modeling for Transect 20. Notice the improvement.*

Onshore-offshore geologic correlation

The onshore structural and stratigraphic framework of the study area was incorporated into the final models. Despite the absence of onshore gravity for the study transects, the regional geology map of northern Gabon (Teisserenc and Villemin, 1990) was imposed on the gravity map (Fig. 5.6), and used to constrain and delineate the stratigraphical and structural trend along each transect. This approach was useful in identifying the onshore stratigraphic correlation and the position of the basement along each transect.

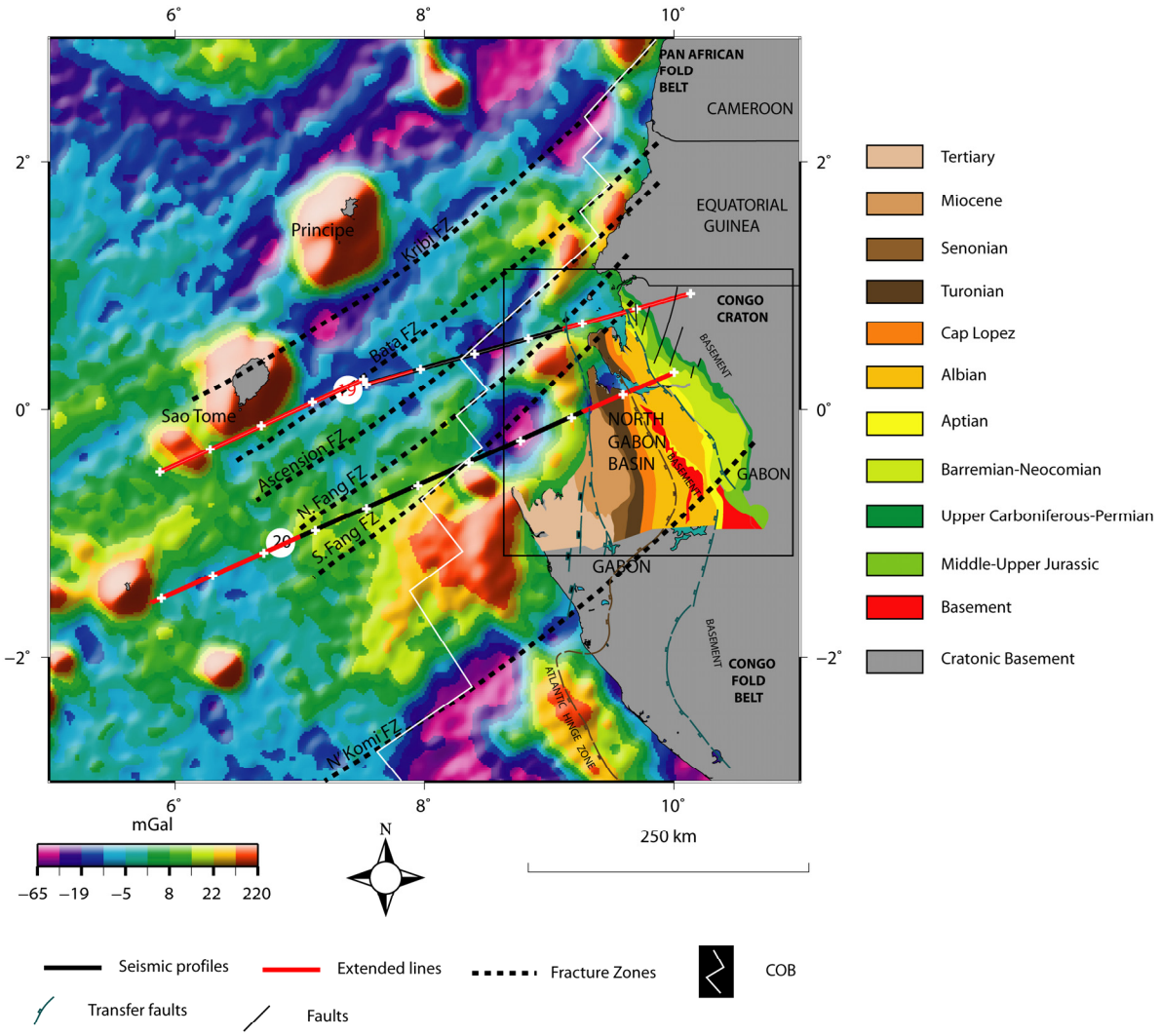

Modified geologic map of North Gabon (Teisserenc and Villemin, 1990) imposed on gravity map of the study area.

***Fig. 5.6**: Onshore structural and stratigraphic framework shown in relation to the regional transects COB, interpreted by Meyers et al. (1996).*

Chapter 6

Discussion

6.1 Geological models

The proposed geological models for this study (Fig. 6.1) were achieved through the complementary role of refined seismic interpretation and gravity modeling. The main highlights leading to the proposed models will be discussed in view of the alternative published seismic reflection interpretation of Rosendahl and Groschel-Becker (2000) for profiles 19 and 20. As earlier stated in Chapter 3, the initial multichannel seismic (MCS) interpretation was based on the published profiles of Rosendahl et al. (2005). However, in the course of gravity modeling, prominent misfits were detected between the observed and calculated gravity anomalies. Several sensitivity steps were taken mainly through a trial- and-error approach to improve the models based on the interpreted seismic reflection profiles (e.g. slightly adjusting the geometry and densities of the identified layers). In spite of these measures, the resultant mean residual errors were still considerably high. On this basis, gravity modeling was used to evaluate two alternative interpretations of the seismic lines (Figs. 6.2 and 6.4), while the annotations used in the seismic lines are shown in Table 6.1. The two alternative interpretations were superimposed on their corresponding seismic reflection data (Figs. 6.3 and 6.5) and areas of correlation and difference were noted and incorporated into the final gravity model.

In line 19, there is a good correlation in both interpretations within the vicinity of the reflection Moho (RM) along both the continental and oceanic domains. The area of major differences is associated with the depth and relief of the top continental crystalline crust reflector. The interpretation of Rosendahl and Groschel-Becker (2000) placed the top basement reflector shallower (i.e. ~2 s twt) than that interpreted by Rosendahl et al. (2005), where it was positioned at ~4 s twt (Fig. 6.2). The implication of this new interpretation is that the basement being brought to a shallower depth will consequently increase the area of the polygon covered by crystalline crustal density. Incorporating and computing this difference into the gravity modeling improves the gravity response and reduces the misfits.

In line 20, there is also a good correlation between the published interpretations of the profile by Rosendahl et al. (2005) and Rosendahl and Groschel-Becker (2000), especially with respect to basement relief. The area of disagreement is beneath the proto-oceanic crust (POC) domain of Rosendahl et al. (2005) and the equivalent outer high (OH) of Rosendahl and Groschel-Becker (2000) (Fig. 6.5). Constraining this shallowing of the reflection Moho (RM) in gravity modeling significantly improved the model and reduced the misfit.

Therefore, the interpretations of Rosendahl and Groschel-Becker (2000) are most preferred to be representative of the relief that best fits the gravity models of this study.

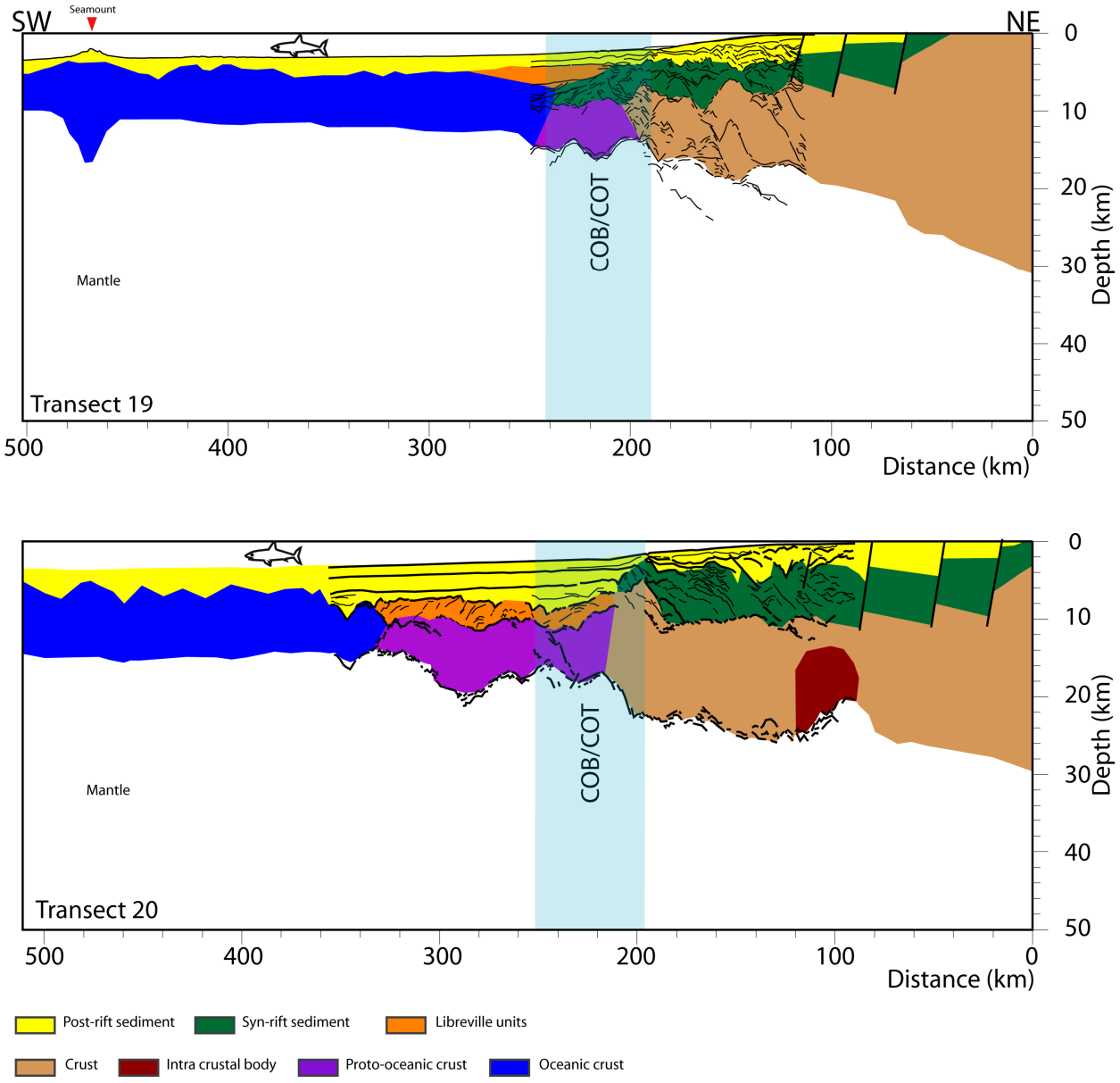

Fig. 6.1: *Crustal scale geological models for the study area.*

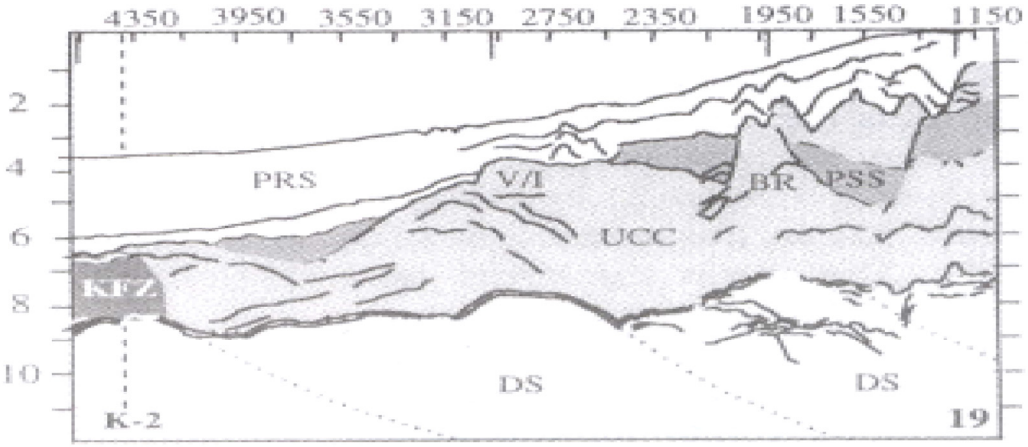

Interpretation by Rosendahl and Groschel-Becker (2000)

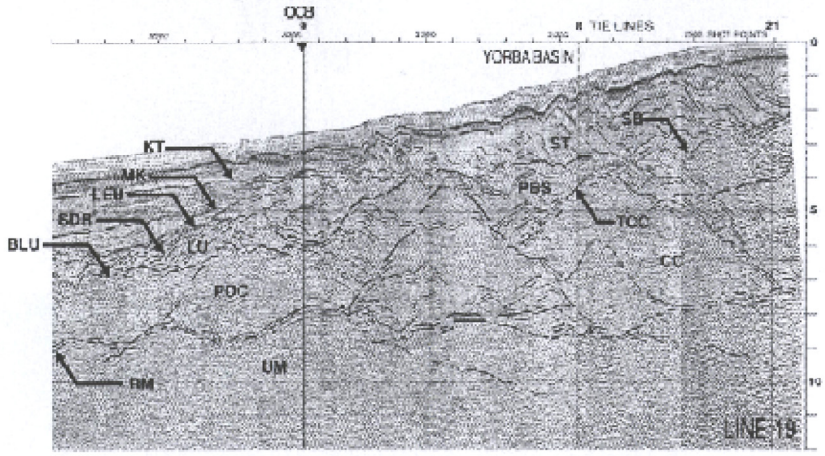

Interpretation by Rosendahl et al. (2005)

Fig. 6.2: *Seismic interpretations of Rosendahl and Groschel-Becker (2000) and Rosendahl et al. (2005) for line 19.*

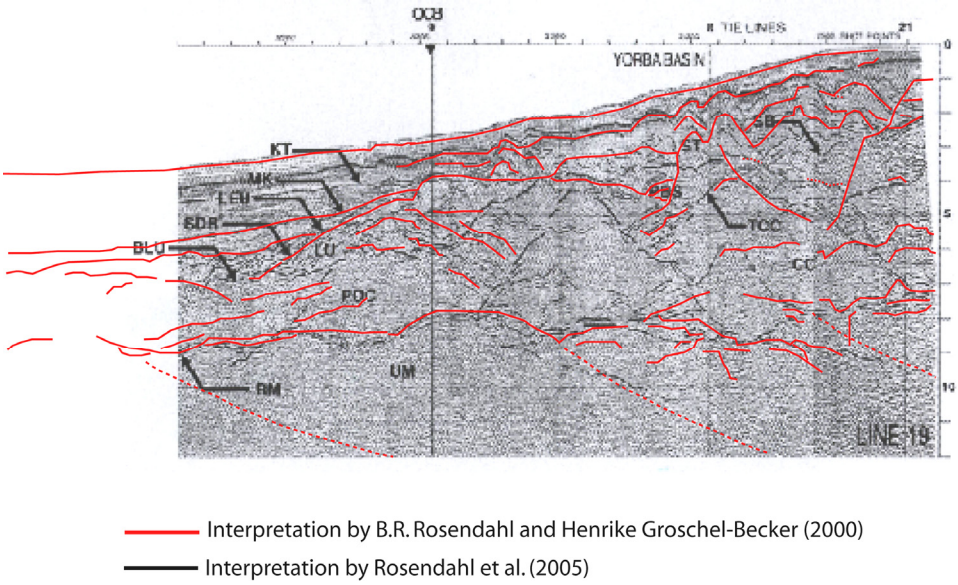

Fig. 6.3: *Correlation of seismic interpretations of Rosendahl and Groschel-Becker (2000) and Rosendahl et al. (2005) for line 19.*

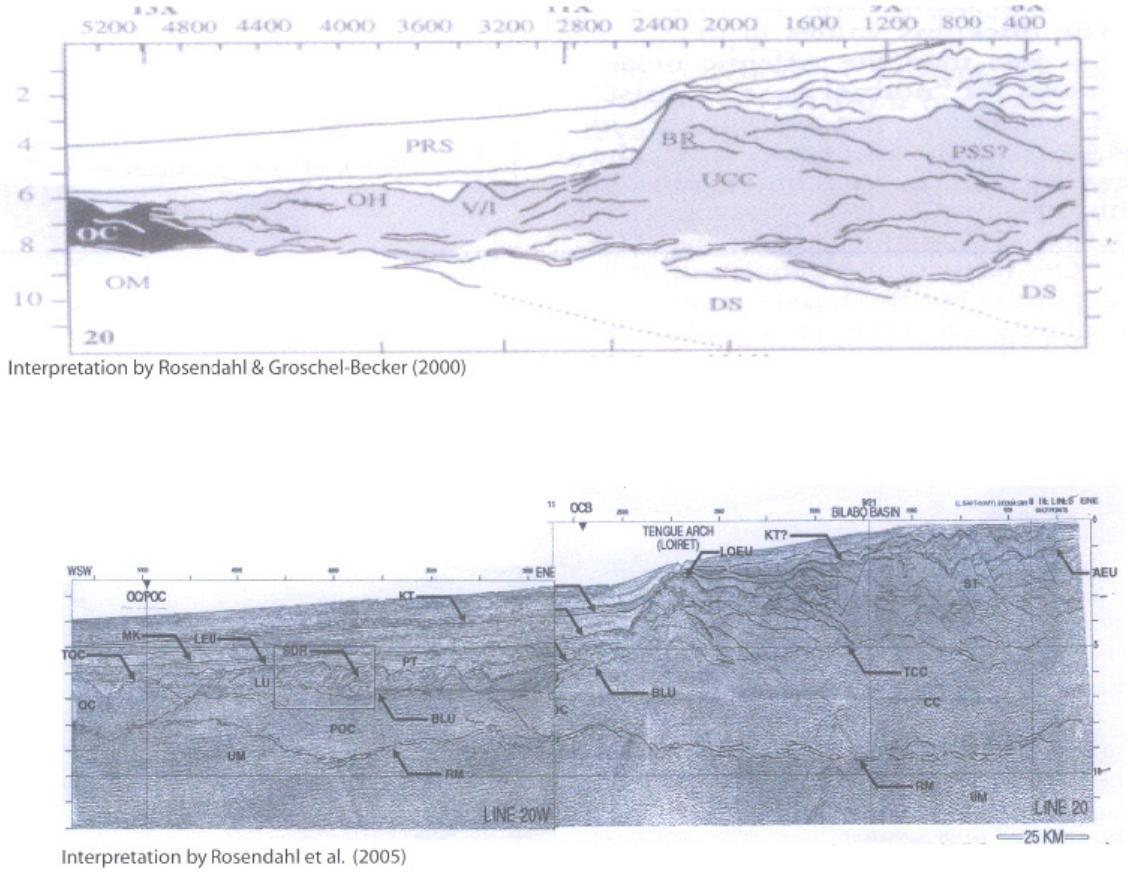

Fig. 6.4: *Seismic interpretations of Rosendahl and Groschel-Becker (2000) and Rosendahl et al. (2005) for line 20.*

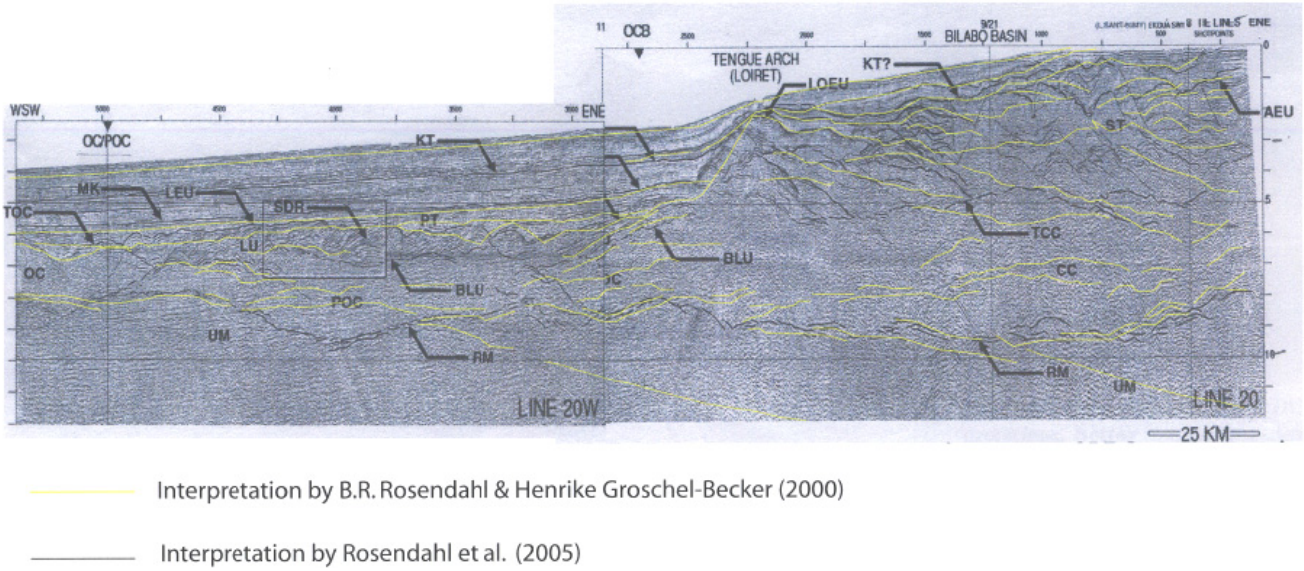

Fig. 6.5: *Correlation of seismic interpretations of Rosendahl and Groschel-Becker (2000) and Rosendahl et al. (2005) for line 20.*

Rosendahl et al. (2005)		**Groschel-Becker (2000)**	
BLU	Base of Libreville unit	BR	Basement ridge
CC	Continental crust	DS	Lower Ductile Sheets which are mainly lower continental crustal and upper mantle rocks
KT	Late Cretaceous to early Tertiary mega-sequence boundary	KFC	Kribi Fracture Zone
LEU	Libreville erosional unconformity (top of Libreville unit; possibly coeval with LOEU)	OC	Oceanic Crust
LOEU	Loiret erosional unconformity (possible coeval with LEU)	OH	Outer High
LU	Libreville unit	OM	Oceanic Mantle
MK	Middle Cretaceous mega-sequence boundary	PRS	Post-Rift Section to be above Break-Up Unconformity and/or above Base of Salt
OC	Oceanic crust	PSS	Pre-Salt Deposits which may include sedimentary and volcanic deposits
PBS	Syn-tectonic and early post-rift fill	UCC	Upper Continental Crustal Sheets which is mainly mid- to upper-level continental crustal rocks
POC	Proto-oceanic crust (first-formed oceanic crust, relatively thick, layered, and deformed)	V/I	Volcanic/Intrusive High
PT	Platform (early to middle Cretaceous carbonate platform constructed on LU)		
RM	Reflection Moho		
SB	Base of salt		
SDR	Seaward-dipping reflectors (probably subaerial volcanic flows)		
ST	Salt (evaporites)		
TCC	Top of continental crust		
TOC	Top of oceanic crust		
UM	Upper mantle		

Table 6.1: *Seismic annotations of profiles 19 and 20*

6.2 Continent-ocean transition

The location of the continent-ocean transition (COT) has been indicated in many crustal-scale studies to correspond to areas of abrupt crustal thinning, depicting a shallowing of the Moho discontinuity (e.g. Keen and Dehler, 1997; Karner and Driscoll, 1999; Tsikalas et al., 2005; Blaich et al., 2008). This expression is observed in the multichannel seismic profiles (MCS) used for this study and in the TAMP modeling results (Figs. 4.4-4.9). The feasibility of this scenario according to Keen (1987) and Buck (1991) is possible if extension prior to breakup is of short duration and associated with high strain rates.

The continent-ocean boundary/transition in the study area is effectively a subsidence boundary that separates deeply subsided oceanic crust and proto-oceanic crust from elevated continental crust across a relatively narrow transition (Rosendahl et al., 2005). The presence of this narrow margin/transition could also be a consequence of colder initial geothermal regimes and stronger rheologies (e.g. Bassi et al., 1993). This transitional window between the continental and oceanic domain is clearly defined by a pronounced negative to positive gradient in the Bouguer-corrected gravity field (Fig. 3.5). The proposed continent-ocean boundary of Meyers et al. (1996) was situated within this window. Furthermore, the transition from the continental to oceanic domain covers an intermediate unit referred to as proto-oceanic crust (POC) (Rosendahl et al., 2005). This unit, as will be described below, is neither fully oceanic nor continental.

To constrain the proposed COB/COT, potential field data (Figs. 4.10-4.11) were used. Additional constraints were based on the MCS profiles. The location of the exact position of the continent-ocean boundary is uncertain when correlated with the expression of the Bouguer gradient. This gradient is not characterized by a strong positive-negative gradient, but a gradual ascending gradient that extends ~60 km for both transects (profile distances ~190-250 km; Figs. 4.10-4.11) and reflects a shallowing of the Moho (i.e. crustal thinning). Similarly, the magnetic field expression at the same distance shows a sudden change in the amplitude response. Therefore, it is most likely that the COB is located within this zone. The 2D forward gravity modeling (Figs. 5.2-5.5) supports this position by the abrupt shallowing of the Moho at ~220-240 km distance. The location of the COB/COT in the seismic reflection profiles of Rosendahl et al. (2005) coincides relatively with this position.

6.2.1 Proto-oceanic crust

In the study area, the transition from continental to oceanic crust occurs across an intermediate zone referred to as the proto-oceanic crust (POC). POC is a heterogeneous type of crust that usually grades seaward into normal oceanic crust. It may have been formed by volcanic effusion of partial melt at the time of continental rupture, and also during initial seafloor spreading. The proto-oceanic crust has been described in different studies as: initial oceanic crust; abnormal crust; fracture zone crust; transitional crust; seaward-dipping volcanic wedges; attenuated continental crust; outer highs; and proto-oceanic crust (e.g. Groschel-Becker, 1996; Meyers, 1995; Meyers et al., 1996a-b; Rosendahl et al., 1991, 1992a; Rosendahl and Groschel-Becker, 1999, 2000; and Wannesson et al., 1991; Wilson et al. 2003). Some studies have defined the proto-oceanic crust as neither purely oceanic nor purely continental in composition and structure (e.g. Wilson et al., 2003), while Rosendahl et al. (2005) define this crust as being fundamentally oceanic in nature. They further presented the idea that all segments of proto-oceanic crust are variants of oceanic crust because the thermal subsidence of POC behaves similarly to that of oceanic crust and that the anomalous magnetic response observed across the proto-oceanic crust requires magnetic susceptibility values of basaltic rocks. This anomalous magnetic response was also observed along the transects in this study (Figs.4.10-4.11).

The composition of proto-oceanic crust (POC) is variable, forming a faulted complex terrain. It could be made up of abducted material, possibly mixed with continental fragments. Meyers et al. (1996) described POC to be composed of (1) highly attenuated blocks of rifted continental crust (RCC), (2) wedges of seaward-dipping reflectors (SDRs) which are presumed to be made up of intermixed mafic volcanics and sediments, (3) mafic lower crust, and (4) possible uplifted mantle rocks. In addition Meyers et al. (1996) characterized POC as expressing variable seismic topography, thickness and width along fracture zones. They further suggested that proto-oceanic crust is probably made up of a combination of dislocated and dike intruded continental blocks, underplated mafic magma, thick volcanic accumulations, unroofed mantle, and sediments eroded from the uplifted rift flanks.

The differences observed in the widths of the proto-oceanic crust in both Transects 19 and 20 (Fig. 6.1) can be attributed to the following factors: (1) the geometry and segmentation of the continent-ocean boundary along fracture zones (Fig. 2.4), (2) segmentation due to volcanism

and extension within rift unit (Meyers et al., 1996), (3) localized mantle diapirism within a spreading cell and eventual outpouring of volcanics (Meyers et al., 1996). Therefore, fracture zones or spreading units play a major role in the distribution of magmatism. It is observed that transform and rifted margin settings also controlled the different width of the proto-oceanic crust (POC) with respect to the geometry of the continent-ocean boundary. In areas where the proto-oceanic crust is broad it correlates with oblique transform segment (e.g. Transect 20) and it is narrow along rifted margin segments (e.g. Transect 19). The continent-ocean boundary along Transect 20 is close to a fracture zone (i.e. S.Fang Fracture Zone) and extends over a wider offset. This could be the expression of the wider width of the proto-oceanic crust (POC) along Transect 20. However, in Transect 19 the rift-shear intersection of the continent-ocean boundary with the Ascension Fracture Zone is sharp. This could explain the narrow width of proto-oceanic crust (POC) along Transect 19. Furthermore, the crust is thinner landward of the continent-ocean transition in Transect 19 than in Transect 20 (Fig. 6.1). This is evidence that Transect 19 has been significantly stretched. Therefore, it is a plausible reason why the POC is narrower in Transect 19 than in Transect 20.

The crustal density of African proto-oceanic crust according to Rosendahl et al. (2005) is at least as great as that of the oceanic crust and possibly higher. This has been confirmed by adjacent gravity modeling studies in part of Equatorial Guinea (e.g. Wilson et al., 2003), where three segments of proto-oceanic crust were investigated through gravity modeling and were found to fit the proposed model with density values ranging from 2.85-3.10 g/cm^3. These high values were attributed to the presence of varying proportion of peridotite which probably emanates during rifting, along fracture zones or from mantle upwelling.

Libreville unit

The Libreville unit has been described to be a Lower Cretaceous angular and erosional unconformity (e.g. Rosendahl et al., 2005). This unit features prominently seaward of the study area and is located in the upper part of the POC (Figs. 3.8-3.9). The interval velocities within the unit according to Rosendahl et al. (2005) exceed 4.5 km/s, as observed in the gravity modeling for transects 19 and 20, where the crustal density of 2.55 g/cm^3 (velocity ~4.9 km/s) and 2.65 g/cm^3 (velocity ~5.5 km/s), respectively, were utilized (Figs. 5.3 and 5.5). The Libreville unit is characterized by pods of seaward-dipping reflector sequences (SDRs) as expressed in the seismic profiles (Figs. 3.8-3.9). The seaward-dipping reflector

sequences (SDRs) vary in sizes and widths. They occur at boundaries that connect rifted continental crust (RCC) and proto-oceanic crust (POC) (Figs. 3.8 and 3.9). Rosendahl et al. (2005) proposed that the Libreville unit might be a mixture of volcanics and sediments. However, they argued that until drill holes penetrate this unit, the origin will still be arguable. They agreed that the African Libreville unit has been sub-aerially exposed (or nearly so) and eroded over a significant period of time, over a broad area. This implies that the unit was emplaced prior to appreciable subsidence of the proto-oceanic crust (POC).

Rosendahl et al. (2005) further indicated that the conjugate Brazilian proto-oceanic crust equivalent of the study area exhibits even more pronounced SDRs within the unit equivalent to the Libreville unit. The conjugate Brazilian SDRs have been interpreted as volcanics related to early opening of the South American and African plates and associated with the formation of oceanic spreading centers (Mohriak et al. 1995a-b, 1998, and 2000a-b). The observed magnetic character within the proto-oceanic crust (Figs. 4.10 and 4.11) and the high interval velocities and density used in the gravity modeling within the seaward-dipping reflectors suggest a probable volcanic origin for the Libreville unit.

6.2.2 Crustal thinning

The progressive crustal thinning across the margin for both transects (Fig. 6.1) stretches from the northeast to the southwest towards the oceanic domain. The Aptian breakup unconformity as recorded in the Gabon Basin (Reyre, 1984a; Teisserenc and Villemin, 1989) was attributed to basinward migration of the rift flank uplift and associated erosion of rift continental features during rift propagation into the oceanic domain. The resultant uplift is feasible, where crustal thinning is greater than the isostatic compensation of the underlying mantle (Braun and Beaumont, 1989), and/or crustal buoyancy from the addition of partial melt below the rift zone (Bonatti and Seyler, 1987). The zone of continental rupture may have been initiated above the thinnest zone of stretched and reheated lithosphere, where mafic melts were injected as dikes into thinned blocks of rifted continental crust (RCC), perhaps accompanied by thermal uplifts (Chalmers, 1991; Bohannon and Eittreim, 1991; Keen et al., 1991). The emplacement of proto-oceanic crust (POC) may have occurred where blocks of rifted continental crust became detached and entrained in the newly formed mafic volcanic crust. Thinning of the rifted continental crust (RCC) across transform-faulted margin segments may be in response to transtensional faulting; erosion of the margin in response to thermal uplift

that is associated with passing of the spreading ridge; and assimilation of the rifted continental crust into the passing spreading ridge (e.g. Scrutton, 1982; Mascle and Blarez, 1987; Todd and Keen, 1989; Reid, 1989; Lorenzo et al., 1992; Lorenzo and Vera, 1992). It is observed that the continental crust is thinner in transect 19 within the vicinity of the continent-ocean transition than in Transect 20.

6.3 Conjugate margins

In many ways, the study area is characterized by oblique opening which resulted from varied transtensional regimes (Fig. 6.6). The area of interest for a conjugate margin discussion is bounded by the Ascension Fracture Zone (AFZ) in the north and the N'Komi Fracture Zone (NFZ) in the south (Fig. 6.6).

The Equatorial Guinea and northern Gabon margins are part of the West African margin which is the conjugate equivalent of the northeastern Brazilian Sergipe-Alagoas margin. The conjugate margins are characterized by having similar tectonic and structural evolutionary features. The margin setting between the conjugate pair of Brazil and Gabon fits into the larger similarities abound in the pre-breakup Brazil-West Africa geological evolution of the margins (Fig. 2.1). These similarities include: (1) Late Jurassic sedimentary strata which consist of coarse grained fluvial sandstones that infill the Afro-Brazilian depression prior to the breakup of the South Atlantic; and (2) segmentation of the margins which is attributed to the influence of oceanic fracture zones that intersect both crustal margins (Fig. 6.7) (although segmentation could also be inherited, giving rise to oceanic fracture zones). Expression of prominent bathymetric structures, transform and transfer faults and oceanic seamounts are distinct features on both sides of the margins. Oblique extension and strike-slip movements are also characteristic trends on the conjugate margins.

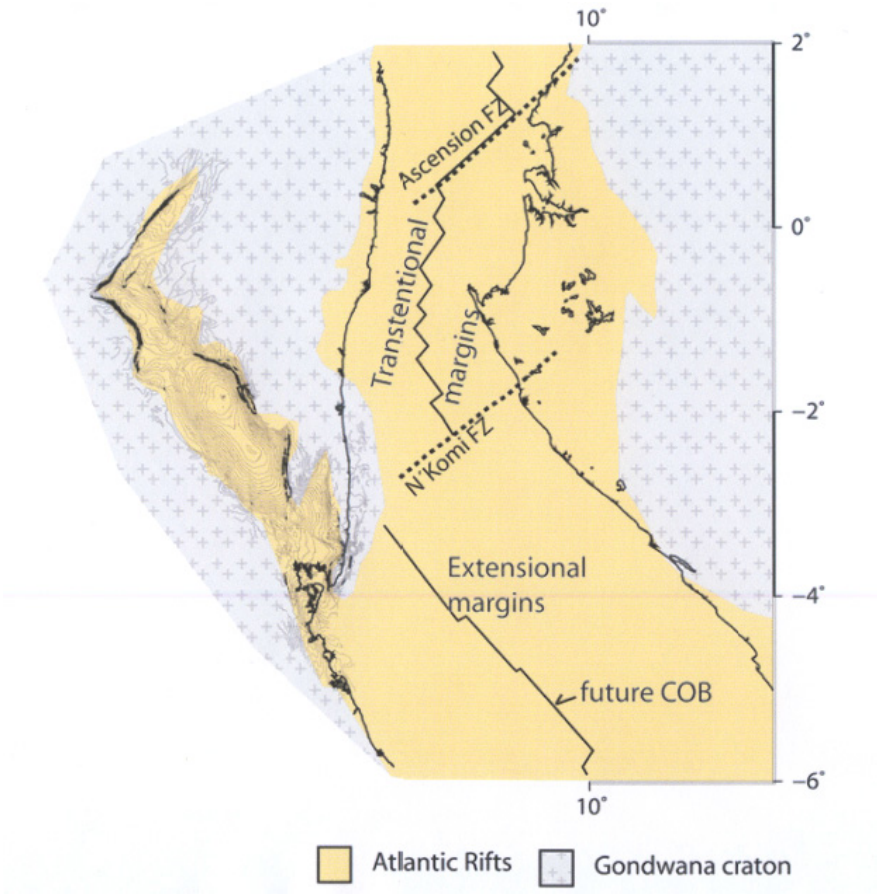

Fig. 6.6: *Initial fit between Africa and South America (Blaich et al., 2008).*

Blaich et al. (2008) argued that the along-margin changes observed in several crustal-scale transects are closely related to a number of fracture zones that affected the northeastern Brazilian margin as well as its conjugate West African margin (Fig. 6.7). Furthermore, the conjugate Salvador-N'Komi and Maceió-Ascencion fracture zones, that stretch across these margins, appear to be first-order structural elements, governing the segmentation and evolution of the conjugate northeastern Brazilian and Gabon margins (Fig. 6.7) (Blaich et al., 2008).

In constraining the conjugate geological models of Brazil and northern Gabon margins, emphasis will be laid , in this study, on Transect A-A' and Transect 19 (Fig. 6.8), where a striking asymmetry typical of rifted margins was observed. These observations include: (1) shallow crustal detachment on the Brazilian side, which points to a simple-shear upper crustal deformation. In the Gabon sector, faults (shear zones) going through the whole crust and even into the mantle were observed. This could be the expression of the lower plate as indicated in

the asymmetric detachment model of Lister et al., (1991). (2) The continental crust is thicker on the Brazilian side than in the Gabon area. This is true if we do not reckon with the onshore part of Transect 19 (i.e. considering from the shelf edge seaward) as observed in Fig. 6.7 and supported by the wide-narrow conjugate pairs configurations of Blaich et al. (2008), where the region covered from the shelf edge to the continent-ocean boundary is wider in Transect A-A' than in Transect 19 (Fig. 6.7). (3) The sediment packages are thinner on the Brazilian side than in the conjugate Gabon. (4) The presence of the proto-oceanic crust (POC), seaward dipping reflector sequences (SDRs) and the wider thickness of the oceanic crust in the Gabon area is evidence of more magmatic activities than in the conjugate part (although, the presence of SDRs is recorded in Transect B-B'). However, there are similarities in the shallowing of the Moho in both transects which are related to extensional regimes. An abrupt change was also observed from the continental domain to ocean domain in Transect A-A' on the Brazilian side but for the conjugate Transects (i.e. 19 and 20), an intermediary unit (referred to earlier as proto-oceanic crust) separates the transition from continental to oceanic domain (Fig. 6.8).

Observations made on Transect 20 revealed that the thickness of the continental crust for Transect 20 is slightly thinner than the conjugate Transect B-B'on the Brazilian side (Fig. 6.9). This difference could be attributed to the onshore extension of Transect B-B' as compared to the marginal onshore extension of Transect 20 (Fig. 2.4). Despite this slight difference, the transect orientations are still within the narrow-narrow conjugate pairs configuration of Blaich et al. (2008). However, both transects are characterized by distinct shallowing of the Moho. The presence of a high velocity body (+7 km/s) in Transect B-B' under-plating the continental crust within the proximity of the continent-ocean boundary (COB) might be the conjugate interpretation referred to as proto-oceanic crust (POC) in Transect 20. This is supported by the high velocity and density assumed in the gravity modeling of this unit. Furthermore, Rosendahl et al. (2005) indicated that the conjugate Brazilian equivalent of the proto-oceanic crust exhibits even more pronounced seaward-dipping reflectors (SDRs). This high velocity unit of transect B-B, though speculative, could be related to the expressed proto-oceanic crust in Transect 20. The Brazilian seaward-dipping reflectors (SDRs) have been interpreted by Mohriak et al. (1995a, b, 1998, and 2000a, b) as volcanics related to early opening of the South American and African plates and associated with the formation of oceanic spreading centers. In general outlook, the correlation of both conjugate transects to pre-breakup (Fig. 6.8 and 6.9) reveals a correlative structural trend and along-strike continuity of the various sub-basins.

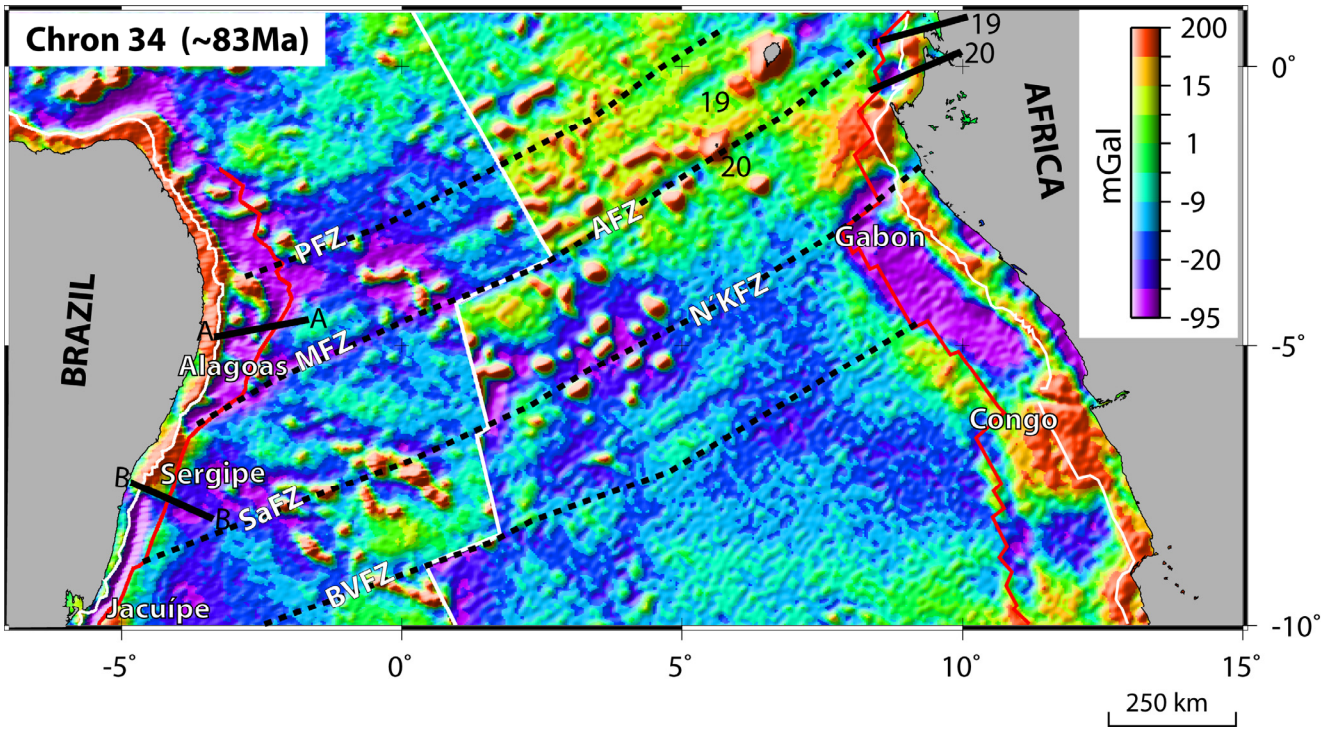

Fig. 6.7: *Correlation of conjugate margins showing location of Transects 19 and 20 with the conjugate A-A' and B-B' (modified from Blaich et al., 2008)*

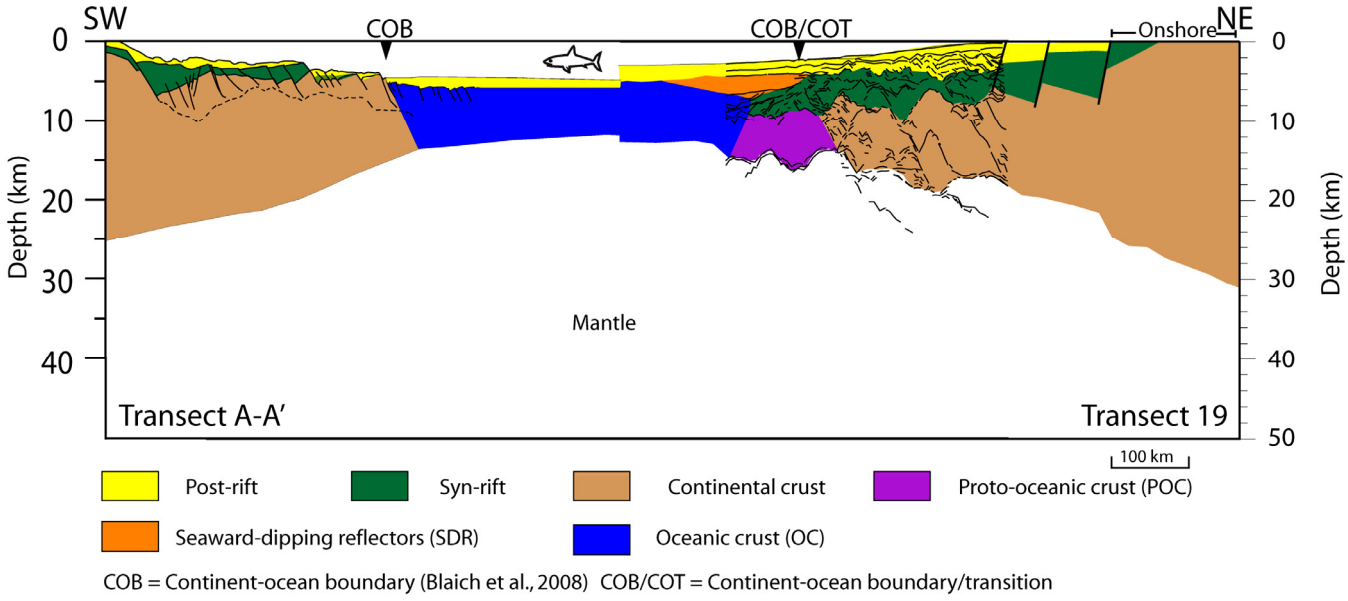

Fig. 6.8: *Modeled crustal-section of the conjugate transects between northeastern Brazil (Blaich et al., 2008) and Transect 19 (this study).*

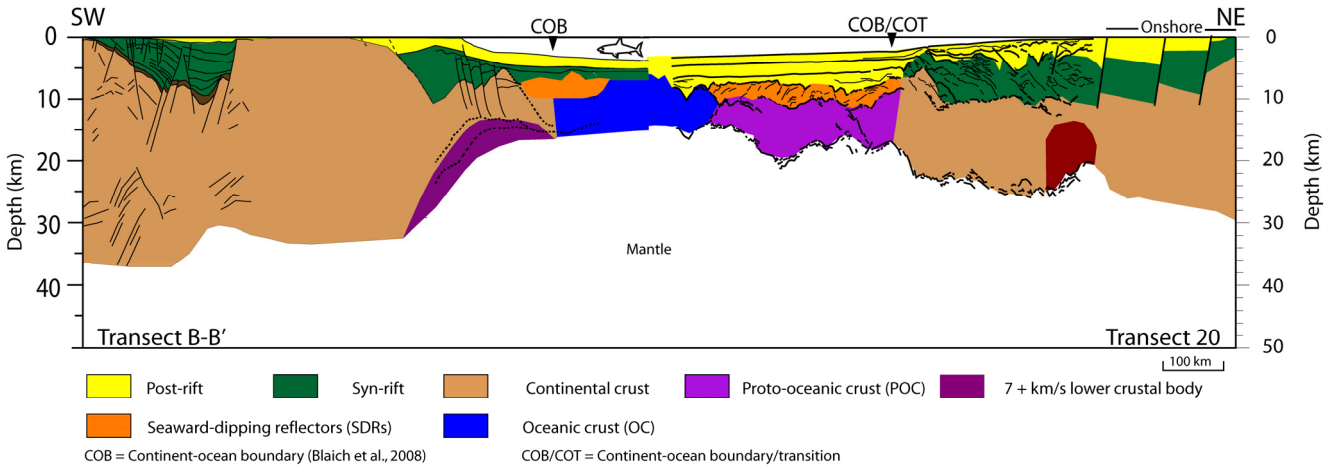

Fig. 6.9: *Modeled crustal-section of the conjugate transects between northeastern Brazil (Blaich et al., 2008) and Transect 20 (this study).*

Furthermore, the asymmetric simple-shear model for this study was constrained through the detachment model of Lister et al. (1991) (Fig. 6.10). This model emphasizes the predictions of detachment models in continental extensions resulting in asymmetric structure on all scale and reveals that asymmetry continues to be accentuated as extension goes on (Lister et al., 1991). They also suggested that complimentary asymmetry and contrasting structural and uplift-subsidence histories will characterize opposing conjugate margin pairs that have undergone continental breakup and formation of ocean basin due to extension. To this end, Lister et al. (1986) proposed two broad classes of passive margins (Fig. 6.10): (1) Upper-plate margins which consist of crust above a detachment zone and (2) Lower-plate margins made up of deeper crystalline rocks overlain by highly faulted remnants of the upper plate.

Therefore, in the proposed conceptualized conjugate model for this study (Fig. 6.11), it was observed by closing the gap to syn-breakup geometry reveals that there are elements or similarities that fit the proposed asymmetric detachment model of Lister et al. (1991). These elements include: (1) Crustal detachment as expressed in the Brazilian sector fitting well with the upper-plate detachment margin of Lister et al. (1991); (2) zones of weakness going through the crust and into the mantle, and (3) magmatic activity on the Gabon margin and the absence of such on the Brazilian side.

However, the observed discrepancy in the syn-sedimentary units of the Brazilian and Gabon sectors raises some questions. These questions are: (1) how much of syn-rift sediments is

represented in Transect 19; (2) how realistic is the whole syn-rift distribution. To constrain this scenario, again the seismic interpretation (Figs. 6.2 and 6.3) will have to be re-evaluated. Perhaps, the whole syn-sedimentary unit is segmented into thicker post-rift than what was interpreted thin syn-rift and pre-rift units. However, the seismic interpretation did not show a clear distinction of these units. Ideally, it is expected the termination of mantle upwelling and subsidence induces post-rift deposits. Therefore, it is very likely that the syn-rift unit is over-estimated. The lack of good seismic images and stratigraphic control limits ability to constrain the true nature of the syn-rift unit and it remains questionable. This hindered a perfect fit of the model in line with the proposed asymmetric detachment model of Lister et al. (1991). However, it could be a possibility that local symmetric pure shear rifting initially occurred, creating accommodation for sediment deposition.

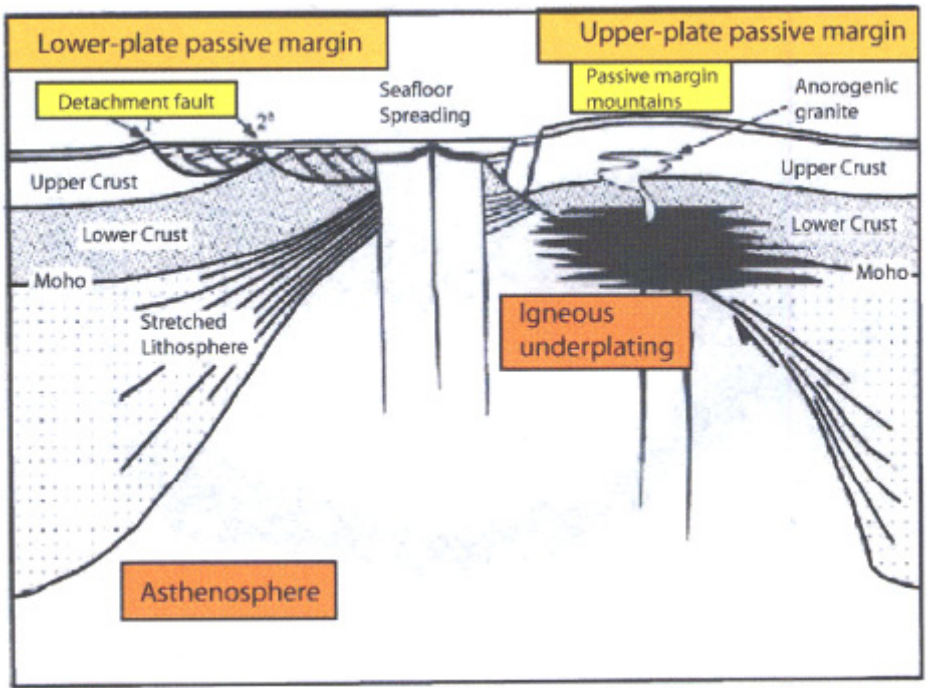

Fig. 6.10: *Upper–plate and Lower-plate passive margins resulting from continental extension by detachment faulting (modified after Lister et al., 1991).*

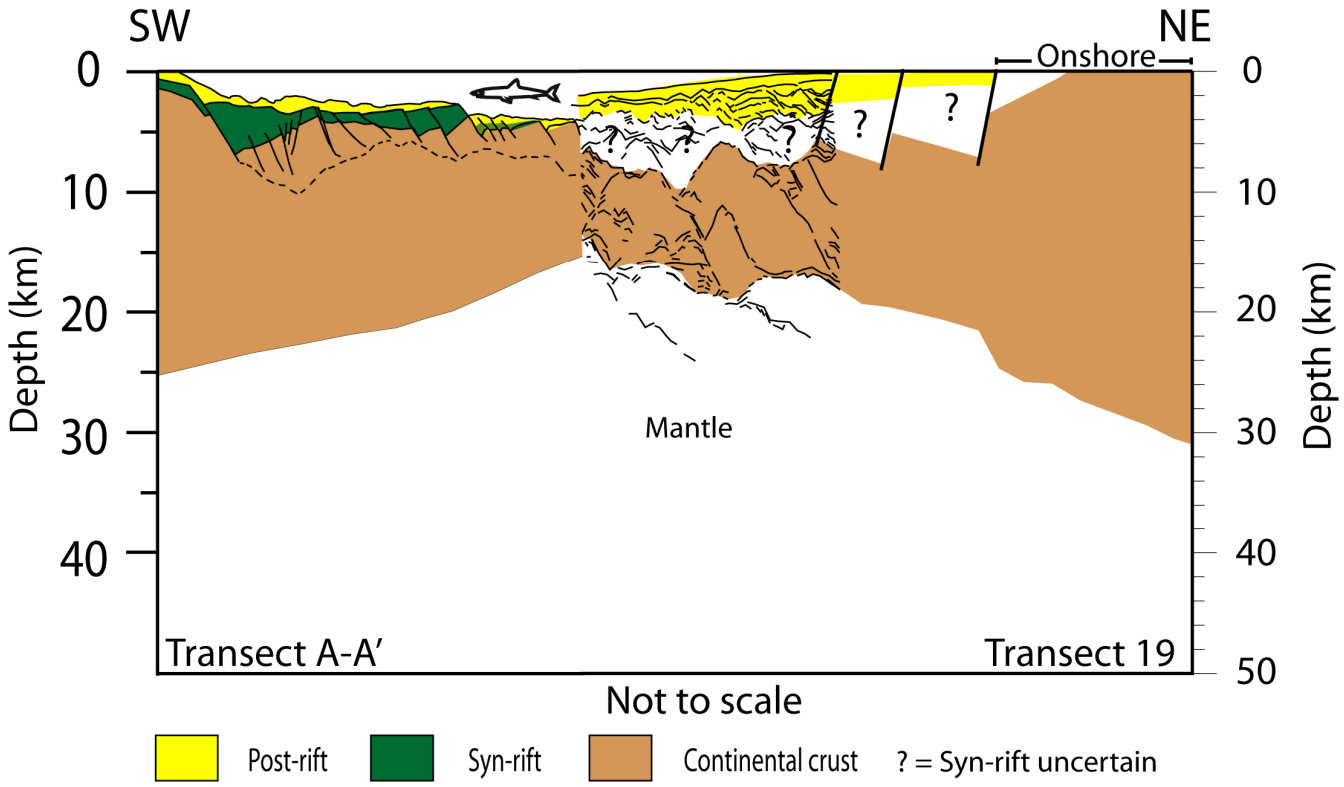

Fig. 6.11: *Conjugate crustal transect between northeastern Brazil (Blaich et al., 2008) and Transect 19 (this study) restored to the approximate position of the COB*

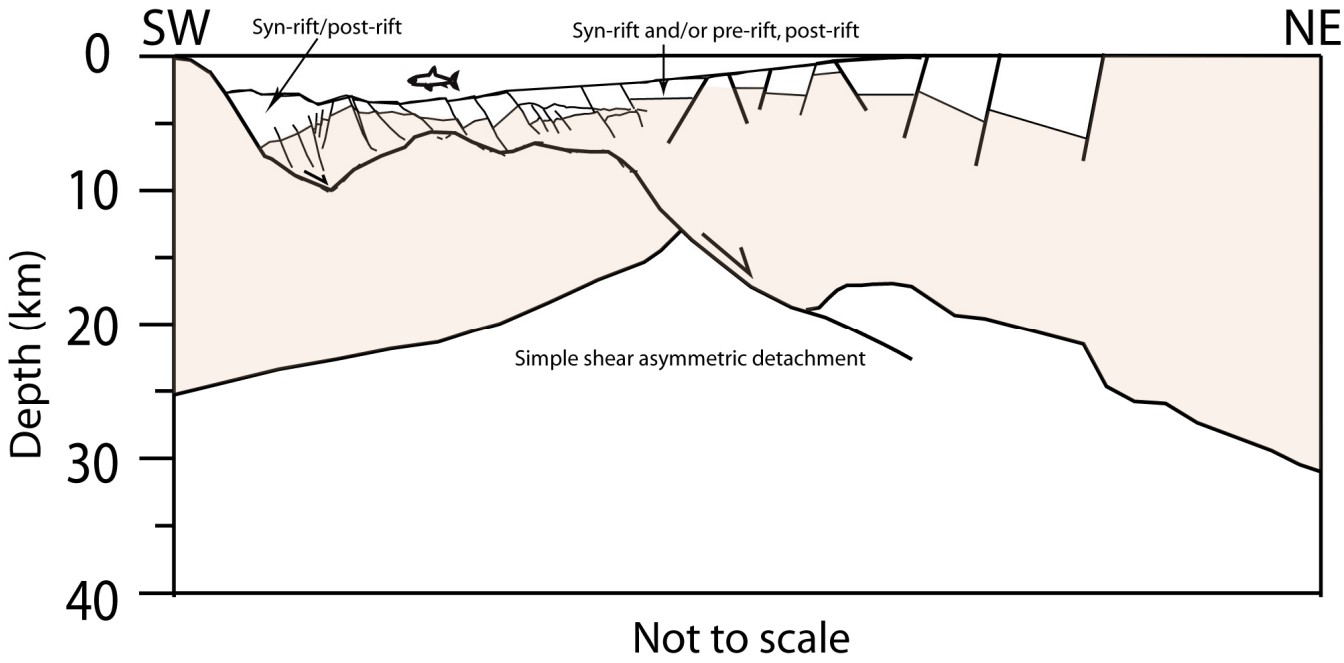

Fig. 6.12: *Simplified conceptual pre breakup model.*

The study area is covered by two tectonic hinge zones: the Eastern and Atlantic hinge zones of Karner and Driscoll (1999) (Fig. 6.13). The Eastern Hinge Zone sits onshore and delineates the eastern limit of extension. It demarcates the syn-rift sediments from the Precambrian basement. Minor faults have been suggested to occur east of the hinge zone, however, it serves as a boundary characterizing a zone of negligible extension from a zone of significantly increased extension (Watts, 1981). The Atlantic Hinge Zone is located mainly offshore and only a fraction steps onshore. The Atlantic Hinge Zone is characterized by a series of short segment, en-echelon high-standing blocks (e.g. Karner and Driscoll, 1999).

The conjugate eastern Brazilian Margin is also characterized by two subparallel tectonic hinge zones (Fig. 6.10): the western/onshore and offshore hinge zones (referred locally as the Alagoas Hinge, adjacent to the Sergipe-Alagoas Basin; Lana, 1990). The onshore/western hinge zone delineates the western extent of Neocomian extension and demarcates syn-rift sediments from Precambrian basement. Minor faulting within the adjacent basement to the west is found in the Tucano Basin (e.g. Roguel, 1990). Karner and Driscoll (1999) also suggested that the hinge zone in this conjugate part separates a region of negligible deformation from a region of severe normal faulting and accommodation generation. They also defined the offshore hinge zone which sits basinward as being constituted by a series of high-standing blocks that demarcate onshore to near shore basins from deeper water offshore equivalent basins.

6.3.1 Margin segmentation

The architectural pattern that characterized the Mesozoic rifting, breakup and early oceanic crust evolution of the South Atlantic margins has been defined by several studies to be controlled by structural inheritance and facilitated by early Precambrian continental lineaments and transfer zones (McConnel, 1974; Guazelli and Carvalho, 1978; Meyers et al., 1996).

The distinct segmentation of the studied margins is attributed to the NE-SW oriented extensional stresses which eventually reactivated Precambrian lithospheric weakness zones. Furthermore, north of the Walvis Ridge/Rio Grande Rise (Figs. 1.1, 2.3 and 6.6), rift zones characterized by varying extensional and subsidence histories are segmented by major transfer systems. These transfer systems may be expressions of the Proterozoic-mobile belt lineaments

that accreted to the African plate during the Transamazonian and Pan-African/Braziliano orogenies. It is very likely that these transfer zones are deeply buried within the crust and therefore continued basinward correlating with oceanic fracture zones (Meyers et al., 1996). The Ascension Fracture Zone (AFZ) is a major oceanic transform-faulted zone that extends into the study area. Other oceanic fracture zones that are prominent within the study area include: the N'Komi Fracture Zone, North and South Fang Fracture Zones, Bata Fracture Zone and the Kribi Fracture Zone. The NE-trending geometry of these fracture and transfer zones of variable length has made the margin to step progressively northeastward by alternating between normal and transform faulted segments, compartmentalizing and isolating, during this process, both continental and oceanic rift-units (Meyers et al., 1996). Blaich et al. (2008) have also shown that the conjugate Brazilian margin is characterized by transfer faults (e.g. Vaza-Barris) and expressions of oceanic fracture zones (e.g. Maceió Fracture Zone) that correlate with the Gabon margin (Fig. 6.7).

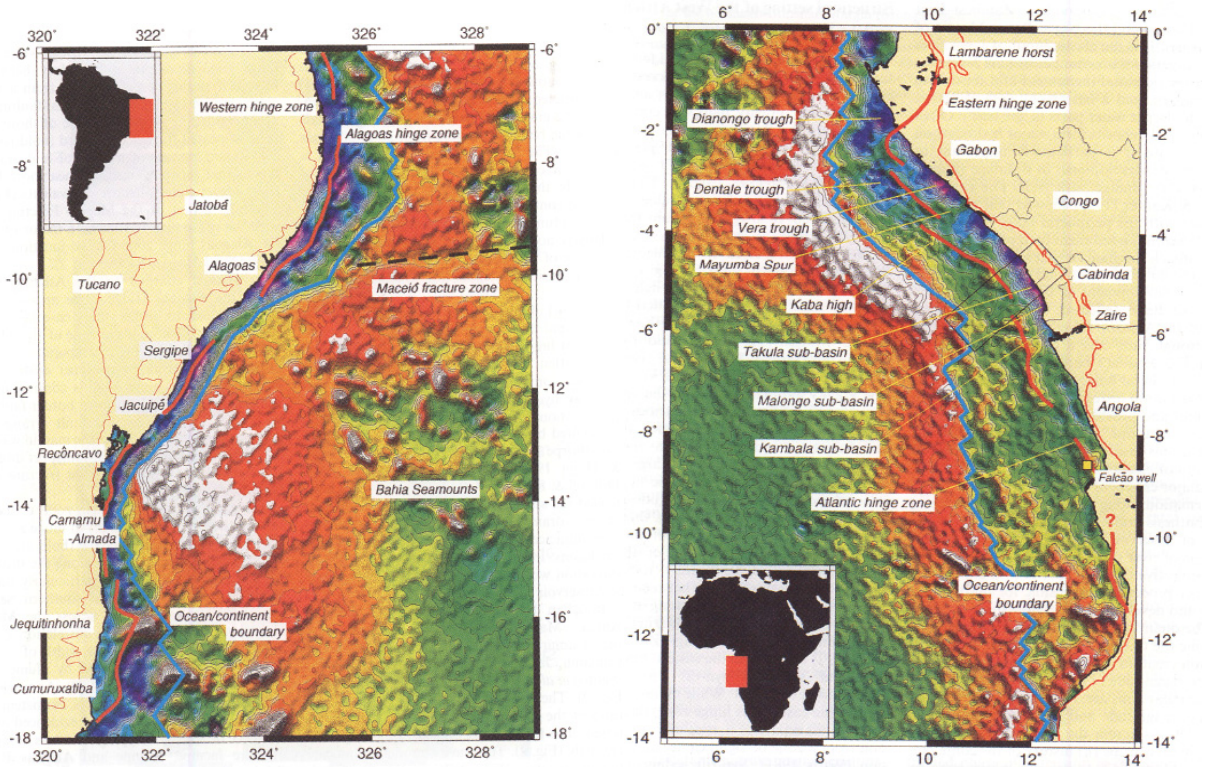

Fig. 6.13: *Bouguer-corrected gravity anomaly fields showing the positions of the Eastern and Atlantic hinge zones on the West African side (right) and Western and Offshore hinge zones on the Brazilian side (left) (Karner and Driscoll, 1999).*

6.3.2 Oblique-shear margin

Oblique-sheared margins are common occurrences on segmented passive continental margins (e.g. equatorial South Atlantic), where the movements of adjacent segments differ according to the changes between the strike of the rift margin and the plate divergence direction (Turner et al., 2003). The structural geometry of the North Gabon margin (Fig. 2.3) is characterized by transfer zones which run oblique to the rifted margin segments. The location and orientation of these transfer zones are likely related to the effect of stress inherent weaknesses in the lithosphere. The Ascension Fracture Zone (AFZ) exhibited oblique-slip faulting and syn-rift half-graben formation that accommodated oblique extension during the period leading up to and immediately following whole lithosphere failure and continental breakup of the study area (Turner et al., 2003). The typically observed geometry of Turner et al. (2003) reveals interplay of stresses induced by extensional regimes changing from normal faults to transform fault systems. These fault systems at rifted margins result in breakup and drift events coinciding with whole lithosphere failure and followed by extrusion of mantle materials to the surface, thus the beginning of spreading. However, breakup in oblique settings results from independent divergent rotation of the margins due to transtensional processes.

Chapter 7

Summary and conclusions

Integration of seismic and potential field data and gravity modeling was utilized to construct two regional crustal-scale transects along the Equatorial Guinea and northern Gabon margins. The analysis has proven to be very robust for unraveling the crustal structure, continent-ocean boundary/transition, margin segmentation, as well as evaluating the conjugate margin setting.

In the construction of the two regional transects, previously published seismic reflection profiles were used that were depth-converted in this study with simplified seismic velocity-depth functions derived from regional consideration and previous studies. Furthermore, gravity modeling was used to test the sensitivity of different alternative seismic interpretations of the same lines and to determine the preferred geometries and densities that are most representative of the crystalline-crust relief for the study area. The two constructed crustal-scale transects were helpful in imaging and obtaining the Moho relief, top crystalline-crust relief, the proto-oceanic crust, and the syn-rift and post-rift sedimentary sequences.

Refinement of the continent-ocean boundary/transition was achieved by the use of the Bouguer-corrected gravity anomaly field, corroborated by the magnetic response. In particular, the continent-ocean boundary/transition is placed along a steep-gradient of the Bouguer-corrected gravity anomaly and where there is a corresponding rapid change in the magnetic anomaly response. The transition from continental to oceanic domain is characterized by an intermediate unit, the proto-oceanic crust separating the continental crust from the normal oceanic crust.

A number of oceanic fracture zones and continental transfer zones/faults, which can be traced landward to Precambrian lineaments, define a distinct margin segmentation along the Equatorial Guinea and northern Gabon margin. The oblique nature of this margin and the juxtaposition between transform and normal faulted regimes has given

the margin a progressive northeast step-like orientation. The margin has been greatly influenced by extensional tectonism.

There is a striking asymmetry between the study area and the conjugate northeast Brazilian margin. In particular, the distance of the shelf-edge from the continent-ocean boundary on the Gabon margin is wider south of the Salvador-N'Komi fracture zones and narrows northwards, while on the Brazilian side it is narrow south of the Maceió-Ascension fracture zones and widens towards the north. Conjugate crustal-scale transects have been compared and evaluated, exhibiting a seawards progressive shallowing of the Moho discontinuity and greater crustal extension as well as asymmetry in their crustal thicknesses.

References

Alan, E. M., and M. A. Khan, 2000. Looking into the Earth: an introduction to Geological Geophysics.

Alkmin, F.F., 2004. O que faz de um cráton um cráton ? O cráton do São Francisco e aas revelações almeidianas ao delimitá-lo. In V. Mantesso-Neto, A. Bartorelli, C.D.R. Carneiro and B.B. Brito-Neves (eds.), Geologia do continente sul-americano: evolução da obra de Fernando Flávio Marques de Almeida, Cap. XVII, p.17-35.

Andersen, O.A., and P. Knudsen, 1998. Global marine gravity field from the ERS-1 and Geosat geodetic mission. Journal of Geophysical Research 103, 8129-8138.

Bassi, G., C.E. Keen, and P.Potter, 1993. Contrasting styles of rifting; models and examples from the eastern Canadian margin. Tectonics 12, 639-655.

Bengtson, P., and E.A.M. Koutsoukos, 1992. Ammonite and foraminiferal dating of the first marine connection between the central and south Atlantic. In: Géologie Africaine: 1er colloque de Stratigraphie et de paleogeographie des basins sedimentaires oust-africains; 2e colloque africain de Micropaleontologie. Bulletin des Centres de Recherches Exploration-Production Elf-Aquitaine Memoir 13 (pp. 403). Libreville, Gabon.

Bertrand, J.M., and E.F.J. de Sá, 1990. Where are the Eburnian-Transamazonian collisional belts? Can. J. Earth Sci., 27, 1382-1393.

Bessoles, B., 1977. Geology de l'Afrique – le craton ouest Africaine. BRGM: Memoir No. 88.

Blaich, O.A., et. al., 2008. Northeastern Brazilian margin: Regional tectonic evolution based on integrated analysis of seismic reflection and potential field data and modelling, Tectonophysics (2008), doi: 10.1016/j.tecto.2008.02.011

Bohannon, R.G. and Eittreim, S.L., 1991. Tectonic development of passive continental margins of the southern and central Red Sea with a comparison to Wilkes Land, Antarctica. Tectonophysics 198, 129–154.

Bonatti, E., and Seyler, M., 1987. Crustal underplating and evolution of the Red Sea rift: uplifted gabbro/gneiss crustal complexes on Zabargad and Brothers islands. J. Geophys. Res., 92, 12803-12821.

Bradley, C.A., and M.N. Fernandez, 1992. Early Cretaceous paleogeography of Gabon/northeastern Brazil: a tectono-stratigraphic model based on propagating rifts. Géologie Africaine: Coll. Géol. Libreville, recueil des Communic., p. 17-30.

Braun, J. and C. Beaumont, 1989. A physical explanation of the relationship between flank uplifts and the breakup unconformity at rifted continental margins, Geology, 17, 760-764.

Breivik, A., P. G. Granholm, B. Krokan and J. E. Rudjord, 1990. Tamp (Tyngde Anomaly Modellerings Program): A Gravity Anomaly Modelling Program. Version 3.1.

Computer program/database documentation series no. 6., Geophysics Research Group, Department of Geology, University of Oslo.

Brink, A.H., 1974. Petroleum Geology of Gabon basin. Am. Ass. Petrol. Geol. Bull., 58, 216-235.

Buck, W.R., 1991. Modes of continental lithospheric extension. Journal of Geophysical Research, V. 96, No. 12, p. 20,161-20,178.

Burke, K., 1969. Seismic areas of the Guinea coast where Atlantic fracture zone reach Africa. Nature, 222, 655-657.

Burke, K., and J. F. Dewey. 1974. Two plates in Africa during the Cretaceous? Nature, 249, 313-316.

Cahen, N.J., N.J. Snelling, J. Delhal, J.R. Vail, M. Bonhomme, and D. Ledent, 1984. The Geochronology and Evolution of Africa. Clarendon Press, Oxford, England, 512 pp.

Cameron, N.R., R.H. Bate, and V.S. Clure, 1999. The oil and gas habitats of the South Atlantic. Geological Society London Special Publication 153, 474 p.

Castro, A.C.M., 1987**.** The northeastern Brazil and Gabon basins: a double rifting system associated with multiple crustal detachment surface. Tectonics, v. 6, no. 6, p. 727-738.

Chalmers, J.A., 1991. New evidence on the structure of the Labrador Sea/Greenland continental margin. J. Geol. Soc. Lond. 148, 899-908.

Chang, H.K., R. O. Kowsmann, A. M. F. Figueiredo, and A. A. Bender, 1992. Tectonic and stratigraphy of the East Brazil Rift system: an overview. Tectonophysics, v. 213, p. 97-138.

Condie, K.C., 1989. Plate Tectonics and Crustal Evolution.

Condie, K., 2005. Earth as an evolving planetary system. Boston: Elsevier academic press.

Cordell, L., and R. G. Henderson, 1968. Iterative three-dimensional solution of gravity anomaly data using a digital computer. Geophysics, v. 33, Issue 4, p. 596-601.

Curie, D., 1984. Ouverture de 1' Atlantique sud et discontinuités intra-plaque : Une nouvelle analyse. PhD thesis, University de Bretagne Occidentale, Brest, pp. 192.

D' Agrella-Filho, M.S., I. G. Pacca, P.R. Renne, T.C. Onstott, and W. Teixeira, 1990. Paleomagnetism of Middle Proterozoic (1.01 to 1.08 Ga) mafic dykes in southeastern Bahia State-Sao Francisco Craton. Brazil Earth Plan. Sci. Let. 101, 332-348.

Dailly, P., 2000. Tectonic and Stratigraphic Dvelopment of the Rio Muni Basin, Equatorial Guinea: the Role of Transform Zones in Atlantic Basin Evolution. Atlantic Rifts and Continental Margins, Geophysical Monograph 115, p. 105-128.

Davison, I., 1988. Comment on "The northeastern Brazil and Gabon Basins: A double rifting system associated with multiple detachment surfaces" by A.C.M. Castro, Jr. Tectonics 6, 1385-1391.

Davison, I., 1999. Tectonics and hydrocarbon distribution along the Brazilian South Atlantic margin. In: N.R.Cameron, R.H. Bate and V.S. Clure (eds.). The Oil and Gas Habitats of the South Atlantic. Geological Society, London, Special Publication, 153, p. 133-151.

De Brito, B, and U.G. Cordani, 1991. Tectonic evolution of South Americaduring the Late Proterozpoic. Precamb. Res. 53, 23-40.

De Matos, R.M.D., 1992. The northeast Brazilian rift system. Tectonics 11, 701-766.

De Ruiter, P.A.C., 1979. The Gabon and Congo salt deposits. Econ. Geol. 74, 419-431.

Dickson, W.G., R.E. Fryklund, M.E. Odegard, and C.M. Green, 2003. Constraints for plate reconstruction using gravity data – implications for source and reservoir distribution in Brazilian and West African margin basins. Marine and Peroleum Geology 20, 309-322.

Ekwueme, B.N., M. Caen-Vachette, and A.C. Onyeagocha, 1991. Isotopic ages from the Oban Massif and southeast Lokoja. Implications for the evolution of basement complex of Nigeria. J. African Earth Sci. 12, 489-503.

Emery, K.O. and E. Uchupi, 1984. The Geology of the Atlantic Ocean. Springer-Verlag, New York.

Fairhead, J.D., 1988. Mesozoic plate tectonic reconstructions of the central South Atlantic Ocean: the role of the West and Central African rift system, Tectonophysics, 155, 181-191.

Garcia, A.J.V., 1991. Paleogeografia do nordeste Brasileiro no Jurassico superior-cretaceo inferior. Geosciencias, 10, 37-56.

Gomes, P.O., B.S. Gomes, J.J.C. Palma, K. Jinno, and J.M. de Souza, 1997. Ocean-Continental Transition and tectonic Framework of the Oceanic Crust at the Continental Margin off NE Brazil: Results of LEPLAC Project. In: W.Mohriak and M.Talwani, eds., Atlantic Rifts and Continental Margins: Geophysical Monograph 115, p. 261-288.

Groschel-Becker, H.M., 1996. Formational processes of oceanic crust at sedimented spreading centers: Perspectives from the West African continental margin and Middle Valley, Juan de Fuca Ridge. University of Miami, 328 p., Ph.D. dissertation.

Guazelli, W., and J. C. Carvalho, 1978. A extensao da Zona de fratura de Vitoria-Trindade no oceano, e seu possivel prolongamento no continente. In F. Carneiro, ed., Aspectos estruturais da margem continental leste e sudeste do Brasil. p. 31-38.

Guiraud, R. and J.C. Maurin, 1992. Early Cretaceous rifts of Western and Central Africa: an overview. Tectonophysics, 213, 153-168.

Jakobsson, M., 2000. Mapping of the Arctic Ocean: Bathymetry and Pliestocene Paleoceanography. Ph.D. thesis. 94 p.

Karner, G.D., and N.W. Driscoll, 1999. Tectonic and stratigraphic development of the West African and eastern Brazilian Margins: insights from quantitative basin modelling. In: N.R.Cameron, R.H. Bate and V.S. Clure (eds.): The Oil and Gas Habitats of the South Atlantic. Geological Society, London, Special Publications, 153, p. 11-40.

Karner, G.D., 2000. Rifts of the Campos and Santos Basins, Southeastern Brazil: Distribution and Timing. In: M.R. Mello and B.J. Katz, eds., Petroleum systems of South Atlantic margins: AAPG Memoir 73, p. 301-315.

Katz, B.J., and M.R. Mello, 2000. Petroleum systems of South Atlantic Marginal basins-An overview, In: M.R. Mello and B.J. Katz, eds., Petroleum systems of South Atlantic margins: AAPG Memoir 73, p. 1-13.

Keen, C.E., 1987. Some important consequences of lithospheric extension. Geol. Soc. London, Sp. Publ. 28, 67-73.

Keen, C.F., B.C. MacLean, and W.A. Kay, 1991. A deep seismic reflection profile across the Nova Scotia continental margin, offshore eastern Canada. Can. J. Earth Sci. 28, 1112-1121.

Keen, C.E. and S.A. Dehler, 1997. Extensional styles and gravity anomalies at rifted continental margins; some North Atlantic examples. Tectonics 16 (5), p. 744-754.

Lana, M.C., 1990. Bacia de Sergipe-Alagoas: Uma hipótese de evoloção tectono-sedimentar. In: De Raja Gabaglia, G.P. and E.J. Milani (eds.). Origem e evolução de bacias sedimentares. Petrobrás.

Ledru, P., J.E. N'Dong, V. Johan, J.-P. Prian, Coste, B., and D. Haccard, 1989. Structural and metamorphic evolution of the Gabon orogenic belt. Collision tectonics in the lower Proterozoic? Precamb. Res. 44, 227-241.

Lehner, P., and P.A.C. de Ruiter, 1977. Structural history of Atlantic margin of Africa, Am. Assoc. Petrol. Geol. Bull., 61, 961-981.

Leyden, R., G. Bryan, and M. Ewing, 1972. Geophysical reconnaissance on the African shelf: 2. Marginal sediments from Gulf to Guinea to Walvis Ridge. AAPG Bulletin, 56, 682-693.

Lister, G.S., M.A. Etheridge, and P.A. Symonds, 1986. Application of the detachment fault model to the formation of passive continental margins. Geology, 14, 246-250.

Lister, G.S., M.A. Etheridge, and P.A. Symonds, 1991. Detachment models for the formation of passive continental margins. Amer. Geophys. Union, Tectonics, Vol. 10, No. 5, 1083-1064.

Lorenzo, J.M., J.C. Mutter, R.L.Larson, and Northwest Australia Study Group, 1992. Development of the continent-ocean transform boundary of the southern Exmouth Plateau. Geology, 19, 843-846.

Lorenzo, J.M., and E.E. Vera, 1992. Thermal uplift and erosion across the continent-ocean transform boundary of the southern Exmouth Plateau. Earth Plan. Sci. Let. 108, 79-92.

Macdonald, D., I. Gómez-Pérez, J. Franzese, L. Spalletti, L. Lawver, L. Gahagan, I. Dalziel, C. Thomas, N. Trewin, M. Hole and D. Paton, 2003. Mesozoic breakup of SW Gondwana: implications for regional hydrocarbon potential of the southern South Atlantic. Marine and Petroleum Geology 20, p. 287-308.

Mascle, J., and E. Blarez, 1987. Evidence for transform margin evolution from the Ivory Coast – Ghana continental margin. Nature, v. 326, p. 376-381.

McConnel, R. B., 1974. Evolution of taphrogenic lineaments in continental platforms. Geologische Rundschau, Stuttgart. v. 63, p. 389-430.

Meyers, J.B., 1995. Rifted continental margin architecture off West Africa, as revealed by deep-penetrating multi-channel seismic reflection and potential field data: University of Miami Ph.D. dissertation, 234 p.

Meyers, J. B., B. R. Rosendahl., H. Groschel-Becker, J. A. Jr. Austin, and P. A. Rona, 1996. Deep penetrating MCS imaging of the rift-to-drift transition, offshore Douala and North Gabon basins, West Africa. Marine and Petroleum Geology, v. 13 nr. 7, p. 791-835.

Meyers, J.B., B.R. Rosendahl, and J.A. Austin, 1996a. Deep-penetrating MCS images of the South Gabon Basin: Implications for rift tectonics and post-breakup salt remobilization: Basin Research, v.8., p65-84.

Meyers, J. B., B. R. Rosendahl., H. Groschel-Becker, J. A. Jr. Austin, and P. A. Rona, 1996b. Deep penetrating MCS imaging of the rift-to-drift transition, offshore Douala and North Gabon basins, West Africa. Marine and Petroleum Geology, v. 13 nr. 7, p. 793-836.

Milani, E.J., and I. Davison, 1988. Basement control and transfer tectonics in the Recôncavo-Tucano-Jatobá rift, northeastern Brazil. Tectonophysics, v. 154, p. 41-70.

Mohriak, W.U., J.H.L. Rabelo, R.D. Matos, and M.C. Barros, 1995 a. Deep Seismic Reflection Profiling of Sedimentary Basins, Offshore Brazil: Geological Objectives and Preliminary Results in the Sergipe Basin. Journal of Geodynamics, v.20, 515-539.

Mohriak, W.U., M.Bassetto, and I.S. Vieira, 1995b. Deep seismic constraints on the crustal architecture of sedimentary basins in the Brazilian margin: Tectonic and exploratory implications. V. Symposio Nacional de Estudus Tectonicos – SNET 95, Boletim de Resumos Expandidos, 246-248.

Mohriak, W.U., M. Bassetto, and I. S. Vieira, 1998. Crustal architecture and tectonic evolution of the Sergipe-Alagoas and Jacuípe basins, offshore northeastern Brazil. Tectonophysics. v. 288, p. 199-220.

Mohriak, W.U., M. Basseto, and I.S Vieira, 2000a. Tectonic Evolution of the Rifted Basins in the Northeastern Brazilian Region. In: W.Mohriak and M.Talwani, eds., Atlantic Rifts and Continental Margins: Geophysical Monograph 115, p. 293-315.

Mohriak, W.U., M.R. Mello, M. Bassetto, I.S. Vieira, and E.A.M. Koutsoukos, 2000b. Crustal Architecture, Sedimentation, and Petroleum Systems in the Sergipe-Alagoas Basin, Northestern Brasil. In: M.R. Mello and B.J. Katz, eds., Petroleum systems of South Atlantic margins: AAPG Memoir 73, p. 273-300.

Mohriak, W.U., 2004. Recursos energéticos associados à ativacão tectônica Mesozóico-Cenozóica da América do Sul. Geologia do Continente Sul-Americano: Evolucão da obra de Fernando Flávio Marques de Almeida, p. 293-318.

Moulin, M., 2003. Etude géologique et géophysique des marges continentals passives: exemple du Zaïre et de l'Angola. PhD thesis, University de Bretagne Occidentale, Brest, 2 Vol., 360 pp. Available at http://www.ifremer.fr/docelec/.

Moulin, M., D. Aslanian, J.L. Olivet, I. Contrucci, L. Matias, L. Geli, F. Klingelhoefer, H. Nouze J.P. Rehault and P. Unternehr, 2005. Geological constraints on the evolution of the Angolan margin based on reflection and refraction seismic data (ZaiAngo Project). Geophysical Journal International 162 (3), p. 793-810.

Nafe, J. E., and C. L. Drake, 1957. Variation with depth in shallow and deep water marine sediments of porosity, density and the velocities of compressional and shear waves. Geophysics, v. 22 Issue3, p. 523-552.

Nøttvedt, A., R.H. Gabrielsen, and R.J. Steel, 1995. Tectonostratigraphy and sedimentary architecture of the rift basins, with reference to the northern North Sea. Marine and Petroleum Geology 12, 8, p. 881-901.

Nürnberg, D. and R.D. Müller, 1991. The tectonic evolution of the South Atlantic from Late Jurassic to present. Tectonophysics, 191, 27-53.

Ojeda, H.A., 1982. Structural framework, stratigraphy, and evolution of Brazilian marginal basins, Am. Assoc. Petrol. Geol. Bull., 66, 732-749.

Pindell, J., and J.F. Dewey, 1982. Permo-triassic reconstruction of western pangea and the evolution of the Gulf of Mexico/Caribbean region, Tectonics, 1(2), 179-211.

Planke, S., 1993. Section: Section plotting, digitizing, and utility program. Version 1.0. Computer program/database documentation series no. 4., Geophysics Research Group, Department of Geology, University of Oslo.

Popoff, M., 1988. Du Gondwana a l'Atlantique sud. Les connexions du fosse de la Benoue avec les bassins du nord-est bresilien jusqu'a l'ouverture du golfe de Guinee au Cretace inferieur. Journal of African Earth Science, v. 7, p. 409-431.

Porada, H., 1989. Pan-African rifting and orogenesis in southern to equatorial Africa and eastern Brazil. Precamb. Res. 44, 103-136.

Rabinowitz, P.D., and J. LaBrecque, 1979. The Mesozoic South Atlantic Ocean and Evolution of Its Continental Margins. Journal of Geophysical Research, B84, p. 5973-6002.

Reid, J., 1989. Effects of lithospheric flow on the formation and evolution of a transform margin. Earth Plan. Sci. Let. 95: 38-52.

Reyre, D, 1984a. Caracteres petroles et evolution geologique d'une marge passive. Le cas du basin bas Congo-Gabon. Bulletin des Centres de Recherches Exploration-Production Elf-Aquitaine, 8, 303-332.

Roguel, N.C., 1990. Analise estructural das falhas ocurentes nas sub-bacias do Tucano sul e central Bahia. Masters Thesis. Universidade Federal de Ouro Preto.

Rosendahl, B. R., H. Groschel-Becker, J. Meyers, and K. Kaczmarick, 1991. Deep seismic reflection study of a passive margin, southeastern Gulf of Guinea. Geology, 19, 291-295.

Rosendahl, B.R., J. Meyers, H. Groschel-Becker, and D. Scott, 1992a. Nature of the transition from continental to oceanic crust and the meaning of reflection Moho. Geology, 40, 721-724.

Rosendahl, B.R., and H. Groschel-Becker, 1999. Deep seismic structure of the continental margin in the Gulf of Guinea: a summary report. In: Cameron, N.R., R.H. Bate, and V.S. Clure (eds.). The Oil and Gas Habitats of the South Atlantic. Geological Society, London, Special Publications, 153, p. 75-83.

Rosendahl B.R., and H. Groschel-Becker, 2000. Architecture of the Continental Margin in the Gulf of Guinea as Revealed by Reprocessed Deep-Imaging Seismic Data. In: Atlantic Rifts and Continental Margins. Geophysical Monograph 115. American Geophysical Union, p. 85-103.

Rosendahl, B.R., W.U. Mohriak, M.E. Odegard, J.P. Turner, and W.G.Dickson., 2005. West African and Brazilian Conjugate Margins: Crustal Types, Architecture, and Plate Configurations. 25th Annual Bob F. Perkins Research Conference: Petroleum Systems of Divergent Continental Margin Basins.

Sandwell, D.T., and W.H.F. Smith, 1997. Marine gravity anomaly from Geosat and ERS-1 altimetry. Journal of Geophysical Research 192, 10039-10054 (v. 15.1).

Scotese, C.R., L.M. Gahagan, and R. L. Larson, 1988. Plate tectonic reconstructions of the Cretaceous and Cenozoic basins. Tectonophysics 155, 27-48.

Scrutton, R.A., 1982. Crustal structure and development of sheared passive continental margins. In: Scrutton, R.A. (Ed.). Dynamics of Passive Margins. Geodynamics Series No. 6, Amer. Geophys. Union, Washington DC, 133–114.

Talwani, M., and O. Eldholm, 1973. Boundary between Continental and Oceanic Crust at the Margin of Rifted Continents. Nature, v.241, p.325-330.

Teisserenc, P., and J. Villemin, 1989. Sedimentary Basin of Gabon – Geology and Oil Systems. In: Edwards, J.D., and P.A. Santogrossi (eds.), Divergent/Passive Margin Basins. AAPG Memoir, 48, 117-200.

Teisserenc, P., and J. Villemin, 1990. Sedimentary Basin of Gabon – Geology and Oil Systems. In: Edwards, J.D., and P.A. Santogrossi (eds.), Divergent/Passive Margin Basins. AAPG Memoir, 48, 117-199.

Teixeira, W., and M.C.H. Figueiredo, 1991. An Outline of Early Proterozoic crustal evolution in the Sao Francisco Craton Brazil. A review. Preamb. Res. 53, 1-22.

Todd, B.J., and C.E. Keen, 1989. Temperature effects and their geological consequences at transform margins. Can. J. Earth Sci. 26, 2591-2603.

Torquato, J.R., and U. Cordani, 1981. Brazil-Africa geological links. Earth-Sci. Rev. 17, 155-176.

Tsikalas, F., O. Eldholm, and J. I. Faleide, 2005. Crustal structure of the Lofoten-Vesterålen continental margin, off Norway. Tectonophysics 404. p. 151-174.

Turner, J.P.,1995. Gravity-driven structures and rift basin evolution: The Rio Muni basin, offshore Equatorial West Africa. AAPG Bulletin, 79, 1138-1158.

Turner, J.P., 1999. Detachment faulting and petroleum prospectivity in the Rio Muni Basin, Equatorial Guinea, West Africa. In: Cameron, N.R., R.H. Bate, and V.S. Clure (eds.). The Oil and Gas Habitats of the South Atlantic. Geological Society, London, Special Publications, 153, 303-320.

Turner, J.P., B.R. Rosendahl, and P.G. Wilson, 2003. Structure and evolution of an obliquely sheared continental margin: Rio Muni, West Africa. Tectonophysics, v. 374, p.41-55.

Unternehr, P. D. Curie, J.L Olivet, J. Goslin, and P. Beuzart, 1988. South Atlantic fits and intraplate boundaries in Africa and South America, Tectonophysics, 155, 169-179.

Ussami, N., G.D. Karner, and M.H.P. Bott, 1986. Crustal detachment during South Atlantic rifting and formation of Tucano-Gabon rift system. Nature, v. 322, p. 629-632.

Wannesson, J., J.C. Icart, and J. Ravat, 1991. Structure and evolution of adjoining segments of the West African margin determined from deep seismic profiling. Continental Lithosphere. Deep seismic reflections. Geodynamics 22. Geophysical Union, p. 275-289

Watts, A.B., 1981. The U.S. Atlantic Continental margin: subsidence history, crustal structure and thermal evolution. In: Geological of Passive Continental Margins: History, Structure and Sedimentologic Record (with special emphasis on the Atlantic margin).

Watts, A.B. and J. Stewart, 1998. Gravity anomalies and segmentation of the continental margin offshore West Africa. Earth and Planetary Science Letters 156, p. 239-252.

Weger, R., B.R. Rosendahl, and M.E. Odegard, 2001. New constraints on rift margin development through integration of deep-imaging seismic interpretation and gravity modeling. Geological Society of America, Annual Meeting 2001, p.301, Abstract.

Wessel, P., and W.H.F Smith, 1998. New version of the Generic Mapping Tools., EOS Transactions v. 79, American Geophysical Union., p. 579., release editor. http://gmt.soest.hawaii.edu/

Wilson, P. G., J. P. Turner, and G. K. Westbrook, 2003. Structural architecture of the ocean-continent boundary at an oblique transform margin trough deep-imaging seismic interpretation and gravity modelling: Equatorial Guinea, West Africa. Tectonophysics v. 374, p. 19-40.